Geological Survey of Canada
Commission géologique du Canada

PAPER
ÉTUDE 88-1F

CURRENT RESEARCH PART F
NATIONAL AND GENERAL PROGRAMS

RECHERCHES EN COURS PARTIE F
PROGRAMMES NATIONAUX ET GÉNÉRAUX

1988

Canada

88-03795/

NOTICE TO LIBRARIANS AND INDEXERS

The Geological Survey's Current Research series contains many reports comparable in scope and subject matter to those appearing in scientific journals and other serials. Most contributions to Current Research include an abstract and bibliographic citation. It is hoped that these will assist you in cataloguing and indexing these reports and that this will result in a still wider dissemination of the results of the Geological Survey's research activities.

AVIS AUX BIBLIOTHÉCAIRES ET PRÉPARATEURS D'INDEX

La série Recherches en cours de la Commission géologique paraît une fois par année; elle contient plusieurs rapports dont la portée et la nature sont comparables à ceux qui paraissent dans les revues scientifiques et autres périodiques. La plupart des articles publiés dans Recherches en cours sont accompagnés d'un résumé et d'une bibliographie, ce qui vous permettra, nous l'espérons, de cataloguer et d'indexer ces rapports, d'où une meilleure diffusion des résultats de recherche de la Commission géologique.

GEOLOGICAL SURVEY OF CANADA
PAPER 88-1F
COMMISSION GÉOLOGIQUE DU CANADA
ÉTUDE 88-1F

CURRENT RESEARCH PART F
NATIONAL AND GENERAL PROGRAMS

RECHERCHES EN COURS PARTIE F
PROGRAMMES NATIONAUX ET GÉNÉRAUX

1988

© Minister of Supply and Services Canada 1988

Available in Canada through

authorized bookstore agents and other bookstores

or by mail from

Canadian Government Publishing Centre
Supply and Services Canada
Ottawa, Canada K1A 0S9

and from

Geological Survey of Canada offices:
601 Booth Street
Ottawa, Canada K1A 0E8
3303-33rd Street N.W
Calgary, Alberta T2L 2A7
100 West Pender Street
Vancouver, British Columbia V6B 1R8

A deposit copy of this publication is also available
for reference in public libraries across Canada

Cat. No. M44-88/1F	Canada:	$5.00
ISBN 0-660-53901-2	Other countries:	$6.00

Price subject to change without notice

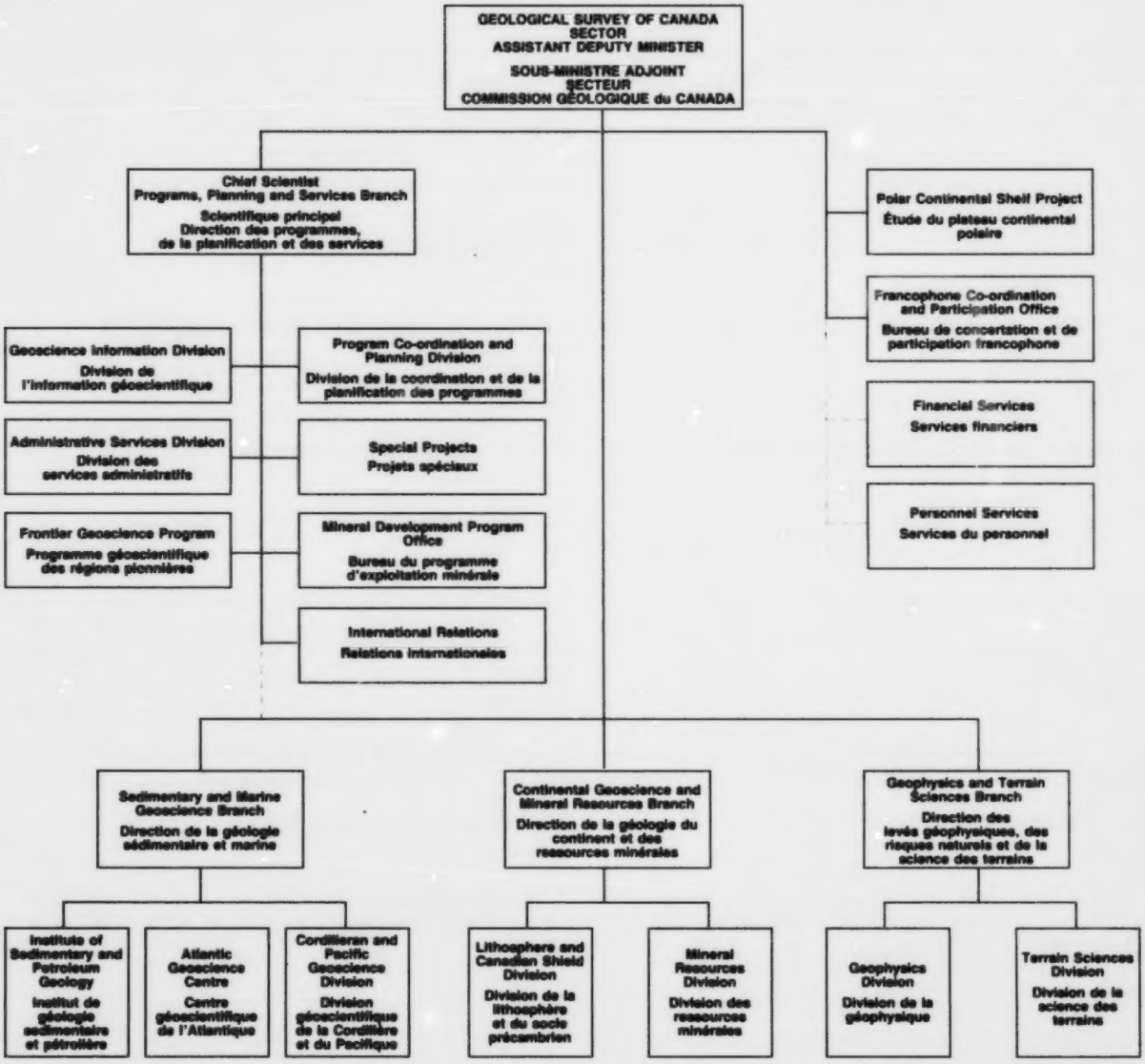
GEOLOGICAL SURVEY OF CANADA
SECTOR
ASSISTANT DEPUTY MINISTER
SOUS-MINISTRE ADJOINT
SECTEUR
COMMISSION GÉOLOGIQUE du CANADA
Chief Scientist
Programs, Planning and Services Branch
Scientifique principal
Direction des programmes,
de la planification et des services
Polar Continental Shelf Project
Étude du plateau continental polaire
Francophone Co-ordination and Participation Office
Bureau de concertation et de participation francophone
Financial Services
Services financiers
Personnel Services
Services du personnel
Geoscience Information Division
Division de l'information géoscientifique
Program Co-ordination and Planning Division
Division de la coordination et de la planification des programmes
Administrative Services Division
Division des services administratifs
Special Projects
Projets spéciaux
Frontier Geoscience Program
Programme géoscientifique des régions pionnières
Mineral Development Program Office
Bureau du programme d'exploitation minérale
International Relations
Relations internationales
Sedimentary and Marine Geoscience Branch
Direction de la géologie sédimentaire et marine
Continental Geoscience and Mineral Resources Branch
Direction de la géologie du continent et des ressources minérales
Geophysics and Terrain Sciences Branch
Direction des levés géophysiques, des risques naturels et de la science des terrains
Institute of Sedimentary and Petroleum Geology
Institut de géologie sédimentaire et pétrolière
Atlantic Geoscience Centre
Centre géoscientifique de l'Atlantique
Cordilleran and Pacific Geoscience Division
Division géoscientifique de la Cordillère et du Pacifique
Lithosphere and Canadian Shield Division
Division de la lithosphère et du socle précambrien
Mineral Resources Division
Division des ressources minérales
Geophysics Division
Division de la géophysique
Terrain Sciences Division
Division de la science des terrains

Separates

A limited number of separates of the papers that appear in this volume are available by direct request to the individual authors. The addresses of the Geological Survey of Canada offices follow:

601 Booth Street,
OTTAWA, Ontario
K1A 0E8

Institute of Sedimentary and Petroleum Geology,
3303-33rd Street N.W.,
CALGARY, Alberta
T2L 2A7

Cordilleran and Pacific Geoscience Division,
100 West Pender Street,
VANCOUVER, B.C.
V6B 1R8

Pacific Geoscience Centre
P.O. Box 6000,
9860 Saanich Road,
SIDNEY, B.C.
V8L 4B2

Atlantic Geoscience Centre,
Bedford Institute of Oceanography,
P.O. Box 1006,
DARTMOUTH, N.S.
B2Y 4A2

When no location accompanies an author's name in the title of a paper, the Ottawa address should be used.

Tirés à part

On peut obtenir un nombre limité de «tirés à part» des articles qui paraissent dans cette publication en s'adressant directement à chaque auteur. Les adresses des différents bureaux de la Commission géologique du Canada sont les suivantes:

601, rue Booth
OTTAWA, Ontario
K1A 0E8

Institut de géologie sédimentaire et pétrolière
3303-33rd St. N.W.,
CALGARY, Alberta
T2L 2A7

Division géoscientifique de la Cordillère
et du Pacifique
100 West Pender Street,
VANCOUVER, Colombie-Britannique
V6B 1R8

Centre géoscientifique du Pacifique
B.P. 6000,
9860 Saanich Road,
SIDNEY, Colombie-Britannique
V8L 4B2

Centre géoscientifique de l'Atlantique
Institut océanographique de Bedford
B.P. 1006,
DARTMOUTH, Nouvelle-Écosse
B2Y 4A2

Lorsque l'adresse de l'auteur ne figure pas sous le titre d'un document, on doit alors utiliser l'adresse d'Ottawa.

CONTENTS

1 | R.G. GARRETT
IDEAS: an interactive computer graphics tool to assist the exploration geochemist

15 | A. LAMBERT, J.O. LIARD, P.N. COURTIER, A.K. GOODACRE, and R.K. McCONNELL
The Geological Survey of Canada absolute gravity program: applications in geodesy and geodynamics

17 | J.R. BÉLANGER
Shaded contour map generation on IBM-compatible microcomputers

21 | V. RUZICKA
Uranium resource investigations in Canada, 1987

31 | R.L. COLES, J. HRUSKA, and H.-L. LAM
Some recent developments in geomagnetic activity forecasting at the Geological Survey of Canada

39 | K.N. DE SILVA
A mathematical model for optimization of sample geometry for radiation measurements

45 | H.-L. LAM
Forecasts of Pc5 magnetic pulsations

53 | H.S. HASEGAWA
Mining induced seismicity

59 | R.A. GIBB and J.B. BOYD
National gravity survey program, 1987-1988

63 | E.E. READY, W.A. KNAPPERS, P.E. STONE, D.J. TESKEY, and R.A. GIBB
Aeromagnetic survey program of the Geological Survey of Canada 1987-1988

INTRODUCTION

In 1987 the Geological Survey of Canada became a Sector within the Department of Energy, Mines and Resources, and was re-organized into the four Branches shown on the accompanying organizational chart. The primary role of the Survey, which was founded in 1842, continues to be to provide an overview of all facets of Canadian geology as a basis for national policy, for planning by government and industry, and for public information.

In order to provide interim results of its program a publication titled "Summary of Research" was initiated in 1963. The title was changed to "Current Research" in 1978 and the report was released three times a year (Part A, B and C). After 1982 Part C was no longer issued and Part B was discontinued in 1987 to encourage greater use of journal publication for short contributions.

Current Research, however, is the one series of GSC publications that gives the public a yearly overview of the range of the Geological Survey of Canada Sector activities. From time to time Current Research has been criticized for its size, as it was necessary for the user to buy a large volume to obtain a few pertinent papers. To introduce greater flexibility, this issue of Current Research is therefore available in six parts that can be purchased separately: four regional volumes, one volume of national and general programs, and a volume that contains abstracts of all the reports. The Parts are:

Part A: Abstracts/Résumés
Part B: Eastern and Atlantic Canada
Part C: Canadian Shield
Part D: Interior Plains and Arctic Canada
Part E: Cordillera and Pacific Margin
Part F: National and General Programs

Identification of the Parts by letters is for convenience only and may be subject to change. Each of Parts B to F includes a paginated Table of Contents for the volume: Table of Contents for the other Parts of this series will be found at the back of each volume.

En 1987 la Commission géologique est devenue un secteur à l'intérieur du ministère de l'Énergie, des Mines et des Ressources et a été réorganisée en quatre directions indiquées sur l'organigramme d'accompagnement. Organisme fondé en 1842, la Commission a comme rôle principal de procurer un cadre d'ensemble de toutes les facettes de la géologie du Canada comme base d'une politique nationale pour la planification du gouvernement et de l'industrie et pour informer le public en général.

Afin de fournir les résultats préliminaires de son programme de recherche une publication ayant titre « Summary of Research » est apparue en 1963. Une nouvelle publication, ayant les mêmes buts, est apparue en 1978 sous le titre « Recherches en cours »; cet ouvrage était diffusé trois fois par année (parties A, B et C). Après 1982 la partie C a été abandonnée et ce fut de même pour la partie B en 1987. L'arrêt de ces publications avait pour but d'adopter une nouvelle forme d'édition pour satisfaire davantage l'usager.

La publication « Recherches en cours » appartient à part entière à la série des publications de la CGC et apporte à chaque année une vue d'ensemble des activités de la Commission géologique maintenant au niveau de secteur. De temps à autre la publication « Recherches en cours » a été critiquée pour son fort volume, plusieurs ont constaté qu'il était nécessaire d'acheter un gros volume uniquement pour n'avoir accès qu'à un petit nombre d'articles. Maintenant, cette publication est disponible en six parties en vente séparément, ce qui procure une plus grande flexibilité pour l'usager. La publication est répartie comme suit: quatre volumes régionaux, un volume couvrant les programmes nationaux et généraux et un dernier contenant les résumés de tous les articles. On y trouve les parties suivantes:

Partie A: Abstracts/Résumés
Partie B: Est et région atlantique du Canada
Partie C: Bouclier canadien
Partie D: Plaines intérieures et région arctique du Canada
Partie E: Cordillère et marge du Pacifique
Partie F: Programmes nationaux et généraux

L'identification des parties par une lettre a été adoptée uniquement par commodité; on pourra éventuellement utiliser une autre façon. Les parties B à F possèdent une table des matières paginée; il est à noter qu'à chacune des parties de cette série on y trouvera à l'endos une table des matières indiquant le contenu des autres parties.

IDEAS: an interactive computer graphics tool to assist the exploration geochemist

Robert G. Garrett
Mineral Resources Division

Garrett, R.G., IDEAS: an interactive computer graphics tool to assist the exploration geochemist; in Current Research, Part F, Geological Survey of Canada, Paper 88-1F, p. 1-13, 1988.

Abstract

A colour interactive graphics computer package (IDEAS) is being developed to meet the data analysis needs of exploration geochemists. At this time enough of the package exists for it to be useful production tool, and it is being used to aid data interpretation and prepare graphics for publication and posters. The current version includes the majority of the plotting, database, and simple statistical functions to be implemented. Some multivariate statistical procedures are in place, and it is in this field that the majority of the remaining work will be undertaken. The package uses a combination of Digital Equipment Corporation (VAX 8700) computing and Tektronix graphics display equipment. The development history of the project is outlined together with a description of current functionality and future enhancements.

Résumé

On met actuellement au point un progiciel d'infographie interactive en couleurs, pour donner aux géochimistes d'exploration les données dont ils ont besoin pour leurs analyses. Actuellement, ce progiciel est suffisamment élaboré pour constituer un outil de production d'une grande utilité, et facilite l'interprétation des données et la préparation du travail graphique pour la mise au point de publications et d'affiches. La version actuelle comprend la majeure partie du traçage, de la base de données, et des simples fonctions statistiques appliquées. Quelques-uns des procédés statistiques multivariés sont déjà en place, et c'est dans ce domaine que la majorité du travail restant sera entrepris. Le progiciel utilise une combinaison du parc informatique de la Digital Equipment Corporation (VAX 8700) et de l'unité d'affichage graphique Tektronix. Dans cet article, on esquisse l'historique du projet, et l'on décrit son développement actuel et les perfectionnements envisagés.

INTRODUCTION

The concept of an interactive computer graphics package tailored to the needs of exploration geochemists crystallized during a review of the Exploration Geochemistry Subdivision's computing requirements in 1979. Prior to that time several interactive graphics programs had been written for use on the Departmental CDC Cyber computing facilities. These were useful for anomaly recognition and general data interpretation; however, they were not "friendly" and use of the CDC Cyber computers placed certain restrictions on their operation.

Between 1980 and 1982, a functional specification was developed under a joint Department of Energy, Mines and Resources — Department of Supply and Services Unsolicited Proposal. Under this Unsolicited Proposal made by Hickling-Smith Inc., a consulting group with computer science and statistics experience, their staff undertook extensive discussions with members of the Subdivision and perpared a functional specification for an interactive graphics package. There was a hiatus in development from 1932 to 1984 when a Digital Equipment Corporation (DEC) VAX computer and colour graphics terminal equipment finally became available to the Subdivision.

During this hiatus a number of key decisions were made. Firstly, the U.S. Geological Survey's GRASP database system was selected as the foundation upon which to develop the new system (Bowen and Botbol, 1975). The reasons for selecting GRASP were several, but the most important were its:

1. Friendliness and extensive on-line help facilities,

2. Ability to process qualified data, e.g., greater than or less than, and blanks in a way consistent with Subdivision usage in geochemical data files,

3. Simplicity of the database — post retrieval processing interface, and

4. Presence in the public domain, making it possible to modify GRASP as required for the interactive graphics project, and distribute the resulting software in whatever way the Geological Survey saw fit.

Secondly, it was decided at an early stage that the graphics software would be written using the GKS (Graphics Kernel System) standard largely developed in Europe (1976-1982) for adoption by the International Standards Organization (ISO) (Enderle et al., 1984). Thirdly, the decision was made to write all software to Fortran 77 standards using the minimal number of system dependent features, and where possible any non-standard Fortran would be isolated in subroutines.

The acquisition of a DEC VAX 11/780 and the VMS Operating System in 1984 by the Geological Survey of Canada and the Department's Computer Science Centre for interactive graphics use permitted development to proceed. The U.S. Geological Survey kindly made a VAX version of GRASP available to the project. Additionally, the selection of VAX technology met requirements for technology transfer. This family of 32 bit machines is extensively used in the mineral exploration industry, and by Geological Surveys, in North America, Europe, the Far East and elsewhere.

Tektronix hardware was selected, because it could be configured as a flexible graphics workstation, consisting of a high resolution 16 colour display, digitizing tablet and plotter(s), with its own internal graphics central processing unit (cpu). The availability of this local computing power reduces the amount of graphics information to be sent from the remote VAX host to the workstation and permits local true zoom and pan functions, thus improving the overall response time. Integral to the decision to use Tektronix equipment was the availability of the company's PLOT10GKS software which met the ISO's level 2.B standard, i.e. interactive input of graphical information and graphical output.

IDEAS DEVELOPMENT

Database

The acronym of IDEAS, Interactive Data Exploration and Analysis System, was finally selected in 1983, and implementation of the functional design began in summer 1984 with the establishment of GRASP on the VAX host as soon as it was available for use. Initially GRASP could undertake the following tasks:

1. Build a database from an existing file of data organized by rows and columns, with up to 99 columns (variables) and an unlimited number of rows (cases/samples),

2. Handle below detection level and other special data qualifiers,

3. Extend a database, temporarily by columns and permanently by rows,

4. Link databases via a common key,

5. List variable names and their data types, i.e., integer, floating point, qualified floating point, dictionary items, long and short character strings,

6. Maintain an alternate dictionary for expanded dictionary names, e.g., mnemonic expansions,

7. Display a help file,

8. Review current session activity and status,

9. Define conditional and logical criteria to be used for subset creation,

10. List, after sorting if required, all or selected fields of the database or a subset,

11. Output, after sorting if required, all or selected fields of the database or a subset to a disk file for subsequent processing or transmission or another facility,

12. Browse through data records using every n-th record, where the user specifies n,

13. Temporarily exit to the operating system, and

14. Compute means, correlation coefficients and a simple linear regression.

Major development work commenced in summer 1985. GRASP uses a sequential file structure to store a database and any subsets, resulting in multiple copies of parts of the database, a feature that can hinder database management.

In particular, these multiple copies make editing and the addition of new derived variables difficult to undertake in a fail-safe manner. The first task was therefore to convert the database structure from sequential to keyed access, specifically the keyed Indexed Sequential Access Method (keyed ISAM), so that each database entry could be read or written individually. The subsets are maintained in a separate keyed ISAM file as lists of pointers (accession numbers) to the members of that particular subset, together with information on the size, parent, time of creation of the subset and a text description. This has many beneficial features, the single copy of the database can be edited and added to irrespective of the subsets. Most importantly, this use of pointers establishes a favourable environment for interfacing the database to the user through the graphics screen by use of GKS numbered graphic segments. Changing the database structure to keyed access allowed the addition of:

1. Subset management for up to 75 subsets,

2. The editing of numeric and short character string data, and

3. The permanent storage of new computed variables with the necessary extensions to the database files,

to the original GRASP software.

Subsequently, other modifications have been made to the database and management components of IDEAS. The original GRASP "sorted-list" facility only permitted ascending order sorts. This has been modified to provide either ascending or descending order sorts, with the latter as the default as usually exploration geochemists are more interested in the high values than the low. The original upper and lower case alphabetic data qualifiers have been replaced by the characters >, <, #, and . The last 3 qualifiers, #, and may be employed in any way the user wishes to indicate some feature of the data. For example, possible analytical interference, or a change in the least significant digit by 1 so that differences of zero between duplicate analyses do not occur. This latter problem is of importance when certain log-log quality control plots are prepared with IDEAS. As in GRASP, selective retrievals can be made on the basis of data qualifiers. However, in the instance of the > and < qualifiers, numeric post-retrieval processing is carried out in a special manner. During numeric post-retrieval processing by GRASP the data qualifiers are ignored, i.e., #5 is treated as 5; however, in IDEAS > and < the values are now respectively doubled or multiplied by 5/8th, i.e., >1 000 is converted to 2 000 and <8 is treated as 5, and the data qualifier is temporarily removed. A module has been implemented to provide a summary of qualified data use. The number of occurrences of missing, unqualified and each qualified data type are displayed together with the maximum and minimum values associated with each. This has proven particularly useful with Instrumental Neutron Activation Analysis (INAA) data where significant variations in the detection level may occur. To improve the response time for help requests, the original sequential help file has been replaced by a keyed ISAM file. This has resulted in a marked improvement, with responses being equally fast for all resquests. This is particularly advantageous as the IDEAS help file is significantly larger than the original GRASP help file, containing in excess of 250 entries totalling some 2 000 lines, and will continue to grow as the system develops.

Graphics

IDEAS really took shape once graphics work commenced after the database system modifications were completed. At the current time the graphics modules are limited to displaying plots with up to 7 000 data points. To date, modules have been written which permit the plotting of:

1. Histograms, including means for up to 3 auxiliary variables,

2. Cumulative probability plots with provision for graphical trimming,

3. Simple x-y plots,

4. Up to 9 data subsets as uniquely coloured and shaped symbols on an x-y plot,

5. A third auxiliary variable as one of up to 9 uniquely coloured and shaped symbols on an x-y plot,

6. Ternary diagrams,

7. Up to 9 data subsets as uniquely coloured and shaped symbols on a ternary diagram,

8. A fourth auxiliary variable as one of up to 9 uniquely coloured and shaped symbols on a ternary diagram,

9. A non-traditional diagram, the box-and-whisker plot,

10. Simple posting maps, using a rectangular co-ordinate scheme, where the value of an integer, floating point or qualified data variable may be displayed beside a cross indicating geographic position.

11. Up to 9 data subsets as uniquely coloured and shaped symbols on a simple map, and

12. A symbol map where the value of a numeric data item can be indicated by one of up to 9 uniquely coloured and shaped symbols.

In the auxiliary variable plots (5, 8 and 12) any data points outside of the symbolized range are indicated by a dot.

Some additional comments on the above procedures are presented below, where the numbers in parentheses refer to module numbers in the above list.

The graphical trimming of cumulative probability plots (2) permits outliers, at either the upper or lower extremes of the data, to be temporarily removed and identified by an up to 12 character "unique character identifiers". The percentiles and cumulative probability plots are then recomputed and displayed for inspection and possible futher trimming. To assist in the selection of trimming levels, "fences" at the approximate 10 % some-outside level may be added to the cumulative probability plots (Fig. 1) following Tukey's procedure (Hoaglin et al., 1986). The concept of a some-outside level (Hoaglin et al., 1986) in this application implies that up to 10 % of the data may plot beyond the "fences", 5 % at each extremity. If more than 5 % of the data fall beyond a "fence" outliers must be suspected. This trimming may be continued until an outlier free background population is isolated (Fig. 2), at which time a list of all the trimmed outliers may be displayed (Table 1) together with summary statistics for the remaining background data (Table 2). Up

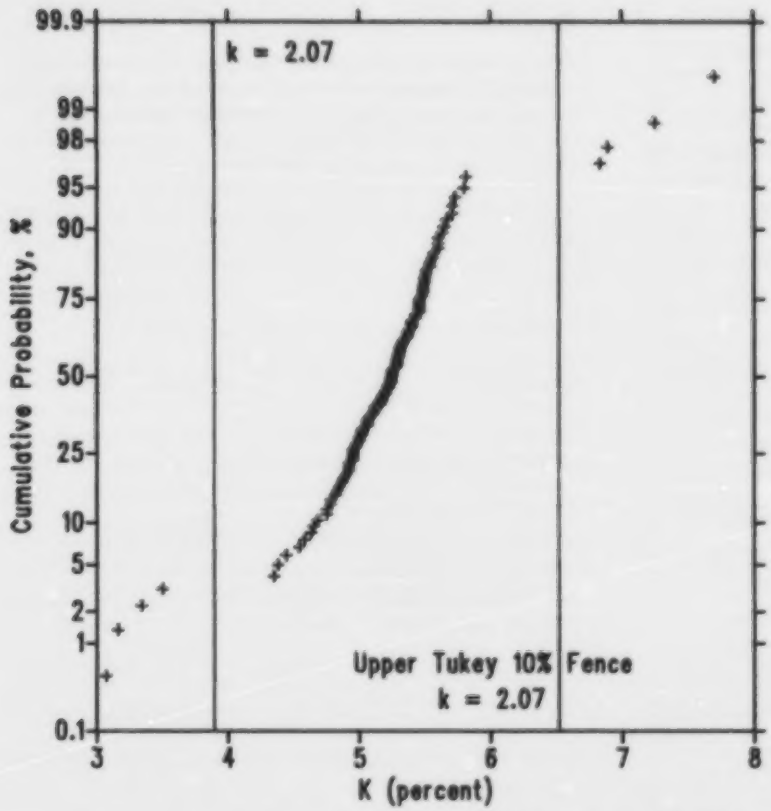

Cut Off Value = 6.511

Points Trimmed = 4

Total Points Trimmed = 4

Total No. of Points = 110

Figure 1. Example of a cumulative probability plot. The fences correspond to a some-outside rate of 10%, i.e., 90% between the fences and 5% outside each fence. In this example the gaps between the central mass of data and the two sets of 4 outliers outside the fences are indicative of true outliers.

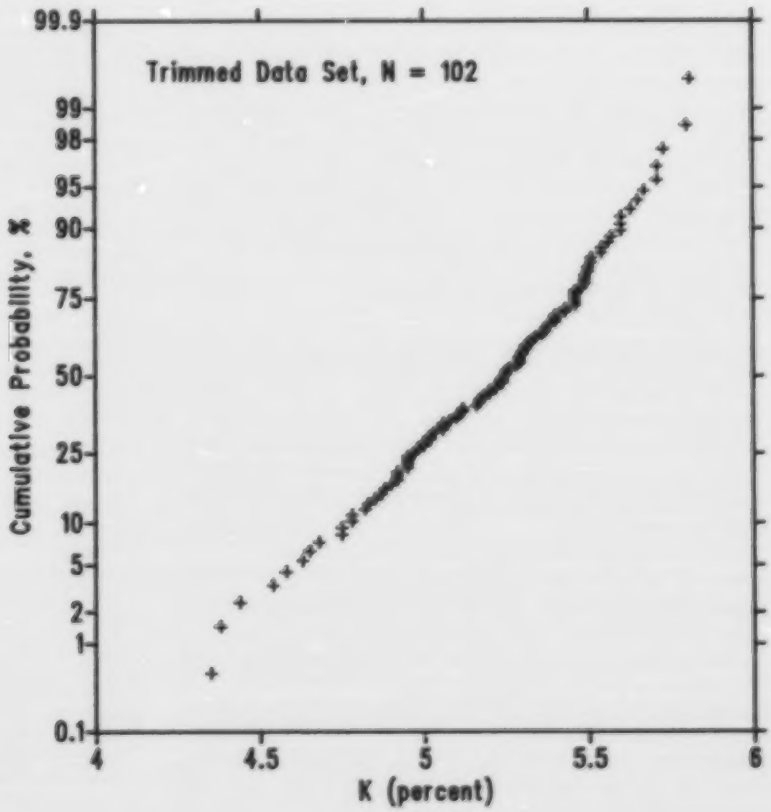

Figure 2. Example of a cumulative probability plot of trimmed data.

to 3 resulting groups, i.e., the lower-outlier, "core", and upper-outlier groups, may be selectively saved as subsets for future display or processing.

The histograms (1) may be annotated with 1 to 3 auxiliary variables. The means for these variables in the cases that fall within the histogram group of the primary variable are displayed to the side of the histogram (Fig. 3). This display has proven particularly useful in the study of the interrelationship of field observations to geochemical laboratory measurements. In the example (Fig. 3) the relative abundance of lakes less than 30 feet deep is clearly seen; but in addition information that indicates a decrease in Loss-on-Ignition and increase in Fe content with increasing depth is also simultaneously displayed. Although Mn generally behaves in a similar fashion to Fe it can also be seen that the sympathetic relationship with Loss-on-Ignition is less pronounced for Mn than if is for Fe in this particular instance.

Histograms, although a popular and widely-used display, lack objectivity by virtue of the arbitrary selection of the starting value, number of histogram groups and their width. In many instances box and whisker plots (9), which are based on the data minima, maxima, 5th, 25th, 50th, 75th and 95th percentiles, are more appropriate than histograms. In particular, they facilitate the graphical comparison of subsets for which data are available for the same variable (Fig. 4). Additionally, the box containing the range of the central 50 % of the data is notched to indicate the location of the median (50th percentile) and its 95 % confidence bounds. Where the notches for subsets do not overlap, the display provides a graphical distribution-free test indicating that the medians of the subsets may well be significantly different at the 95 % confidence level.

The auxiliary variable plots (5 and 8) permit the display of a trace element content in the context of major components, e.g., Zn versus the Fe and Mn in lake or stream sediments, or a trace element against Ca + Mg, Na + K and Fe + Ti in a ternary diagram for a differentiated series of igneous rocks. Both of these displays heve proven useful. Figure 5 is an example where U (ppm) content has been plotted against the r1 (x) and r2 (y) differentiation indices (de la Roche et al., 1980). Each plotted point corresponds to a granitoid pluton, and it can be seen that the high U plutons fall into two clusters; one cluster corresponding to more felsic plutons and the other to syenitic bodies. It is worth noting that cation measures r1 and r2 were computed from the major element compositional data on a demand basis using the "define" command.

The spatial display modules (10-12) provide for rectangular co-ordinate systems, e.g., UTM or simple local grids; no provision has been made for geodetic co-ordinates or the projections required by them. In some instances of high data density on the posting display (10) the values may overplot on one another. To resolve this clutter problem a graphical editing procedure is provided so that the numeric values may be rearranged spatially so they do not overlap. As part of all the mapping modules (10-12) a facility has been implemented which allows a geological or topographic map to be placed on a digitizing tablet and be "slaved" to the map displayed on the screen. In this manner the position of any location of interest may be transferred to the screen as a highlighted open circle centred on the digitized position. Optionally, a marker can be left at this position for later annotation, or the target circle may be deleted.

In order to identify outliers the simple plot and the map posting procedures (3, 6 and 10) include a facility where up to eight points, selected from the screen display with the graphics cursor, may have their plotting symbol changed. The new unique symbol and "unique character identifier" of the selected point are displayed to the side of the plot. The example (Fig. 6) contains the same data and x-y axes as Figure 5, the outlier identification function has been used to identify the 1:250 000 NTS map sheet numbers and pluton field identifiers of the high U background syenitic plutons. If more than eight points are to be identified, the previous eight are set back to the default marker, and then additional sets of up to eight points may be identified.

To ease the task of preparing data subsets a graphical procedure has been implemented in the non-subset display routines, i.e., the x-y, ternary and map displays (3, 5, 6, 8, 10, 12). The user simply draws a polygon using the graphics cursor around the group of points to be included in a subset, this is followed by a prompt for the subset name and description. The subsets may be used for any future display or processing as the user desires.

Table 1. List of trimmed outliers. Note that the mean and standard deviation of the background (untrimmed) data are displayed. These are used in the computation of the SND (Standard Normal Deviate) values and their corresponding probabilities, which indicate the probability of an outlier being a member of the background population under the assumption of normality.

DATA SET NAME: ogdy.dat DATE: 2-JUL-87

CORE DATA MEAN = 5.282 CORE DATA S.D. = 0.3266 SIZE = 102

TABLE OF OUTLIERS

NT	I	UNIQUE	IDENTIFIER	VALUE	SND	PROB
1	63	105I	091	3.070	-6.530	0.00000
2	78	105I	092	3.160	-6.254	0.00000
3	68	105I	090	3.340	-5.703	0.00000
4	67	105I	089	3.500	-5.213	0.00000
5	81	105I	111	6.830	4.984	0.00000
6	82	105I	112	6.890	5.168	0.00000
7	79	105I	107	7.250	6.270	0.00000
8	80	105I	108	7.700	7.648	0.00000

Table 2. Summary Statistics for the graphically trimmed background population. Note that 2 estimates of the standard deviation are provided. One from the Interquartile Range, and the other via hte usual computation of mean and variance.

```
SUMMARY STATISTICS FOR: k

TABLE OF EMPIRICAL PERCENTILES          NUMBER OF OBSERVATIONS =  182

MAXIMUM VALUE                  5.8100
99.9th PERCENTILE              5.8090
  99th PERCENTILE              5.7993
  98th PERCENTILE              5.7296
  95th PERCENTILE              5.6690
  90th PERCENTILE              5.5970
  80th PERCENTILE              5.4900
  75th PERCENTILE              5.4600
  70th PERCENTILE              5.4000
  60th PERCENTILE              5.3100
  50th PERCENTILE              5.2450
  40th PERCENTILE              5.1640
  30th PERCENTILE              5.0230
  25th PERCENTILE              4.9725
  20th PERCENTILE              4.9260
  10th PERCENTILE              4.7800
   5th PERCENTILE              4.6310
   2nd PERCENTILE              4.4420
   1st PERCENTILE              4.3806
MINIMUM VALUE                  4.3500

MEDIAN =   5.2450     I-Q RANGE =  0.48750     S.D. =  0.36138
MEAN   =   5.2024     VARIANCE  =  0.10664     S.D. =  0.32655     CV% =  6.3
```

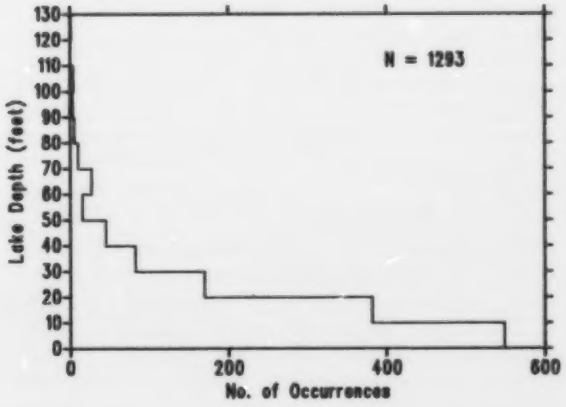

LOI (%)	Fe (%)	Mn (ppm)
11.00	3.500	3250.0
18.25	4.100	752.0
25.20	5.707	923.3
23.52	8.250	2195.0
23.50	3.095	713.1
18.77	4.000	2487.0
24.71	4.200	897.7
28.57	3.012	822.1
24.71	3.903	1232.1
25.70	3.549	694.7
29.05	2.752	457.3
39.59	1.907	341.0

Figure 3. Example of a histogram drawn by IDEAS and annotated with information for 3 auxilliary variables.

Univariate and bivariate statistics

A selection of statistical routines are available, including computations for.

1. Sumary statistics, e.g., range, mean, standard deviation, etc.,
2. Empirical percentiles,
3. Normality testing (3 tests),
4. Generalized power transformations (Box — Cox procedure),
5. One-way (two-level unbalanced) Analysis of Variance, both parametric and non-parametric Kruskal — Wallis procedures, for up to 9 groups, including homogeneity of variance tests (2),
6. Paired t-test,
7. Spearman rank correlation coefficients,
8. Pearson product-moment correlation coefficients, and
9. Simple linear regression.

The thrust of the univariate statistical and simple graphics modules is to facilitate graphical inspection and comparison of data in the spirit of what statisticians refer to as exploratory data analysis (EDA) (Turkey, 1977; Velleman and Hoaglin, 1981). Experience has shown that the trained or inquisitive eye studying graphical presentations is far more efficient at detecting patterns and outliers (anomalies) than statistical computations. Descriptive statistics will always have a place for the exploration geochemist and IDEAS generates those in common use. For confirmatory data analysis (CDA), or hypothesis testing, the normality tests and analysis of variance modules are provided.

In fact normality is less of a concern than many non-statisticians believe. Three normality tests are provided, the first two of which are commonly used in statistical studies;

they are the Shapiro — Wilk (Shapiro and Wilk, 1965), modified Anderson — Darling (Stephens, 1974) and Lin — Mudholkar tests (Nelson, 1983). However, it is not expected that the general user will or should make extensive use of these tests.

Analysis of variance (ANOVA) is useful dool for statistically determining if subset means are, or are not, significantly different (Anderson and McLean, 1974). In the context of this, the porperty of homogeneity of variance (homoscedasticity) is far more important than normality. Therefore two appropriate tests, the Bartlett (Anderson and McLean, 1974) and Levene (Levene, 1960) tests, are built right into the ANOVA module. The results of the ANOVA on the data subset means must be reviewed for credibility in tems of these homoscedasticity test results. In addition to the traditional ANOVA and computation of variance components (Table 3) a non-parametric (distribution-free) alternative, the Kruskal — Wallis test (Miller and Kahn, 1962), is undertaken. The ANOVA module also provides for the computation of subset means together with a multiple comparison following a procedure of Tukey's (Gill, 1978), Table 4. This is of assistance in identifying the actual subsets which have significantly different means from each other, as the ANOVA can only indicate that one or more means are significantly different from the remainder. Finally, in the case of a 2 group ANOVA with equal-sized samples a paired t-test may be undertaken if it is appropriate.

The paired t-test may be undertaken independently and is particularly appropriate if one wishes to determine if two procedures, perhaps concerning sample preparation and/or analysis, lead to similar or significantly different results when applied to a group of samples (Koch and Link, 1970). This procedure finds its most extensive use in IDEAS in studying the results of different analytical techniques applies to the same physical sample, e.g., gold determined by INAA versus gold by an acid leach and graphite furnace AAS procedure.

The inclusion of a module for determining optimal transformations to normality following the procedure of Box and Cox (Howarth and Earle, 1979) may not seem in the spirit of EDA. However, previous work has shown that use of this procedure on non-normal data after the user has removed any outliers or obvious members of other data populations can provide useful information. For instance, when an element is present dominantly in discrete mineral grains a Poisson distribution is likely; when a body of rock has undergone hydrothermal alteration a negative skew may develop; and where a process is time-dependent a reciprocal law may play an important role. The results of the optimal transform module can be effectively used to shed light on the term of the physical and chemical processes underlying the data distribution. In general the technique is used in this EDA mode rather than to determine the coefficients of the generalized power transform to fulfill the normality requirements of a CDA technique.

The provision of both Spearman and Pearson correlation coefficients permits the quantification of systematic monotonic non-linear pair-wise relationships as well as linear patterns. For this reason the Spearman coefficients are the default, as the presence of any systematic relationship is of interest, whether or not it is linear. Relationships can usually be linearized by an appropriate transformation if such is required. The Spearman coefficients are also more resistant to the effects of outliers, which can "lever" Pearson coefficients to unrealistically high values. In contrast, the Pearson coefficient is displayed in the x-y and bivariate regression plot modules, where various linearizing transforms would be inspected. The simple regression module is a natu-

Table 3. Example of an ANOVA table with the hypothesis test for equality of means and the computation of the variance components.

ONE-WAY ANOVA FOR VARIABLE: k

SOURCE OF VARIABILITY	SUM OF SQUARES	DEGREES OF FREEDOM	MEAN SQUARE	F-RATIO	SIGNIFICANCE
BETWEEN	2.299	2	1.149	3.12	0.9520 *
WITHIN	39.38	107	0.3680		
TOTAL	41.68	109	0.3823		

NS = NOT SIGNIFICANT, F < 0.95
* = F > 0.95 BUT < 0.99
** = F > 0.99 BUT < 0.999
*** = F > 0.999

SOURCE OF VARIABILITY	MEAN SQUARE	UNIT SIZE	VARIANCE COMPONENT	PERCENTAGE OF TOTAL	COEFFICIENTS	
BETWEEN	1.149	3	0.2798E-01	7.07	1.00	27.93
WITHIN	0.3680	110	0.3680	92.93	1.00	
TOTAL	0.3823		0.3960			

STD. ERROR OF THE MEAN = 0.1388

GRAND MEAN = 5.2835
APPROXIMATE (CONSERVATIVE) 95% CONFIDENCE LIMITS: 4.6485 5.7664
APPROXIMATE (RADICAL) 95% CONFIDENCE LIMITS: 4.9441 5.4628

Table 4. Example of the non-parametric Kruskal and Wallis statistic and the subset means display together with the matrix indicating significantly different means.

```
KRUSKAL & WALLIS NON-PARAMETRIC ANALYSIS OF VARIANCE

SUBSET    SIZE     SUM OF RANKS

alsk        6          223.5
grnt       36         2351.
grdr       68         3530.

KRUSKAL & WALLIS H STATISTIC =   6.1718
SIGNIFICANCE OF THE STATISTIC:   0.9543 *

DO YOU WISH TO DISPLAY THE SUBSET MEANS? y

SUBSET    SIZE       MEAN       STD. ERROR      95% CONFIDENCE BOUNDS

alsk        6       4.8783       0.2299         4.2873         5.4694
grnt       36       5.3942       0.1363         5.1177         5.6706
grdr       68       5.1312       0.5621E-01     5.0192         5.2432

TUKEY'S 95% CRITICAL DIFFERENCE =   0.44894

MATRIX OF SIGNIFICANT (95%) DIFFERENCES

   GROUP          1     2     3

3  grdr           -     -     *
2  grnt           *     *
1  alsk           *
```

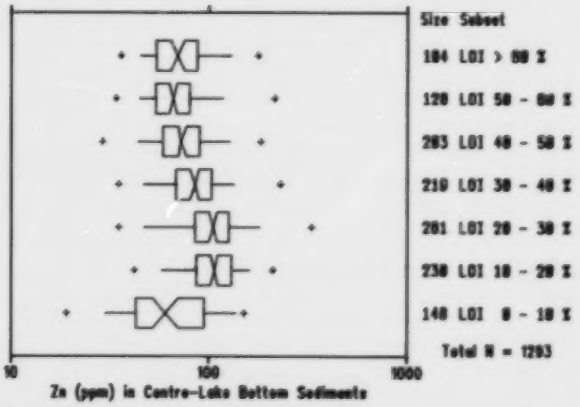

Figure 4. Example of a box and whisker plot drawn to illustrate the relationship between Loss-on-Ignition and Zn in centre-lake bottom sediments.

ral extension of the search for linearity. In addition to the regression coefficients a number of additional statistics are computed, hypothesis tests for the intercept being equal to zero and for the significance of the reduction in the sums of squares due to the regression are undertaken.

Multivariate statistics

Implementation of the multivariate statistical modules commenced in 1987. Currently there is an upper limit of 36 to the number of variables that can be processed in the multivariate procedures at any time. As with the limit on cases, i.e., 7 000, this was decided upon after discussions with the users; however, should more variables need to be processed simultaneously the required changes can be made quite easily.

To date one module is completed which undertakes a multivariate trimming (MVT) procedure employing the multivariate equivalent of a cumulative probability plot. The method is based on plotting the ranked Mahalanobis distances (c.f., univariate standard normal deviates) against Chi-square (Fig. 7), with degrees of freedom equal to the number of variables (Gnanadesikan, 1977). Initially after a summary statistics display (Table 5) a number of trial inspection plots, where arbitrary fractions of the most extreme data are temporarily trimmed and the Mahalanobis distances for all cases recomputed, are displayed (Fig. 8) in order to gain an insight on the data structure and an idea of how many gross outliers may exist (Garrett et al., 1982). Once a satisfactory starting plot is selected the extreme members, outliers, are graphically trimmed with the cursor and their "unique character identifiers" displayed. The univariate summary statistics and the correlation matrix for the trimmed data set are then presented with a new Chi-square plot. Trimming continues iteratively until the plot appears linear with a homogeneous distribution of points (Fig. 9). Finally, a list of all the trimmed outliers (Table 6) may be displayed, together with the summary statistics of the remaining "core" data (Table 7). As with the univariate probability plots the outliers and "core" data groups may be selectively saved as subsets for future display or processing. In the geochemical context, the "core" represents a multivariate background population, and the outliers are prime candidates for detailed interpretation in terms of mineral occurrences or other features of interest. The procedure is useful in determining the extreme members of a multivariate data set. By treating all variables simultaneously the "multiple jeopardy" problem is avoided, where accumulating the top few percent of each variable separately for detailed inspection usually leads to a disproportionately large list of candidates for further study. The MVT procedure is also a useful precursor to other multivariate techniques

where outliers could seriously distort the analysis, or non-multivariate-normality would contradict the assumptions of the techniques to be used. As such it is an effective exploratory data analysis tool in the multivariate domain.

PROVISIONS FOR HARDCOPY

A major feature of IDEAS is that through the use of GKS the graphical output may be edited, i.e., titles and labels changed, and additional annotative text added. A Tektr[illegible] multi-pen plotter allows camera-ready publication quality black line diagrams to be prepared directly during an IDEAS session, as has been done for this report. Currently the various colours on the video display are mapped to different pen widths. It was the need for publication quality black line diagrams that led to the decision to limit a number of the graphic displays to 9 data subsets or concentration levels as 10 unique marker types are available under GKS, and one is not suitable as a plot symbol. Alternately, the colour display on the screen may be dumped to an ink-jet plotter; this output is suitable for inspection and interpretation, or may be used in poster presentations.

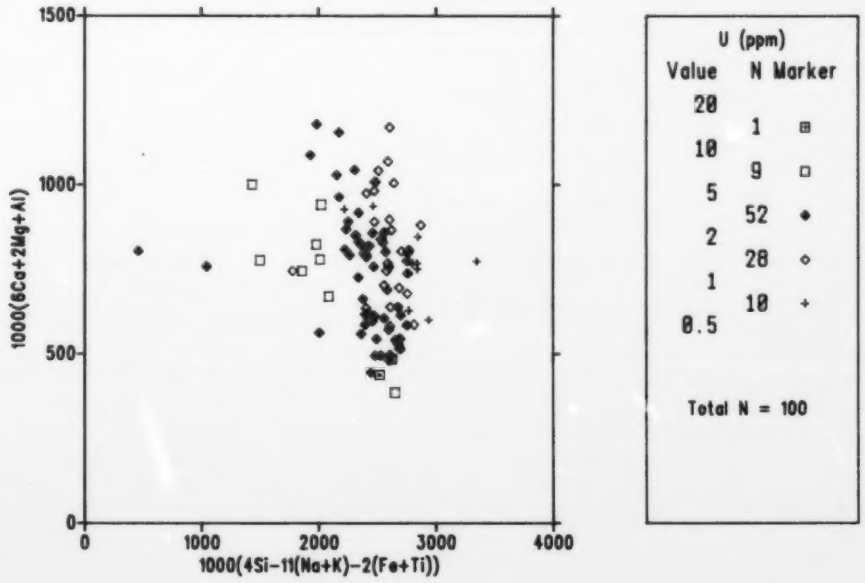

Figure 5. Example of an x-y plot coded by the value of an auxilliary variable.

Table 5. Initial Summary Statistics display of the multivariate data.

```
 5. ca
 6. na
 7. k
 8. ti
 9. mn
10. ba
11.

DATA SET NAME: ogdy.dat                                    DATE:  6-JUL-87

                    MULTIVARIATE OUTLIER INVESTIGATION

          ITERATION: 0     POPULATION SIZE = 110     TRIM % = 0.0

   VARIABLE              MEAN          VARIANCE        STD.DEV          CV %

   1 si                 30.74             3.627          1.904          6.20
   2 al                 8.119            0.2550         0.5050          6.22
   3 fe                 2.869            0.6144         0.7839         27.32
   4 mg                 1.356            0.3174         0.5634         41.56
   5 ca                 2.887            0.6886         0.7801         27.02
   6 na                 1.687         0.3134E-01         0.1770         10.50
   7 k                  5.283            0.3823         0.6183         11.88
   8 ti                 3540.         0.8979E+06          947.6         26.76
   9 mn                 645.0         0.2873E+05          169.5         26.28
  10 ba                 984.2         0.8317E+05          288.4         29.30
```

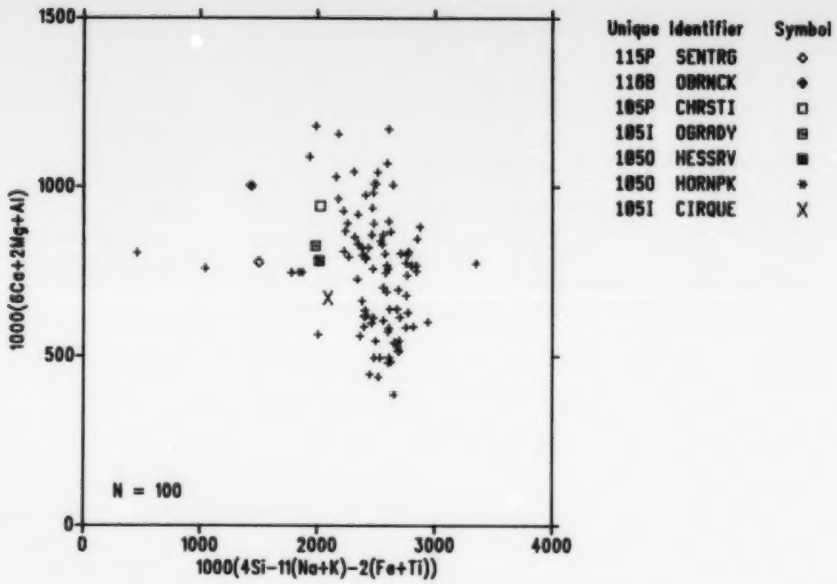

Figure 6. Example of an x-y plot labelled with the unique character identifiers via changes in plot symbology.

FUTURE DEVELOPMENTS

Future graphical developments call for the implementation of a "zoom-in" feature on the x-y plot and map displays (3-5, 10-12). The user will be prompted for the lower-left and upper-right corners of the area to be redisplayed. After determining graphically acceptable plot limits the area will be redisplayed with all appropriate title, axis labelling and legend information.

Two additional database related modules are planned. The first permits the logical combination of pre-existing subsets through the use of Boolean operators. The second permits variables to be conditionally recoded, this facility is particularly useful when working with multiple geochemical thresholds dependent on categorical field data, e.g., lithology.

In the realm of simple statistical procedures, a 2-dimensional contingency table module will be added to IDEAS. This tool it particularly useful for studying categorical and coded data, e.g., field data.

It is planned to prepare a number of additional multivariate graphical and statistical modules for inclusion in IDEAS. These include a canonical variable module, 2 cluster analysis procedures (one graphical and the other statistical), a principal component (factor) analysis module, a multilinear regression package, a logistic discriminant module, and finally, an empirical classification procedure which will include the ability to undertake multivariate analysis of variance.

In November, 1987 the Geological Survey of Canada upgraded its DEC VAX 11/780 to a VAX 8700. Both machines run the VMS Operating System and no conversion problems were encountered. Perhaps of greater interest are the possibilities for migrating the IDEAS software to smaller computers so as to provide a stand-alone or networked workstation. DEC offers its MicroVAX family of super-microcomputers, i.e., the II and 2000 machines. However, whereas this solution is appropriate in a regional or small office where several people or projects can share the cost of the computing resources, it tends to be too costly for a single user workstation. The obvious advantage of the above solution is the availability of VAX Fortran and the VMS operating system for the MicroVAXes. An alternative would be to use one of the new 32 bit super-microcomputers using the Intel 80386 or Motorola 68020 microprocessors. If this was done the

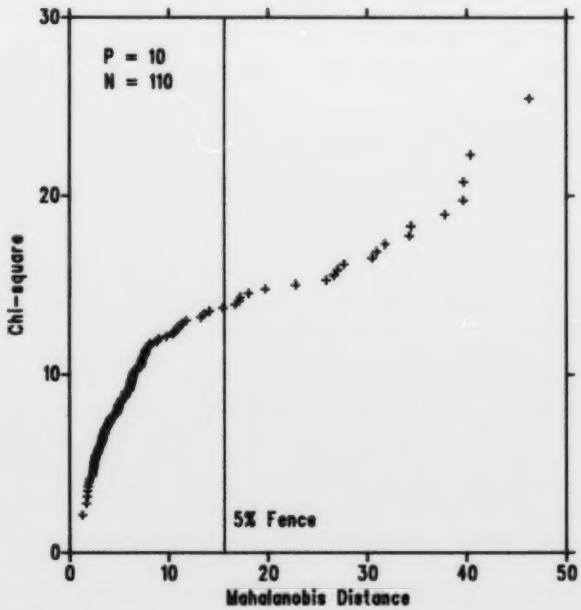

Figure 7. Example of a Chi-square (multivariate probability) plot. The fence corresponds to a some-outside rate of 5%. In this example 20 points lie above the fence, 14 in excess of the expected 6, which is indicative that some true outliers exist.

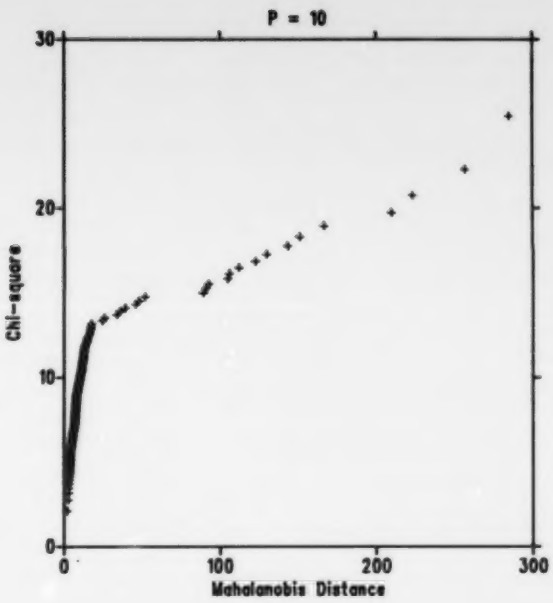

MVT % entered = 15.0

Cases trimmed = 17

Actual trim % = 15.5

Unique Identifier		D-sq
105I	100	105.8
105I	044	104.6
105I	015	92.4
105I	016	90.8
105I	112	89.0
105I	060	52.8
105I	114	48.0

Figure 8. Example of a multrivariate trim robust start trial. Note the unique character identifiers of the most extreme members of the data set displayed by the plot.

Table 6. List of multivariately trimmed outliers. Note that the Mahalanobis distances (D-SQ) are with respect to the final kernel subset means and covariances (correlations). The H (I) column is a measure of leverage which can be computed from the Mahalanobis distance (Velleman and Welsch, 1981) and indicates the extent to which that outlier would perturb a linear model. The probability (DPROB) is the Chi-square based estimate of group membership in the kernel subset, in the example all the probabilities are less than 0.0005%.

DATA SET NAME: ogdy.dat DATE: 8-JUL-87

TABLE OF OUTLIERS

CRITICAL PROBABILITY FOR TRIMMING = 0.0007

NT	I	UNIQUE IDENTIFIER		D-SQ	H(I)	DPROB
1	80	105I	100	543.7	4.998	0.00000
2	68	105I	090	502.6	4.620	0.00000
3	70	105I	092	446.3	4.104	0.00000
4	79	105I	107	442.2	4.066	0.00000
5	21	105I	037	332.1	3.056	0.00000
6	22	105I	038	315.8	2.907	0.00000
7	69	105I	091	275.7	2.538	0.00000
8	67	105I	089	253.6	2.336	0.00000
9	81	105I	111	251.3	2.314	0.00000
10	74	105I	100	213.0	1.963	0.00000
11	1	105I	015	209.7	1.933	0.00000
12	2	105I	016	199.1	1.836	0.00000
13	40	105I	060	153.7	1.420	0.00000
14	24	105I	044	151.5	1.399	0.00000
15	39	105I	059	132.0	1.220	0.00000
16	82	105I	112	131.0	1.211	0.00000
17	8	105I	022	117.0	1.082	0.00000
18	42	105I	062	107.0	0.9910	0.00000
19	106	105I	138	88.37	0.7464	0.00000
20	73	105I	099	77.45	0.7196	0.00000

Table 7. Summary Statistics for the graphically trimmed multivariate kernel subset. Note the marked reduction, by in excess of 50% in some cases, in the coefficients of variation (cv%) due dominantly to decreases in the standard deviations with the removal of outliers.

```
MOVE CURSOR TO NOTE STARTING POSITION AND PRESS A (PUCK) KEY
IS THE NOTE AND ITS POSITION CORRECT?

HAVE YOU FINISHED ADDING NOTES?


ENTER A <CR> TO CLEAR THE SCREEN AND CONTINUE


DATA SET NAME: ogdy.dat                                    DATE:  8-JUL-87

                    MULTIVARIATE OUTLIER INVESTIGATION

          ITERATION: 4     POPULATION SIZE = 80     TRIM % = 27.3

 VARIABLE          MEAN          VARIANCE        STD.DEV          CV %

 1 si             30.58            1.368          1.169          3.82
 2 al             8.150           0.1617         0.4021          4.93
 3 fe             2.976           0.1786         0.4227         14.20
 4 mg             1.359           0.1446         0.3803         27.99
 5 ca             2.979           0.1898         0.4356         14.62
 6 na             1.654       0.6437E-02     0.8023E-01          4.85
 7 k              5.253       0.6425E-01         0.2535          4.83
 8 ti             3632.        0.2220E+06          471.2         12.97
 9 mn             678.8             6267.          79.16         11.66
10 ba             1030.        0.2433E+05          156.0         15.15
```

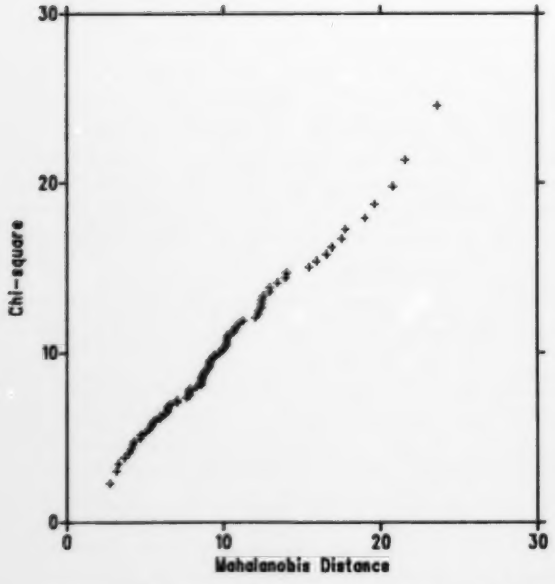

Figure 9. Example of a chi-square plot for a multivariately trimmed data set.

move to a UNIX, or UNIX-like, operating system might be made. Although such a move involves more effort it increases software portability and machine/vendor independence, which was one reason GKS was selected as the graphics software package.

Current plans call for the continued development of IDEAS until it contains all the features identified in the functional specification, and those others required by the Subdivision at this time. In parallel, a number of other software packages are being, or will be, evaluated or developed in the Subdivision. IDEAS will be integrated with these to provide a unified computing environment. Following a period, probably of one year, of extensive testing the final version of IDEAS will be released to the geoscience community. Several procedures for such a release are available, the two extremes being simple open-filing at a nominal cost, or release, possibly on a widely available microcomputer family, by a software house.

DISCUSSION

IDEAS is meeting the majority of the Geological Survey of Canada's exploration geochemist's needs, and those of other geoscientists with spatially distributed point data who are interested in detecting outliers (anomalies) and identifying and interpreting the underlying patterns of statistical and spatial variation in their data. IDEAS is considered to be an evolving system, the underlying structure facilitates the addition of further modules. As user experience grows, modifications and new features are being suggested and being integrated into the system as appropriate.

At this time the major use of IDEAS has been with regional geochemical and detailed study data derived from Federal — Provincial Mineral Development Agreement (MDA) funded surveys. Usage is now being extended to support other Geological Survey geochemical R & D projects and overseas CIDA surveys. To this end an additional Tektronix terminal, digitizing tablet and ink-jet plotter have been purchased so that "production" and "development" can continue without mutual interference.

To date user response has been fabourable, and the creation of IDEAS databases has been facilitated with the implementation of a software package that automatically generates an IDEAS data definition file from the Geochemical Information Services System (GISS) file description stored archivally with the data for all Subdivision surveys on the Departmental CDC Cyber facilities. Other users are compiling their databases on MS-DOS based microcomputers in their offices employing commercial software packages such as dBASE III and Rbase System V and then using the public domain data communications package KERMIT to transfer their data to the Geological Survey VAX for IDEAS use.

ACKNOWLEDGMENTS

A large group of people have been involved with the IDEAS project since its inception in 1979. During the Hickling — Smith Unsolicited Proposal (1980-81) T.I. Goss, G. Jackson and J. Nash all played important roles in preparing the functional specification. The U.S. Geological Survey made the VAX version of GRASP available and permitted R.W. Bowen to install it and provide valuable assistance in system familiarization in 1984. Between 1985 and 1987 a series of University of Waterloo Co-op program students worked on various aspects of IDEAS. C.E. Lee, M.S. Pearson, C.D. Lichtenfeld, F. Khalily Araghy and W.A. Quesnel all made significant contributions to the developments of IDEAS. Lastly, thanks are due to D.J. Ellwood of the GSC for his assistance and advice on many matters since the inception of the project. The role of management in the success of this long term project must be acknowledged. Progressing from a concept to a usable system has been a lengthy process, without their continued support over the years the project would have been stillborn.

REFERENCES

Anderson, V.L. and McLean, R.A.
1974: Design of Experiments — A realistic approach; Marcel Dekker, New York, 418 p.

Bowen, R.W. and Botbol, J.M.
1975: The Geological Retrieval and Synopsis Program (GRASP): U.S. Geological Survey, Professional Paper 966, 87 p.

de la Roche, H., Leterrier, J., Grandclaude, P., and Marchal, M.
1980: A classification of volcanic and plutonic rocks using r_1r_2-diagram and major element analyses; its relationships with current nomenclature; Chemical Geology, v. 29 (3-4), p. 183-210.

Enderle, G., Kansy, K., and Pfatt, G.
1984: Computer Graphics Programming: GKS — The Graphics Standard; Springer Verlag, New York, 542 p.

Garrett, R.G., Goss, T.I., and Poirier, P.R.
1982: Multivariate outlier detection — an application to robust regression in the earth sciences; Joint Statistical Meetings of the American Statistical Association, Cincinnati, Ohio, 1982. Abstracts, p. 101.

Gill, J.L.
1978: Design and Analysis of Experiments in the Animal and Medical Sciences; Iowa State University, Press, Ames, v. 1, 409 p.

Gnanadesikan, R.
1977: Methods for Statistical Data Analysis of Multivariate Observations; John Wiley, New York, 311 p.

Hoaglin, D.C., Inglewicz, B., and Tukey, J.W.
1986: Performance of some resistant rules for outlier labelling; American Statistical Association, Journal, v. 81, no. 396, p. 991-999.

Howarth, R.J. and Earle, S.A.M.
1979: Application of a generalized power transformation to geochemical data; Methematical Geology, v. 11 (1), p. 45-62.

Koch, G.S. and Link, R.F.
1970: Statistical Analysis of Geological Data; John Wiley, New York, v. 1, 375 p.

Levene, H.
1960: Robust tests for equality of variances; *in* Contributions to Probability and Statistics, ed. I. Olkin; Stanford University Press, Palo Alto, California, p. 278-292.

Miller, R.L. and Kahn, J.S.
1962: Statistical Analysis in the Geological Sciences; John Wiley, New York, 483 p.

Nelson, B.B.
1983: Testing for normality; Journal of Quality Technology, v. 15 (3), p. 141-143.

Shapiro, W.W. and Wilk, M.B.
1965: An analysis-of variance test for normality (complete samples); Biometrika, v. 52 (3-4), p. 591-611.

Stephens, M.A.
1974: EDF statistics for goodness of fit and some comparisons; American Statistical Association, Journal, v. 69, no. 347, p. 730-737.

Tukey, J.W.
1977: Exploratory Data Analysis; Addison — Wesley, Reading, Massachusetts, 688 p.

Velleman, P.F. and Hoaglin, D.C.
1981: Applications, Basics and Computing of Exploratory Data Analysis; Duxbury Press, Boston, Massachusetts, 354 p.

Velleman, P.F. and Welsch, R.E.
1981: Efficient computing of regression diagnostics; American Statistican, v. 35 (4), p. 234-242.

The Geological Survey of Canada absolute gravity program: applications in geodesy and geodynamics

A. Lambert, J.O. Liard, P.N. Courtier, A.K. Goodacre, and R.K. McConnell
Geophysics Division

Lambert, A., Liard, J.O., Courtier, P.N., Goodacre, A.K., and McConnell, R.K., The Geological Survey of Canada absolute gravity program: applications in geodesy and geodynamics; in Current Research, Part F, Geological Survey of Canada, Paper 88-1F, p. 15-16, 1988.

Abstract

A transportable absolute gravimeter recently acquired by the Geological Survey of Canada has an accuracy estimated to be better than 20 microgals (200 nms^{-2}) and a precision of better than 5 microgals. By measurements at selected stations in the Canadian Gravity Standardization Net the instrument will provide a country-wide datum accuracy of about 25 microgals. This accuracy satisfies one of the requirements for achieving a geoid accurate to 10 cm over Canada. Regular annual measurements at 8 to 10 stations in eastern Canada using the instrument in a differential mode would allow the testing of theoretical models of Laurentide post-glacial rebound within 5 to 10 years. The instrument should also provide the datum control now lacking in existing independent high-precision gravity networks for the study of earthquake processes.

Résumé

Un gravimètre absolu transportable acquis récemment par la Division de la géophysique a une justesse estimée supérieure à 20 microgals (200 nms^{-2}) et une précision supérieure à 5 microgals. Par les mesures faites à des stations choisies dans le réseau canadien de normalisation de la gravité, l'instrument fournira des données à l'échelle du pays d'une justesse d'environ 25 microgals. Cette justesse répond à une des conditions pour établir un géoïde à 10 cm près sur le Canada. Des mesures régulières annuelles à 8 à 10 stations dans l'est du Canada en utilisant l'instrument dans un mode différentiel permettront d'évaluer les modèles théoriques du rebondissement isostatique postglaciaire des Laurentides dans 5 à 10 ans. L'instrument devrait aussi permettre le contrôle des données qui manque actuellement avec les réseaux gravimétriques très précis existants et indépendants pour l'étude des processus des tremblements de terre.

The Geophysics Division of the Geological Survey of Canada recently acquired a transportable absolute gravimeter (JILA-2) developed by the Joint Institute for Laboratory Astrophysics (JILA), University of Colorado (Fig. 1). The instrument was designed to be easily transported and operated under non-laboratory conditions. The time and length standards for the calculation of the acceleration of a freely falling prism are provided by a rubidium oscillator and a frequency-stabilized He-Ne laser. Other features of the apparatus are a servo-controlled dra-free chamber which follows the falling prism and an isolation device called a super spring that isolates a reference prism from ground vibrations. Laboratory testing in Ottawa and measurements in Boulder, Calgary and Winnipeg have been carried out in order to identify sources of systematic error and to develop field procedures. In collaboration with J. Faller and colleagues at JILA a number of changes have been made to the JILA-2 apparatus since its delivery, including improvements in the acquisition and maintenance of the dropping chamber vacuum, calibration of the laser wave-length standard, reduction in vibration of the dropping chamber during operation, more stable illumination of the fringe detector and reduction of scaler-counter noise level. At the present stage of development the accuracy of the Canadian apparatus is estimated to be better than 20 microgals (200 nms^{-2}). Tests indicate that the apparatus has a precision of better than 5 microgals.

An important application of regional gravity data is the computation of geoidal undulations. Reduction of erors in geoidal undulations over Canada to the 10 cm level will require the use of an improved global gravity model, improvement in regional gravity coverage, reduction of height and terrain correction errors and adequate control of gravity datum and scale. All regional gravity measurements in Canada are referred to the Canadian Gravity Standardization Net (CGSN) whose datum and scale are controlled at present by stations of the International Gravity Standardization Net 1971 (IGSN71). The lack of absolute control of IGSN71 at high latitudes could result in datum errors as large as hundreds of microgals in the Canadian high Arctic. Computational methods combining terrestrial gravity data with satellite gravity models require that systematic errors in regional gravity date be less than about 300 microgals in order to achieve a geoidal accuracy of 10 cm. Absolute gravity measurements with an accuracy of 20 microgals at nine stations of ghe CGSN would ensure a country-wide datum accuracy of about 25 microgals which is more than adequate for the geoidal accuracies presently sought.

Another important application of absolute gravimetry in Canada is the monitoring of temporal changes in gravity associated with various dynamic processes. Taking advantage of the high precision of the Canadian absolute apparatus (JILA-2) we propose to test Laurentide post-glacial rebound models by differential gravimetry. It can be shown that regular absolute gravity measurements with a precision of 5 microgals at 8 to 10 stations in Eastern Canada would allow the testing of theoretical models within 5 to 10 years, assuming a present range of gravity-change rates of 2.2 microgals/yr. To monitor these same stations through a network established using spring-balance gravimeters would be more

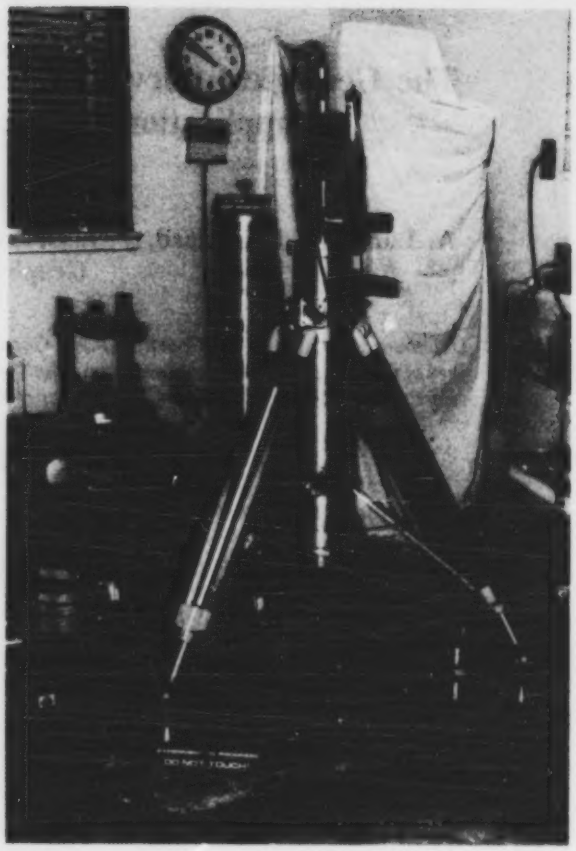

Figure 1. The GSC absolute gravimeter in operation at a laboratory of there Geophysics Division.

expensive and less precise. Assuming a present range of uplift rates of 1.2 cm/yr in Canada, relative vertical displacements associates with the post-glacial rebound would be detected with the same confidence and in the same period of time by annual VLBI/GPS measurements provided a vertical precision of better than 3 cm is achievable. Monthly mean sea level observations which have a precision of about 8 cm in Hudson Bay are equally sensitive but are restricted geographically and require continuous operation.

High-precision local gravity networks, established over the last decade on Vancouver Island and at Charlevoix, Quebec for the study of earthquake processes, generally have an internal accuracy of about 3 microgals with respect to the network means. However, the network means themselves are poorly defined as a result of the difficulty and expense of carrying out external ties. Network simulation studies show that absolute measurements with a precision of 3 microgals at two points in each network in conjunction with measurements at the Canadian Absolute Gravity Station (CAGS) in Ottawa would provide datum control compatible with the internal precision of these special networks.

Shaded contour map generation on IBM-compatible microcomputers

J.R. Bélanger
Terrain Sciences Division

Bélanger, J.R., Shaded contour map generation on IBM-compatible microcomputers; in Current Research, Part F, Geological Survey of Canada, Paper 88-1F, p. 17-20, 1988.

Abstract

A software system has been developed to produce contour maps with the use of a microcomputer. The program does not require a graphics card ans uses a dot-matrix printer to reproduce the desired maps. The software system is divided into two modules: the first interpolates dots on a regular grid from irregular checkpoints; the second produces the contour map using halftones. Each of these modules can be used separately, thus allowing the user to replace the modules with his own software or to prepare several contour maps using the interpolated values simply by varying the specifications.

Résumé

Un logiciel a été mis au point pour produire des cartes en courbes de niveau (cartes isarithmiques) sur micro-ordinateur. Le programme ne nécessite aucune carte graphique et reproduit les cartes voulues sur imprimante matricielle. Le logiciel est divisé en deux modules: interpolation des points d'une grille à quadrillage régulier à partir de points de contrôle irréguliers et la production de la carte en courbes de niveau à l'aide de demi-teintes. Chacun des modules peut être utilisé indépendamment permettant à l'utilisateur de remplacer les modules par son propre logiciel ou de produire plusieurs cartes en courbes de niveau à partir des valeurs interpolées en variant les spécifications.

INTRODUCTION

A computer program was developed to produce shaded contour maps (isarithmic maps) on a microcomputer. The program, written in FORTRAN 77 requires no graphic card and produces contour map on dot matrix printers (Epson, IBM Proprinter and compatibles).

The program named SHADEMAP is divided into two independent modules: interpolation of regularly spaced grid points from irregularly distributed control points and contouring of the grid values. Either part of the program can be used independently so the user can supply his own interpolated values, bypassing the interpolation module, or use a different contouring program to plot the gridded (interpolated) values (see Fig. 1).

The program is designed to be used interactively and the instructions were kept to a minimum to facilitate its use. A source listing is provided so the user can modify the program to meet his own requirements.

The program is not copyrighted but cannot be resold. Any modification to improve the efficiency or flexibility of the program is encouraged and a report on any significant modifications would be appreciated.

INTERPOLATION

The interpolation program generates a regular grid of interpolated values from irregularly spaced data points. Each grid point is interpolated from the surrounding data points (between 5 and 10 depending on the distribution of the data) based on the distance of the grid point to the data points, and on a shadow zone projected by closer data points on the data points located farther away. The program uses the inverse square of the distance between a grid point and a data point, the reason for using the inverse "square" of the distance rather than using higher exponent or linear distance is based on the following observations: when using higher exponents (such as inverse cube distance) the interpolation generates relatively flat surfaces with sharp gradients over a small interval "between" control points; when inverse linear distance is used, the surface between points tend to be flat with steep gradients "at" the control points. When using the inverse square distance the gradient between control points tends to be more gradual. To overcome the problem caused by clustered control points located in the vicinity of the grid, a shadow zone is created behind each data point from the grid point. The influence of a data point that falls in the shadow zone of another point is reduced based on the cosine of angle (Fig. 2). The screening effect is essential in this algorithm since no slope factor is taken into consideration.

The program stores the interpolated points in a file called "OUTDAT" which serves as input to the contouring program so the data can be contoured several times using different specifications.

Specifications

(The numbers refer to prompts generated by the program as given in Fig. 3). The specifications are used to produce the example in Figure 4.

1. If the response is "yes" the program initiates the interpolation program otherwise the program jumps to the contouring section.

2. The limits of the maps are given in Cartesian co-ordinate system. The values can be in any units (centimetre, metres, inches or any user defined units).

3. The program will generate a grid of interpolated values according to the following specifications: 1 = 400 grid points, 2 = 900, 3 = 1600, 4 = 2500, 5 = 3600, 6 = 4900 . The number of grid points in the X and Y directions will be proportionate to the dimensions of the map.

4. Format of the X, Y and Z values supplied on file "INDAT" used by the interpolation program. The options are:

— FORTRAN format: the XYZ values must be specified as real numbers (e.g. Fformat) even if the actual data are integer numbers (i.e. have no decimal points) ex: 2x, F5.0, 7x, F6.0, 17x, F4.1

— Unformatted: the data supplied on the "INDAT" file is unformatted

— List directed: the values on file "INDAT" conforms to list directed input, i.e. the 3 values are separated either by blanks or comma with optional decimal points.

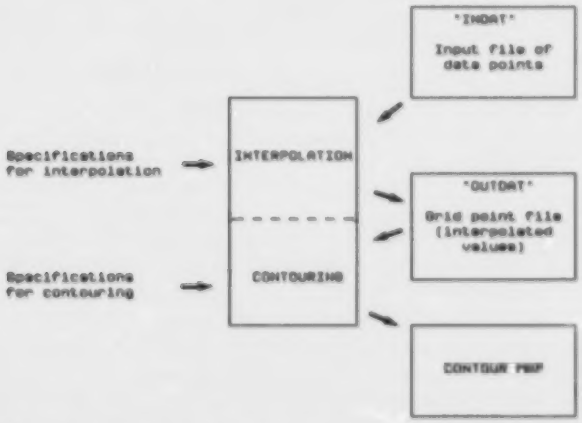

Figure 1. Flow chart showing the structure of the computer program

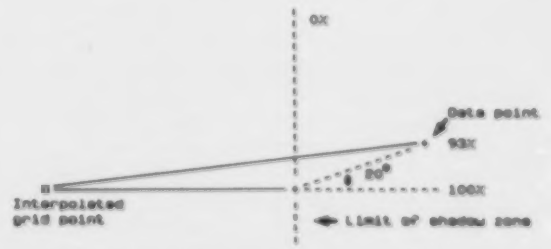

Figure 2. Example of shadow zone created by data points located close to an interpolated grid point

5. This option permits the user to place the X, Y and Z values in any order in the record. The first value is the position of the X co-ordinate, the second value the position of the Y co-ordinate, and the third value is the position of the Z value; e.g. 2, 3, 1 means that the X co-ordinate is the second number in the record the Y co-ordinate is the third number in the format and the Z value is the first number in the record.

6 & 7 When reading the data the program will ignore (consider as invalid) the values specified as null.

8. This message tells the user that the program is reading the input data on the file called "INDAT" which should be on the default drive and directory.
— Stop reading data at count 1000. This message appears if there are more than 1000 points in the input files. This value is based on array dimensions and can be increased if required.

9. Number of data points read on file "INDAT" located inside the limits specified previously in prompt 2. If no data are found inside the map limits, the program stops.

10. The data points are sorted before the interpolation in order to speed up the search for control points. This is a comment sent by the program to report on the status of the processing.

11. Overlying control points are grouped and their Z values are averaged.

12. The program can print the X, Y and Z values supplied in the input file as shown on the example (Fig. 3).

13. The program informs the user on the number of grid cells that will be interpolated in the X and Y directions.

14. The program keeps the user informed on the status of the interpolation since a very fine grid can take several minutes to be interpolated.

15. Minimum and maximum interpolated values, which might be slightly different than the original data point values as the grid locations will not necessarily fall exactly at the same location as the data points.

CONTOURING

The contouring program, which can be used independently from the interpolation program, produces shaded contour maps from a grid of regularly spaced points. The grid values are read from a binary file (unformatted) named OUTDAT, which contains three sets of records.

— The first record contains: the limits of the map (X-Y minimum and maximum) as specified by the user during the interpolation program. The number of grid points in the X and Y directions. The number of data points supplied by the user for interpolation.

```
1 DO YOU WANT TO CALL THE INTERPOLATION PROGRAM?...
  Y

2 BORDERS: X-MIN,X-MAX,Y-MIN,Y-MAX...
  1.30,1.20

3 INTERPOLATED GRID POINTS: 1=COARSE....6=VERY FINE...
  3
4 FORMAT OF INPUT DATA VALID FORMATS ARE: FORTRAN FORMAT
                                          UNFORMATTED
                                          L=LIST DIRECTED
  L

5 POSITION OF X-Y-Z VALUES IN FORMAT...
  1,2,3

6 NULL VALUES IGNORED?...
  Y

7 VALUE CONSIDERED AS NULL...
  0.

8 READING DATA

9 NO OF DATA READ...   81

10 SORTING THE DATA

11 NUMBER OF INPUT POINTS AFTER GROUPING:  . 81

12 DO YOU WANT  A LISTING OF DATA POINTS?...
  Y
          X-Y-Z:      2.00      11.80      1.20
          X-Y-Z:      3.00       4.00      2.60
          X-Y-Z:      5.00      17.80      2.00
          X-Y-Z:      5.80       8.50      2.50
          X-Y-Z:      6.00      15.20      3.50
          X-Y-Z:      6.00      12.10      3.60
          X-Y-Z:      9.50      12.10      4.20
          X-Y-Z:     10.00       7.70      4.80
          X-Y-Z:     11.00      10.80      4.90
          X-Y-Z:     12.00      14.00      1.60
          X-Y-Z:     13.00      13.50      4.10
          X-Y-Z:     14.00       4.80      4.50
          X-Y-Z:     15.40      10.30      3.70
          X-Y-Z:     15.60       1.50      2.30
          X-Y-Z:     18.70      19.00      2.80
          X-Y-Z:     21.30       4.30      2.50
          X-Y-Z:     23.00       5.80      3.30
          X-Y-Z:     25.50       4.90      4.10
          X-Y-Z:     25.60       2.70      4.80
          X-Y-Z:     25.80       2.30      3.70
          X-Y-Z:     26.00      10.50      2.10

13 NUMBER OF GRID POINTS IN X-DIRECTION=   48
                    IN Y-DIRECTION=   31

14 100.0 % OF GRID INTERPOLATED

15 MIN. AND MAX. INTERPOLATED VALUE...      1.2       6.9

16  DO YOU WANT TO CONTOUR THE DATA?...
  Y

17 DO YOU WANT A HISTOGRAM ?...
  Y

18 HOW MANY COLUMNS IN HISTOGRAM (MAX.: 25)...?
  10

    ******* HISTOGRAM OF  INTERPOLATED POINTS *******

          .00       .69-
          .69      1.38-
         1.38      2.06-**
         2.06      2.75-************************
         2.75      3.44-****************************************
         3.44      4.13-*******************************
         4.13      4.82-********************
         4.82      5.50-*************
         5.50      6.19-*************
         6.19      6.88-**********

19 DIVIDE DATA INTO HOW MANY CLASSES (MAX. 10)...?
  5

20 SPECIFY SHADE INTENSITY (1=WHITE, ... 10=BLACK) AND UPPER LIMIT OF EACH CLASS

21 INTENSITY, LIMIT OF CLASS- 1 ...
  1,3

  INTENSITY, LIMIT OF CLASS- 2 ...
  2,4

  INTENSITY, LIMIT OF CLASS- 3 ...
  4,5

  INTENSITY, LIMIT OF CLASS- 4 ...
  6,6

  INTENSITY, LIMIT OF CLASS- 5 ...
  10,7

22 WIDTH (IN CM) OF OUTPUT MAP...
  15

23 POST THE DATA POINTS?...
  Y

24  TITLE...
  Test Map

25  JUSTIFIED: LEFT(L), RIGHT(R) OR CENTERED(C)...
  C

26  SUBTITLE...
  Interpolation : 3

27  DO YOU WANT A LEGEND?...
  Y
```

Figure 3. Prompts and specifications to the interpolation and contouring program. Numbers 1 to 15 refer to the interpolation whereas numbers 16 to 27 are used to produce the contour map

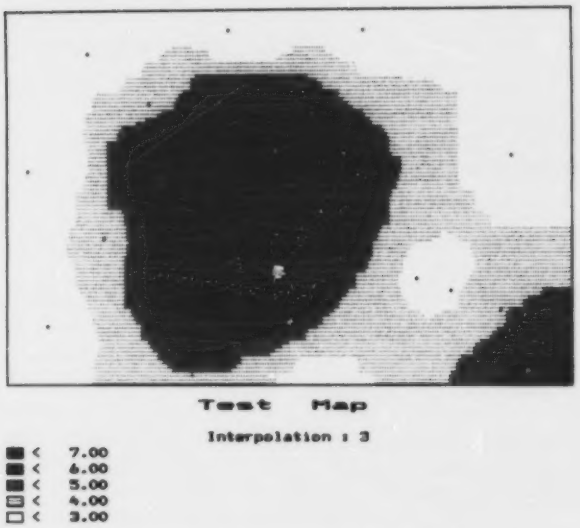

Figure 4. Example of contour map produced by the program

— A second set of records contain the X, Y and Z values of the data points.

— The third set of records contains the grid point values.

Specifications

16. If the answer is "YES" the program proceeds with the contouring phase otherwise it will stop and the grid file "OUTDAT" is saved.

17. To help the user to specify the class intervals, the program can display a histogram of the interpolated data distribution on the console.

18. The histogram will be displayed using the number of columns (or bars) specified by the user (up to a maximum of 25 columns). The range of the histogram will correspond to the minimum and maximum grid values.

19. The program permits a maximum of ten classes: the ten different grey levels are obtained by dithering a 3 x 3 matrix.

20 & 21. Only the upper limit of each class must be specified, the lower limit of the first class will correspond to the lowest interpolated value.

22. The width (X dimension of the plot) of the map cannot exceed 20 cm (unless the program is modified for a larger carriage size). The height (Y-dimension) will be calculated by the program and has no maximum limit.

23. A "+" will be posted at the location of the data points. The symbol might be difficult to identify in areas filled with grey levels 6-7-8 due to its similarity to the dot pattern used for these classes.

24 & 25. The title can be from 0 to 40 characters long. It can be centred, right or left justified.

26. The subtitle can be from 0 to 40 characters long and will be written below the title.

27. The legend gives the correspondence between each class and shade (or dot pattern) on the map.

The map in Figure 4 was reproduced on a IPM-PC AT, with a clock speed of 8 MHz, using grid size options of 1, 3 and 4 (giving grid sizes of 360, 1488 and 3387) and 21 control points. The interpolation took 21 seconds, 90 seconds and 210 seconds respectively, which shows a linear relationship between the number of grid points and seconds used for the interpolation (approximately 16.5 points per second). Other tests using 280 control points showed an increase in the interpolation time to 13 points per second.

The time required for contouring the map is directly proportional to the size of the output map and depends on the type of printer used, as the actual processing for the example in Figure 4 took 20 seconds and the printing took 3 minutes.

The program source code will be available as a GSC Open File on a diskette. The Open File version will include options to allow the use of wide carriage printer and to mask areas of the map (i.e. to delete the shading, such as in lakes); these options are being implemented by F.M. Nixon of the Geological Survey of Canada.

Uranium resource investigations in Canada, 1987

V. Ruzicka
Mineral Resources Division

Ruzicka, V., Uranium resource investigations in Canada, 1987; in Current Research, Part F, Geological Survey of Canada, Paper 88-1F, p. 21-30, 1988.

Abstract

Investigations on the Eagle Point deposit, Saskatchewan, indicate that it formed polygenetically from solutions derived from the Athabasca Group rocks and by reactions with the basement rocks. The processes were associated with thermal events affecting the Athabasca Basin region.

Chemical analyses of samples from the Cigar Lake and Key Lake deposits, Saskatchewan, indicate that these two deposits exhibit many similarities, but in detail each is unique.

Geochronological observations on the Collins Bay 'B' deposit and Natona Bay occurrence, Saskatchewan, show that their formation took place contemporaneously with other deposits associated with the sub-Athabasca unconformity.

A sample from the former Foster property in Cobalt area containing a high grade uranium-thorium-zinc mineral assemblage and apparently belonging to the older (sulphidic, i.e. pre-silver-arsenide) period of mineralization, was discovered in the Mining Museum at Cobalt, Ontario.

Résumé

Les analyses du gisement d'Eagle Point (Saskatchewan) indiquent que ce gisement s'est formé de façon polygénétique à partir de solutions issues des roches du groupe d'Athabasca et par réaction aux roches du socle. Ces processus ont été associés aux événements thermiques qui ont affecté la région du bassin d'Athabasca.

L'analyse chimique d'échantillons provenant des gisements de Cigar Lake et de Key Lake (Saskatchewan) indique que ces deux gisements présentent de nombreuses caractéristiques semblables mais qu'ils sont uniques dans le détail.

Des observations géochronologiques du gîte « B » de Collins Bay et de la venue de Natona Bay (Saskatchewan) indiquent que leur formation a eu lieu en même temps que les autres gisements associés à la discordance sub-Athabasca.

Un échantillon provenant de l'ancienne propriété Foster dans la zone de Cobalt et contenant un assemblage minéral à haute teneur en uranium-thorium-zinc et datant probablement de la période de minéralisation la plus ancienne (sulfurée, c.-à-d. avant l'argent-arséniure) a été découvert dans le musée minier de Cobalt (Ontario).

INTRODUCTION

In 1987 studies of Canadian uranium resources were conducted by members of the Mineral Resource Appraisal Secretariat on occurrences in the Athabasca Basin region and selected other areas in the Churchill, Bear, Superior and Southern structural provinces of the Canadian Shield, on areas favourable for uranium mineralization in the northern part of Canadian Cordillera and on selected parts of the Appalachian Orogen. The author conducted most of his research on uranium-bearing areas and uranium occurrences of the Churchill, Superior and Southern structural provinces and of the Appalachian Orogen.

As in previous years Canada was the world's leading producer and exporter of uranium in 1987 with production of uranium in concentrates exceeding 11 000 tonnes. The production centres are at Elliot Lake, Ontario (Quirke, Panel, Stanleigh and Denison mines), at Key Lake (Gaertner and Deilmann open pits), at Rabbit Lake — Collins Bay (Collins Bay 'B' Zone) and at Cluff Lake (Claude open pit and Dominique-Peter underground operations), Saskatchewan. Locations of the production centres are shown in Figure 1.

As of 1, January 1987, the total known Canadian Reasonably Assured and Estimated Additional I uranium resources (according to classification of the International Atomic Energy Agency) recoverable at prices up to $300/kgU amounted to 567 000 tonnes U (Whillans, 1987) as compared to 545 000 tonnes U a year before. The resources increased due to advanced exploration of the Eagle Point and Cluff Lake deposits in Saskatchewan and the Kiggavik (formerly Lone Gull) deposit in the District of Keewatin. Locations of areas with deposits containing Measured, Indicated and Inferred uranium resources are shown in Figure 1.

Expenditures in exploration for uranium by the industry in 1986 exceeded 32 million Canadian dollars and attained slightly higher levels than in 1985. According to a preliminary survey, the total exploration expenditures in 1987 are estimated to be even higher than in 1986.

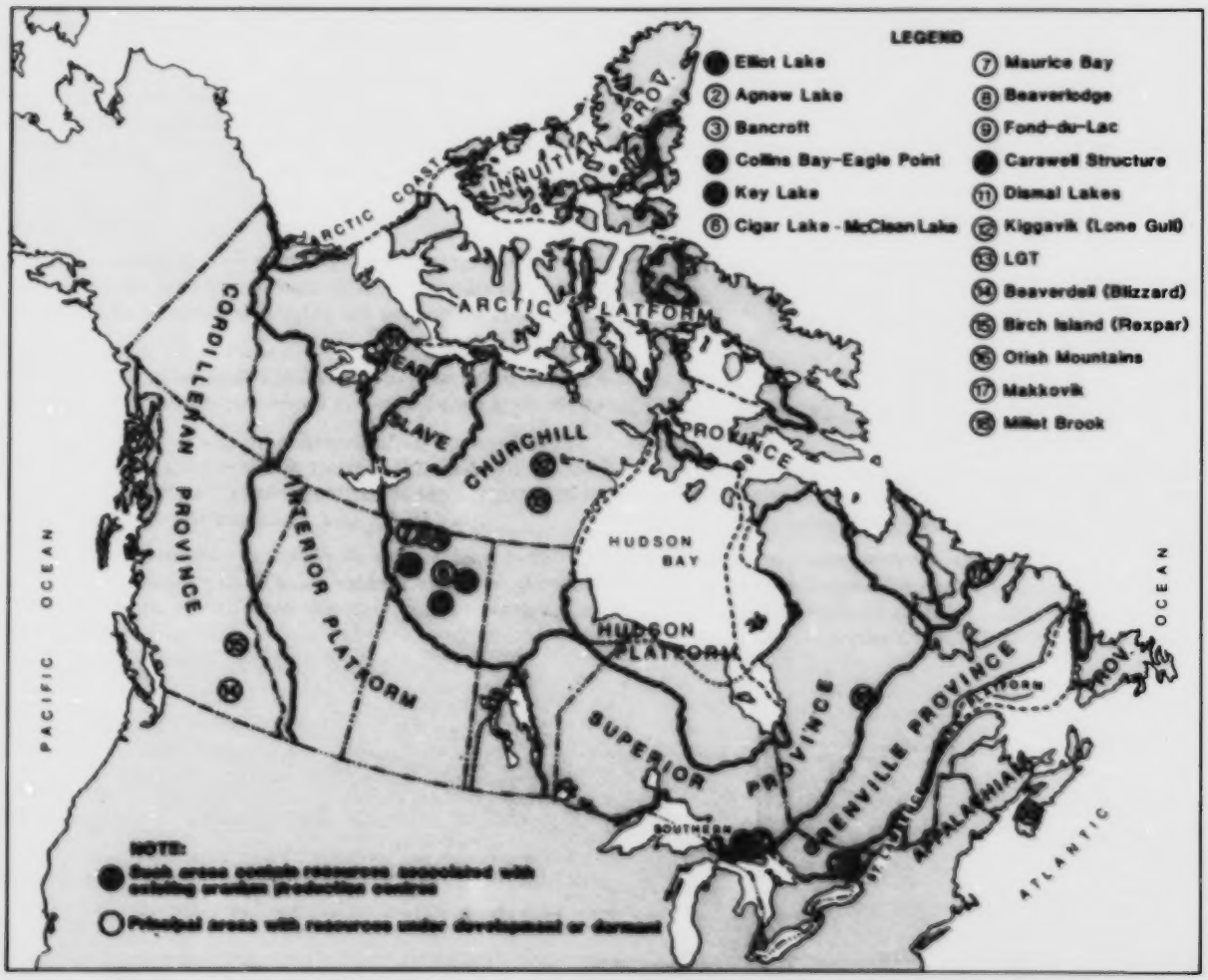

Figure 1. Areas containing uranium resources associated with production centres and principal areas with resources under development or dormant as of October, 1987.

In 1987 advanced exploration was focussed particularly on areas favourable for unconformity-associated deposits in the Athabasca Basin region, Saskatchewan and Thelon Basin region, Northwest Territories, but grass-root prospecting and exploration were also conducted in other parts of Canada; e.g. in the Bear Structural Province and in the Cordilleran and Appalachian orogenic belts. The seven-year moratorium on uranium exploration and mining in British Columbia terminated early in 1987. In New Brunswick field studies continued under the Federal-Provincial Mineral Development Agreement.

All areas under active exploration and all producing deposits were studied. Some results of these studies are presented in this paper.

INVESTIGATIONS ON EAGLE POINT DEPOSIT

By the end of July, 1987, the Eagle Point deposit has been tested by 530 drillholes, among which 285 holes were in the Eagle Point South and 245 in the Eagle Point North segments. The drillholes identified several orebodies in the southern segment of the deposit (according to Eldorado Resources Limited names: Main zone, Upper zone with satellitic orebodies, Intermediate zone, and Island zone) and three ore zones (01, 02 and 03) in the northern segment. As of September 1987 global geological resources of uranium of the Eagle Point deposit amounted to 3 356 912 tonnes of ore grading 1.53 % U and containing 51 229 tonnes U (Eldorado Resources Limited, 1987).

Mineralization of the Eagle Point deposit is lithologically controlled by a suite of Aphebian metamorphic rocks unconformably overlying Archean granitoid rocks (Eldorado Resources Limited, 1987). The Aphebian rocks are in turn unconformably overlain by clastic sedimentary rocks of the Athabasca Group. The Aphebian suite comprises graphitic paragneiss, biotite-, garnet-, cordierite- and sillimanite-, quartz-feldspar gneisses in various proportions, conglomerate, quartzite, calc-silicate, skarn and marble. This suite is intercalated by lenses and dykes of pegmatoid rocks and by segregations of quartz.

The mineralization is structurally controlled by Collins Bay and Eagle Point reverse faults (generally dipping between 40 and 55° to the southeast) and by faults parallel and subparallel to them, by steeply dipping normal faults and by cross faults.

In the vicinity of faults and adjacent to mineralized areas the host rocks are altered by illitization, chloritization and kaolinization; hematization is most common in the vicinity of high grade mineralization. Intensity of alteration is controlled by density of fracturing, which is more extensive in the southern segment (Eagle Point South) than in the northern segment (Eagle Point North) of the deposit.

The principal ore-forming mineral is pitchblende which occurs in several forms and generations: in veins and masses filling open spaces; as tiny veinlets in quartz grains (Fig.2); as disseminations (Fig.3); and in schlieren-like form intimately associated with clay minerals (Fig.4). Thorium-free uranium heptaoxide (' U3O7; Ruzicka and Littlejohn, 1982), is similar to 'tetrauraninite' reported by Voultsidis et al.(1982) from the Key Lake deposit. Amorphous pitchblende occurs in very finely disseminated form in carbon (Fig.5; and Ruzicka and LeCheminant, 1987).

The oxidation zone of the Eagle Point deposit is deep. Secondary uranium minerals have been found at about 130 m below the present surface. Sooty (hydrated) pitchblende occurs at a depth about 300 m below the surface.

The oldest U-Pb isotope age of the mineralization is about 1400q25 Ma (Eldorado Resources Limited, 1987). Additional U-Pb isotope analyses on three pitchblende samples from the southern segment of the deposit (from 173, 233 and 377 m depth) and on one sample from the northern segment (from 207 m) were interpreted (R.I.Thorpe of the Geological Survey of Canada, written comm., 1987) as indicating an absolute age of the mineralization of about 707 and 65 Ma. These dates and the mineralogical observations indicate that either the 1400 Ma old mineralization was rejuvenated or that several mineralization periods took place in formation of the deposit. The polygenetic nature of uranium mineralization is typical for all the deposits associated with the sub-Athabasca unconformity (Laine, 1985; Ruzicka, 1984; Ruzicka and LeCheminant, 1987). Taking into account a conceptual genetic model for the unconformity-associated deposits (Ruzicka, in press), geochronological evidence, and mineralogical features (presence of secondary uranium minerals attesting to a great depth of the oxidation zone), it can be reasonably

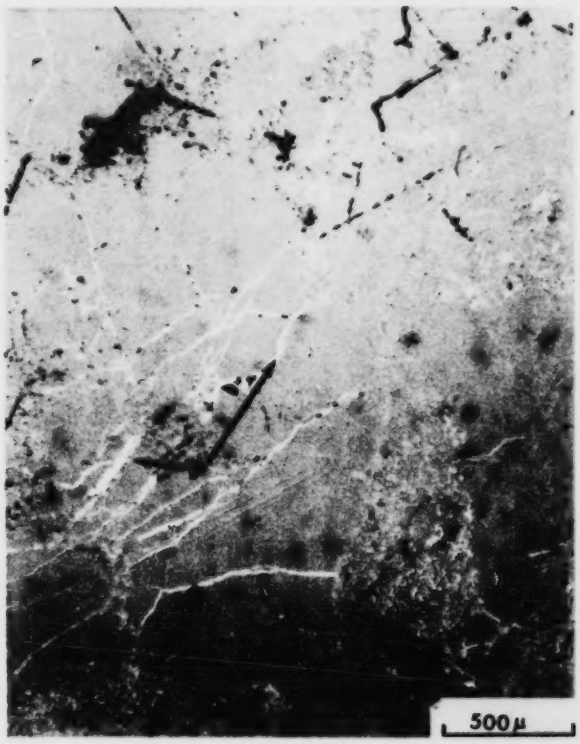

Figure 2. Pitchblende veinlets (white) in quartz. Eagle Point deposit, Saskatchewan. Reflected plain light.

assumed that (a) the Eagle Point deposit formed from solutions derived from the Athabasca Group rocks during their diagenesis; (b) these solutions reacted with the Aphebian basement rocks; and (c) the processes were associated with several thermal events affecting the Athabasca Basin region.

COMPARISON OF ELEMENTAL ASSEMBLAGES OF CIGAR LAKE AND KEY LAKE DEPOSITS

The Cigar Lake and Key Lake deposits are located in the eastern and southern part of the Athabasca Basin respectively. The distance between them is about 104 km. The Cigar Lake deposit occurs at the base of the Athabasca Group rocks at an average depth of about 430 m beneath the present surface, whereas the depth of the Key Lake deposit is on average about 100 m.

Mineralogical studies on both deposits (Ruzicka and LeCheminant 987; Voultsidis et al.,1982) indicated many common features, e.g. presence of similar mineral assemblages and similar alteration phenomena. On the other hand there are dissimilarities in gangue minerals and in copper and arsenide suites.

To clearly elucidate these features, selected samples from both deposits were chemically analyzed and the results statistically treated.

For comparative studies of elemental assemblages in these two largest Canadian polymetallic deposits, which are associated with the sub-Athabasca unconformity, seventeen samples from selected mineralized parts of the Cigar Lake deposit and eleven samples from the Key Lake deposit were analyzed for ten oxidic and twenty-eight elemental constituents and Loss on Ignition (Table 1). The samples were selected so that their uranium contents reflected distribution of ore grades of the deposits. Number of analyses (n), arithmetic means (x) and standard deviations (s) of the constituents are shown in Table 2.

Results of preliminary investigations indicate that the elemental assemblages of the Cigar Lake and Key Lake deposits exhibit certain features that make each deposit unique.

Uranium contents in the selected samples from the Cigar Lake deposit are higher (x = 15.96 %U and s = 14.59) than in samples from the Key Lake deposit (x = 4.9 %U and s = 7.68) thus reflecting differences in average grades of their resources.

Contents and distribution patterns of some components (e.g. SiO2, La, Sc, Sr and V) are similar in both deposits. These features apparently indicate that the sources and conditions of transport and deposition were similar for both deposits.

Figure 3. Pitchblende (white) in fractures in a corroded quartz grain (intermediate grey) and disseminated in matrix of quartzite. Eagle Point deposit, Saskatchewan. Reflected plain light.

Figure 4. Schlieren-like pitchblende (white) in micaceous and kaolinized matrix of quartzite; intermediate grey = corroded quartz grains. Eagle Point deposit, Saskatchewan. Reflected plain light.

On the other hand average contents of some constituents (e.g. As, Cu, and Ni) differ substantially. The Cigar Lake samples contain larger amounts of Cu and Pb, whereas the Key Lake samples are rich in As and Ni. This feature is clearly reflected in the paragenetic mineral succession of the Cigar Lake deposit, where the copper mineral assemblage represents a separate stage in the ore-forming processes (i.e. the 'Stage II' of Fouques et al., 1986, or 'Oligomictic Stage' of Ruzicka and LeCheminant, 1987) whereas this stage at the Key Lake deposit is missing.

Differences in the mineralization processes are also reflected in comparison between the average contents of the elements in the samples and their clarkes of crustal abundance (i.e. 'concentration ratio'; Table 2). In the Key Lake samples, for instance, the As contents exceed 50 000 times, Ni and Ag more then 200 times their crustal clarkes. The uranium concentration ratio is about 16 000. In the Cigar Lake samples the Pb contents exceed more than 1000 times and Cu more than 50 times their clarkes with a uranium concentration ratio of more than 50 000. These observations correspond in general with estimates of U and Ni resources in both deposits. The U/Ni ratio in the Key Lake deposit is approximately 1:0.55 (A.de Carle, pers. comm., 1987) whereas in the Cigar Lake deposit the U/Ni ratio is 1:0.078 (Fouques et al., 1986).

To investigate processes that participated in formation of the Cigar Lake and Key Lake deposits, uranium contents and selected constituents in samples from both deposits were statistically correlated (Table 4) and graphically presented by line diagrams (Fig. 7). The statistical analysis showed very high correlation coefficients between uranium and total iron oxides and uranium and manganese oxides in samples from the Key Lake deposit (rU/Fe = 0.99; rU/Mn = 0.96). The line diagrams (Fig. 7) confirmed positive correlation in samples containing more than 0.21 %U. Thus both methods indicate deposition of uranium in the Key Lake deposit along with iron and manganese. On the other hand the same methods applied to samples from the Cigar Lake deposit revealed between U and Fe_2O_3 and U and MnO a very low degree of correlation ($r_u/Fe_2O_3 = 0.07$; $r_u/MnO = 0.003$), which was confirmed by the irregular pattern on the line diagrams (Fig. 7).

Correlation coefficents between contents of uranium and individual elemental constituents may be influenced by a 'nugget' effect of high contents of some components. This must be the case with the Cigar Lake deposit analyses, where several samples contain more than 20 % U and one sample even 53 % U. Analyses of samples from this deposit, for instance, show positive correlation between uranium and sodium oxide ($r_u/Na_2O = 0.78$) and between uranium and calcium oxide ($r_u/CaO = 0.56$) (Table 4) but their line diagrams (Fig. 7) indicate very loose relationship. Strong correlation

Figure 5. Autoradiograph (positive image) of pitchblende-bearing (light grey spots) carbon [kerabitum] (black). Eagle Point deposit Saskatchewan.

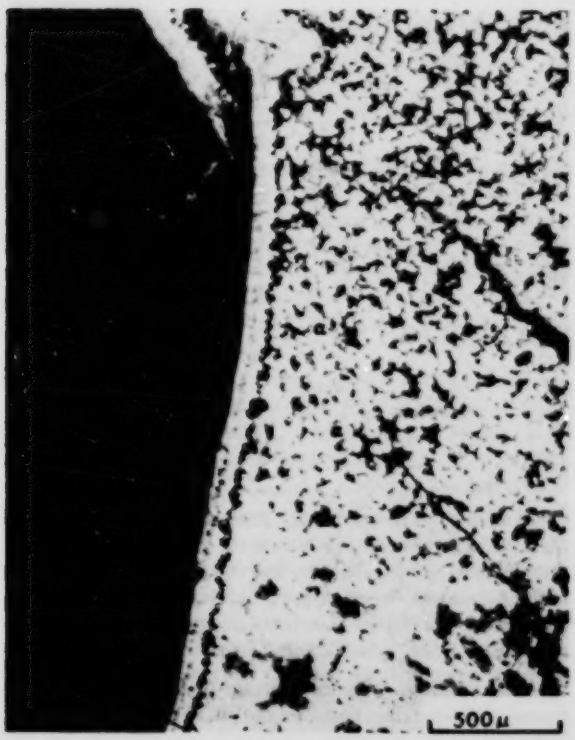

Figure 6. 'Tetrauraninite' ($\propto$) [$\propto U_3O_7$] (cubes) from Eagle Point deposit, Saskatchewan. Reflected plain light.

Table 1A. Chemical analyses of selected samples from the Cigar Lake deposit, Saskatchewan; data in per cent. Footnote: NA = analysis not available; NF = not found; U analyzed by delayed neutron activation method by Atomic Energy Limited. All other analyses by GSC: Samples 1 to 10 analyzed spectrochemically; samples 11 to 17 by ICP method except for LOI, which was analyzed chemically.

Element /Oxide	Sample 1	2	3	4	5	6	7	8	9	10	11	12	13	14	15	16	17
SiO2	>64.2	42.8	>64.2	32.1	10.7	>64.2	64.2	32.1	64.2	>64.2	64.2	21.7	86.6	5.67	4.69	4.99	14
Al2O3	3.7	9.5	1.9	3.7	3.7	2.8	13.2	5.7	5.7	3.8	9.5	16	8.15	3.41	1.72	2.3	9.42
Fe2O3	4.3	28.6	10	21.5	7.1	10	28.6	21.5	14.3	2.1	10	11.8	0.2	3.84	1.16	15.3	3.62
CaO	0.28	0.98	0.28	2.1	2.8	0.28	0.98	2.1	2.1	0.1	1.4	0.66	0.09	2.23	7.2	1.32	0.94
Na2O	<.04	NA	<.04	NA	NA	<0.04	NA	NA	NA	<0.04	NA	0.16	0.1	0.17	0.26	0.12	0.17
MgO	0.33	0.83	0.5	0.323	0.17	0.83	0.83	1.16	1.16	0.83	1.16	9.7	0.32	4.06	2.51	1.62	1.86
TiO2	0.83	0.83	0.5	1.67	2.5	0.33	1.17	0.83	1.67	0.5	1.67	6.45	0.29	0.84	0.45	0.39	2
P2O5	<0.23	NF	<0.23	<.023	<0.23	NF	<0.23	<0.23	<0.23	NF	<.23	0.3	0.05	0.14	0.17	0.2	0.31
LOI	NA	NA	NA	NA	NA	NA	NA	NA	NA	NA	NA	14.1	1.5	7.5	5.1	5.1	6.7
MnO	0.026	0.26	0.194	0.194	0.194	0.09	0.258	0.258	0.387	0.004	0.194	0.08	0.01	0.12	0.09	0.26	0.05
K2O	NA	NA	NA	NA	NA	NA	NA	NA	NA	NA	NA	0.28	2.14	0.12	0.13	0.03	0.63
Ag	NA	NF	NF	NA	NA	NF	NF	NF	NF	NF	NF	NA	NA	NA	NA	NA	NA
As	NF	NF	0.1	NF	NF	NF	NF	NF	NF	<0.1	NF	NF	NA	NA	NA	NA	NA
Au	NF	NF	NF	NF	NF	NF	NF	NF	NF	NF	NF	NA	NA	NA	NA	NA	NA
B	0.02	0.07	0.01	0.03	0.02	0.02	0.07	0.03	0.03	0.02	0.05	NA	NA	NA	NA	NA	NA
Ba	0.01	0.03	0.003	0.03	0.015	0.003	0.03	0.03	0.02	0.003	0.02	0.007	0	0.01	0.048	0.023	0.024
Be	0.001	0.003	0.0005	0.0015	0.0005	0.0005	0.005	0.001	0.003	0.0005	0.003	0.0057	0.0002	0.003	0.0037	0.0043	0.0054
Bi	NA	NA	NF	NA	NA	NF	NA	NA	NA	NF	NA	NA	NA	NA	NA	NA	NA
Ce	NF	NF	NF	<.005	<.005	NF	NF	NF	NF	NF	NF	NA	NA	NA	NA	NA	NA
Co	NA	<.0.001	0.05	NA	NA	0.005	NA	NA	NA	0.005	NA	0.11	0.0041	0.12	0.032	0.091	0.1
Cr	0.005	0.01	0.003	NA	NA	0.002	0.01	0.007	0.007	0.002	0.007	0.033	0.0007	0.082	0.1	0.096	0.093
Cu	0.003	0.003	0.002	0.007	0.015	0.0005	0.005	0.03	0.05	0.01	0.05	3.2	0.0013	0.25	0.53	0.25	1.1
La	NF	NF	NF	<.0003	<.003	NF	NF	NF	NF	NF	NF	0.013	0.0037	0.083	0.12	0.01	0.1
Mo	<.001	NF	0.005	<.001	<.001	NF	NF	NF	NF	NF	NF	NA	NA	0.4	NA	0.163	0.92
Nb	NF	NF	NF	NF	NF	NF	NF	NF	NF	NF	NF	NA	NA	NA	0.084	0.103	0.096	0.092
Ni	0.005	<.001	0.03	NA	NA	0.01	NA	NA	NA	0.002	NA	0.4	0.0024	4.4	0.1	0.14	0.18
Pb	0.1	0.7	0.03	0.7	3	0.005	0.5	5	3	0.015	1.5	0.19	0.014	7.7	5.4	7.7	6.4
Sb	NF	NF	NF	NF	NF	NF	NF	NF	NF	NF	NF	NA	NA	NA	NA	NA	NA
Sc	0.003	0.015	<.0001	0.015	0.05	<.0001	0.01	0.02	0.02	0.0005	0.01	NA	NA	NA	NA	NA	NA
Sn	NF	NF	NF	NF	NF	NF	NF	NF	NF	NF	NF	NA	NA	NA	NA	NA	NA
Sr	0.003	0.02	0.001	0.03	0.05	0.003	0.015	0.03	0.02	0.0015	0.015	NA	NA	NA	NA	NA	NA
Ta	NF	NF	NF	NF	NF	NF	NF	NF	NF	NF	NF	NA	NA	NA	NA	NA	NA
Th	NF	NF	NF	NF	NF	NF	NF	NF	NF	NF	NF	NA	NA	NA	NA	NA	NA
U	5.2	17.4	1.4	22.4	53	0.0879	18	17.5	28	0.495	27.5	2.05	0.0072	23.7	25.8	2.66	26.1
V	0.05	0.15	0.02	0.1	0.1	0.02	0.15	0.07	0.07	0.015	0.07	0.12	0.0025	0.11	0.11	0.11	0.12
Y	0.03	0.07	0.02	0.1	0.1	0.003	0.05	0.1	0.1	0.007	0.03	NA	NA	0.098	0.147	0.17	0.165
Yb	0.003	0.01	0.0015	0.01	0.015	0.0003	0.005	0.01	0.01	0.0007	0.003	0.0016	0.0003	0.018	0.02	0.029	0.02
Zn	NF	NF	NF	NF	NF	NF	NF	NF	NF	NF	NF	0.029	0.0016	0.027	0.0054	0.014	0.14
Zr	0.07	0.05	0.05	0.15	0.2	0.03	0.15	0.07	0.1	0.05	0.15	0.33	NA	NA	NA	NA	0.186

between uranium and calcium oxide (r = 0.84) exists, on the other hand, in samples from the Key Lake deposit (Table 4 and Fig. 7). Results of this simple correlation indicate again that both deposits have some specific features that make them unique.

COLLINS BAY 'B' DEPOSIT

The Collins Bay B deposit, which is located between the Rabbit Lake and Eagle Point deposits, is currently being exploited by open pit. It contains polymetallic mineralization associated with the sub-Athabasca unconformity (Jones, 1980; Ruzicka, 1986).

The deposit is structurally controlled by intersection of the Collins Bay reverse fault with the sub-Athabasca unconformity and lithologically by the clastic sedimentary rocks of the Athabasca Group that rest unconformably on Aphebian graphitic paragneiss. The orebody is surrounded by a clay (essentially illite, some kaolinite and chlorite) envelope.

The uranium ores are thorium-free and occur in two forms: monometallic, consisting of pitchblende and coffinite; and polymetallic where these uranium minerals are associated with sulphides of iron, copper, nickel and molybdenum, arsenides of nickel and cobalt, and sulphoarsenides of nickel, copper and iron.

Two samples of the polymetallic ore collected from the northeastern wall of the open pit about 20 m below the surface were analyzed by Geospec Consultants Limited of Edmonton for U and Pb isotopes. Their isotope ratios were found as follows: $^{207}Pb/^{206}Pb$: 0.07191 and 0.07990; $^{206}Pb/^{238}U$: 0.02573 and 0.1306; $^{207}Pb/^{235}U$: 0.2551 and 1.438.

These ratios were interpreted to indicate an absolute age of mineralization of 1212 ± 1 Ma (R.I. Thorpe, written comm., 1987). The age dates for mineralization of the Collins Bay B deposit are fully compatible with dates for other deposits associated with the sub-Athabasca unconformity (Laine, 1985).

NATONA BAY OCCURRENCE

The Natona Bay occurrence has been discovered by the Saskatchewan Mining and Development Corporation about 22 km to the northeast of Cigar Lake. It is apparently associated with the same regional fault that controls localization of the Cigar Lake deposit and with the sub-Athabasca unconformity, which occurs about 250 m below the surface.

The occurrence represents a large nugget of pitchblende, coffinite, nickeline, rammelsbergite, gersdorffite, galena,

Table 1B. Chemical analyses of selected samples from the Key Lake deposit, Saskatchewan; data in per cent. Footnote: NA = analysis not available; NF = not found; U analyzed by delayed neutron activation method by Atomic Energy Limited. All other analyses by GSC: Samples 1 to 3 analyzed spectrochemically; samples 4 to 11 by ICP method except for LOI, which was analyzed chemically.

Element /Oxide	Sample 1	2	3	4	5	6	7	8	9	10	11
SiO2	3	4.3	10.7	34.9	69.6	55.3	36.2	39.8	39.6	72.1	71
Al2O3	3.8	1.9	5.7	14.4	13.8	25.2	30.2	33.9	37.2	14.3	14.2
Fe2O3	1	21.5	28.6	17	0.46	1.44	9.7	0.35	1.1	0.77	3.4
CaO	0.07	2.1	2.8	0.89	0.13	0.18	0.22	0.15	0.17	0.12	1.59
Na2O	<0.04	NA	NA	0.49	0.07	0.09	0.07	0.08	0.15	0.06	2.62
MgO	0.5	0.7	1.5	2.47	1.29	5.82	0.65	0.75	7.21	3.26	1.62
TiO2	0.5	0.12	0.5	0.17	0.92	1.15	1	0.65	0.36	0.18	0.43
P2O5	NF	NF	NF	0.08	0.04	0.07	0.1	0.08	0.1	0.05	0.11
LOI	NA	NA	NA	8.9	10.1	10	14.3	12.9	13.3	5.2	1
MnO	0.001	0.39	0.39	0.14	0.01	0.01	0.02	0.01	0.01	0.01	0.04
K2O	NA	NA	NA	2.73	3.47	0.66	0.2	0.28	0.34	0.88	3.53
Ag	NF	0.007	<.0002	NA	NA	NA	NA	NA	NA	NA	NA
As	<.1	30	1	NA	NA	NA	NA	NA	NA	NA	NA
Au	NF	NF	NF	NA	NA	NA	NA	NA	NA	NA	NA
B	0.01	0.02	0.03	NA	NA	NA	NA	NA	NA	NA	NA
Ba	0.001	0.05	0.07	0.18	0.019	0.006	0.005	0.003	0.001	0.002	0.069
Be	0.0003	0.0015	0.003	0.0023	0.0004	0.0015	0.003	0.0014	0.0014	0.0005	0.0001
Bi	NA	NA	NA	NA	NA	NA	NA	NA	NA	NA	NA
Ce	NF	NF	NF	NA	NA	NA	NA	NA	NA	NA	NA
Co	0.015	0.5	0.05	0.0064	0.0011	0.024	0.0081	0.17	0.0046	0.0009	0.0004
Cr	0.001	0.003	0.015	0.031	0.011	0.017	0.018	0.0058	0.014	0.0036	0.001
Cu	0.003	0.3	0.2	0.053	0.0021	0.0022	0.031	0.038	0.0002	0.0048	0
La	NF	NF	NF	0.072	0.0026	0.005	0.01	0.0061	0.0089	0.0016	0.0037
Mo	NF	NF	NF	NA	NA	NA	NA	NA	NA	NA	NA
Nb	NF	NF	NF	NA	NA	NA	NA	NA	NA	NA	NA
Ni	0.15	10	3	0.022	0.0099	0.32	1.3	4.8	0.38	0.13	0.0028
Pb	0.003	2	3	1.1	0.038	0.079	0.13	0.18	0.057	0.025	0.022
Sb	NF	NF	NF	NA	NA	NA	NA	NA	NA	NA	NA
Sc	0.0003	0.02	0.02	NA	NA	NA	NA	NA	NA	NA	NA
Sn	NF	NF	NF	NA	NA	NA	NA	NA	NA	NA	NA
Sr	0.002	0.015	0.03	NA	NA	NA	NA	NA	NA	NA	NA
Ta	NF	NF	NF	NA	NA	NA	NA	NA	NA	NA	NA
Th	NF	NF	NF	NA	NA	NA	NA	NA	NA	NA	NA
U	0.199	17	20	12.1	0.0015	0.0261	4.28	0.21	0.0181	0.093	0.0004
V	0.01	0.05	0.1	0.14	0.011	0.15	0.18	0.11	0.27	0.023	0.0043
Y	0.01	0.2	0.15	NA	NA	NA	NA	NA	NA	NA	NA
Yb	0.0007	0.02	0.02	0.0079	0.00004	0.0006	0.0017	0.0005	0.0002	0.0002	0.00008
Zn	0.02	<.01	<.01	0.012	0.016	0.029	0.038	0.046	0.043	0.0066	0.0045
Zr	0.02	0.005	0.03	NA	NA	NA	NA	NA	NA	NA	NA

sphalerite, chalcopyrite, pyrite, bravoite and molybdenite. This assemblage is accompanied by clay, chlorite, carbonate, hematite and chalcedony.

Three samples of thorium-free pitchblende from the polymetallic assemblage have been analyzed by Geospec Consultants Limited of Edmonton for U and Pb isotopes.

The isotope ratios have been determined as follows: $^{207}Pb/^{206}Pb$: 0.08431, 0.08309 and 0.08489; $^{206}Pb/^{238}U$: 0.2900, 0.2451 and 0.4663; $^{207}Pb/^{235}U$: 3.371, 2.808 and 5.458.

These ratios have been interpreted to indicate an absolute age of mineralization in the range of 1277 to 1303 Ma (R.I. Thorpe, written comm., 1987).

DISCOVERY OF URANIUM-THORIUM-ZINC MINERALIZATION IN THE COBALT AREA, ONTARIO

During field metallogenic studies of the Huronian Supergroup in the Cobalt area, Ontario, a sample labelled 'Sphalerite — zinc ore' and catalogued by the Cobalt Mining Museum under No. 212 was identified as containing uranium and thorium.

The sample, weighing approximately 300 g, consists of vein material, mainly yellowish-brown translucent sphalerite grains, each about 3 to 5 mm long and 1 to 3 mm wide. Megascopic examination and radiometric analysis of the sample, using gamma- ray spectrometer McPhar TV-1A, indicated that the sample contains about 2.2 % eU and 9.3 % eTh in a highly radioactive black interstitial mass, tentatively identified as uranothorite.

Field examination of the provenance area of the sample, which is at present occupied by an ore-processing plant owned and operated by Agnico-Eagle Mines Limited, did not reveal the exact location of the sample collection site. However, it can be reasonably assumed that the sample was collected from, or from the vicinity of, No. 5 vein on the former Foster property. Petruk (1971) observed sphalerite, galena, chalcopyrite, pyrite and pyrrhotite in 'Keewatin' cherty interflow rocks from this property and quoted Thomson (1961), who reported assays of a selected sample taken from this mineralized interflow of 20.15 % Zn, 8.5 % Ag, 0.58 % Cu, 0.28 % Co, 1.53 % Ag and traces of Au. However, no uranium has been ever reported from this locality.

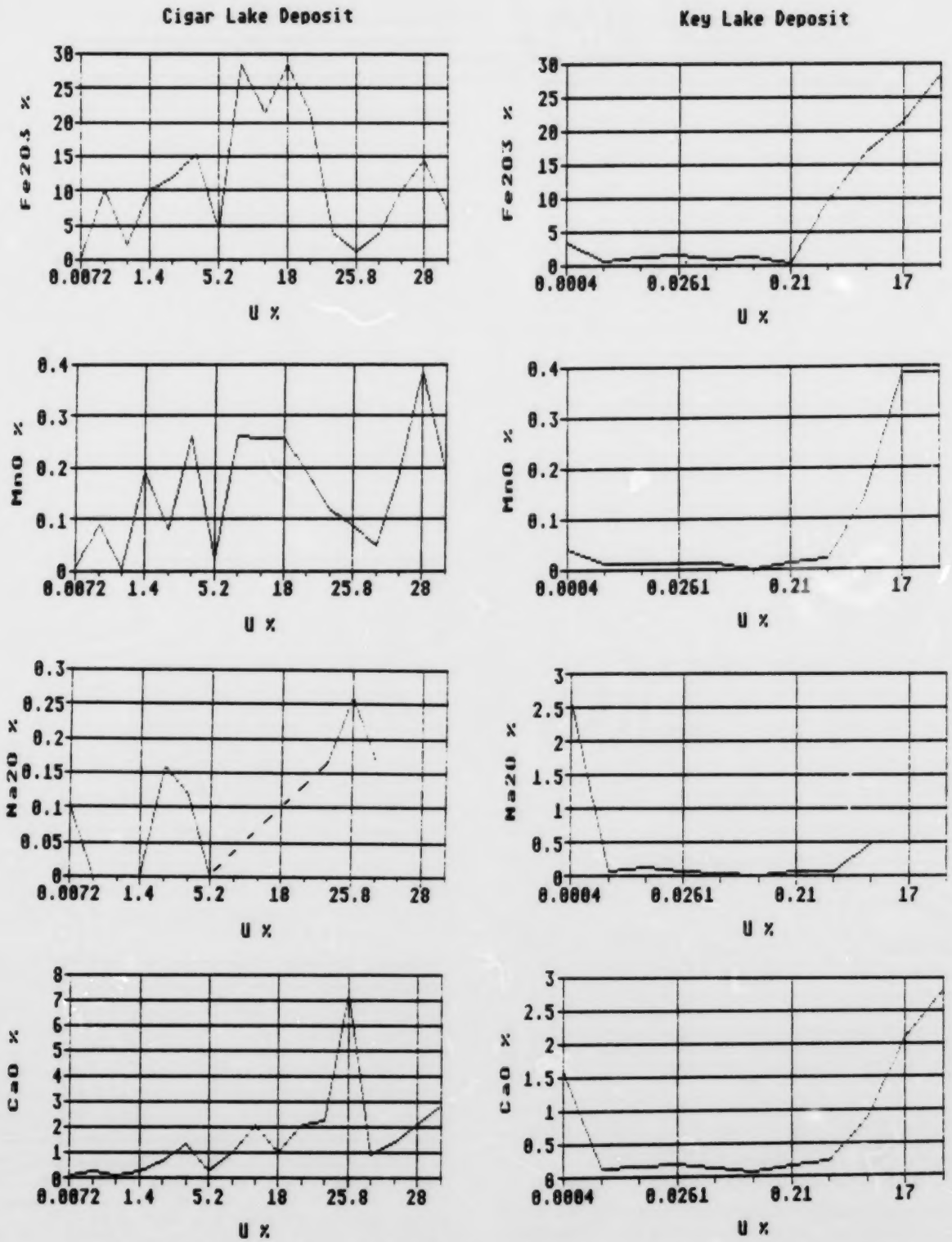

Figure 7. Line diagrams showing relationship between uranium and Fe_2O_3, MnO, Na_2O and CaO contents in samples from the Cigar Lake and Key Lake deposits as recorded in Tables 1A and 1B.

Table 2. Average contents (x) in per cent, number of samples (n) and standard deviations (s) of chemical analyses of selected samples from mineralized parts of Cigar Lake and Key Lake deposits, Saskatchewan. Footnote: NA = analysis not available; NF = not found.

Element/ Oxide	Cigar Lake Deposit x	n	s	Key Lake Deposit x	n	s
SiO2	41.46	17	27.26	45.2	11	23.5
Al2O3	6.13	17	4.18	17.7	11	12.2
Fe2O3	11.41	17	9.11	7.76	11	10.09
CaO	1.52	17	1.69	0.77	11	0.96
Na2O	0.11	10	0.08	0.41	9	0.84
MgO	1.66	17	2.29	2.47	11	6
TiO2	1.35	17	1.47	0.54	11	0.35
P2O5	0.18	17	0.1	0.07	11	0.05
LOI	6.67	6	4.18	9.46	8	4.48
MnO	0.16	17	0.11	0.09	11	0.15
K2O	0.56	6	0.8	1.51	8	1.47
Ag	NF	8		0.002	3	0.004
As	0.018	11	0.04	10.37	3	17.01
Au	NF	11		NF	3	
B	0.034	11	0.021	0.02	3	0.01
Ba	0.018	17	0.013	0.037	11	0.055
Be	0.0002	17	0.002	0.638	11	1.724
Bi	NF	3		NA		
Ce	0.001	11	0.002	NF	3	
Co	0.052	10	0.049	0.075	11	0.149
Cr	0.031	15	0.04	0.011	11	0.009
Cu	0.324	17	0.794	0.058	11	0.099
La	0.02	17	0.039	0.01	11	0.021
Mo	0.107	14	0.259	NF	3	
Nb	0.025	15	0.043	NF	3	
Ni	0.479	11	1.306	1.83	11	3.12
Pb	2.468	17	2.869	0.6	11	1.01
Sb	NF	11		NF	3	
Sc	0.01	11	0.014	0.013	3	0.011
Sn	NF	11		NF	3	
Sr	0.017	11	0.015	0.016	3	0.014
Ta	NF	11		NF	3	
Th	NF	11		NF	3	
U	15.96	17	14.59	4.9	11	7.68
V	0.082	17	0.047	0.095	11	0.085
Y	0.079	15	0.055	0.12	3	0.098
Yb	0.009	17	0.009	0.005	11	0.008
Zn	0.013	17	0.034	0.021	11	0.015
Zr	0.122	13	0.085	0.018	3	0.013

Table 3. Ratios between elemental contents in selected samples from the Cigar Lake and Key Lake deposits and their crustal clarkes; data in ppm.

Element	Clarke ppm a	Cigar Lake ppm b	Key Lake ppm c	Ratio (b/a) d	Ratio (c/a) e
Si	270000	194000	211000	0.72	0.78
Al	80000	32000	94000	0.4	1.18
Fe	50000	80000	54000	1.6	1.08
Ca	30000	10900	5500	0.36	0.18
Na	24000	800	3000	0.03	0.13
Mg	21000	10000	14900	0.48	0.71
Ti	5000	8100	3200	1.62	0.64
P	1000	800	300	0.8	0.3
Mn	900	1200	700	1.33	0.78
K	26000	4600	12500	0.18	0.48
Ag	0.07	0	20	0	285.71
As	2	180	103700	90	51850
Au	0.004	0	0	0	0
B	10	340	200	34	20
Ba	430	180	370	0.42	0.86
Be	3	20	14	6.67	4.67
Ce	45	10	0	0.22	0
Co	25	520	750	20.8	30
Cr	200	310	110	1.55	0.55
Cu	60	3240	580	54	9.67
La	39	200	100	5.13	2.566
Mo	2	1070	0	535	0
Nb	20	250	0	12.5	0
Ni	80	4790	18300	59.87	228.75
Pb	16	24680	6000	1542.5	375
Sb	0.62	0	0	0	0
Sc	18	100	130	5.56	7.22
Sn	2.5	0	0	0	0
Sr	350	170	160	0.49	0.46
Ta	2	0	0	0	0
Th	10	0	0	0	0
U	3	159600	49000	53200	16333.33
V	150	820	950	5.47	6.33
Y	30	790	1200	26.33	40
Yb	3	90	50	30	16.67
Zn	70	130	210	1.86	3
Zr	160	1220	180	7.63	1.13

Table 4. Correlation coefficients (r) and regression constants (A and B) between contents of uranium and selected components in samples from Tables 1A and 1B.

Constituents	Cigar Lake Deposit n	A	B	r	Key Lake Deposit n	A	B	r
U/Fe2O3	17	10.72	0.04	0.07	11	1.38	1.3	0.99
U/CaO	17	0.48	0.07	0.556	11	0.25	0.11	0.84
U/Na2O	10	0.07	5.18	0.78	9	0.42	-0.01	-0.02
U/MgO	17	2.05	-0.02	-0.16	11	2.77	-0.09	-0.3
U/TiO2	17	1.11	0.01	0.15	11	0.63	-0.02	-0.4
U/MnO	17	0.11	0.003	0.38	11	0.001	0.019	0.96
U/Co	17	0.04	0.001	0.325	11	0.02	0.01	0.5
U/Cu	17	0.45	-8.21	-0.15	11	0.001	0.011	0.89
U/Ni	11	0.002	0.05	0.43	11	0.68	0.24	0.56
U/V	17	0.06	1.53	0.48	11	0.09	0.0004	0.03

Correlation coefficient:

$$r = (n.\Sigma xy - \Sigma x.\Sigma y)/[n.\Sigma x^2 - (\Sigma x)^2].[n.\Sigma y^2 - (\Sigma y)^2]$$

Regression equation:

$$y = A + Bx$$

The locality is in an area of Archean rocks containing cherty interflows; the Archean rocks are unconformably overlain by metasedimentary rocks of the Gowganda Formation of the Huronian Supergroup. The Archean-Aphebian sequence is intruded by the Kerr Lake diabase dome. In addition to the above mentioned mainly sulphidic mineral assemblage, which is associated with the cherty interflow rocks, a much larger, younger and mainly arsenide assemblage occurs in the No. 5 and accompanying veins (Petruk, 1971).

ACKNOWLEDGMENTS

Co-operation of J.P. Fouques of Cogema Canada Limited, N. Andrade of Eldorado Resources Limited, A. deCarle of Key Lake Mining Corporation and C. Roy of the Saskatchewan Mining Corporation is sincerely acknowledged. G.M. LeCheminant of the Geological Survey of Canada provided mineral determinations and photomicrographs for this paper. Chemical analyses were made by GSC laboratories. U/Pb isotope analyses were made by Geospec Consultants Limited, Edmonton. Critical reading of the manuscript by R.T. Bell is appreciated.

REFERENCES

Eldorado Resources Limited,
1987: Geology of uranium deposits of the Rabbit Lake — Collins Bay area; unpublished document for participants of the International Atomic Energy Agency excursion to Collins Bay, Key Lake and La Ronge Core Library, September 1987; 20 p.

Fouques,J.P., Fowler,M., Knipping,H.D., and Schimann,K.
1986: The Cigar Lake uranium deposit: discovery and geological characteristics; *in* Uranium Deposits of Canada, ed. E.L.Evans; The Canadian Institute of Mining and Metallurgy, Special Volume 33, p.218-229.

Jones,B.
1980: The geology of the Collins Bay uranium deposit, Saskatchewan; The Canadian Institute of Mining and Metallurgy, Bulletin, v. 73, no. 818, p. 84-90.

Laine,R.
1985: Conclusion: the Carswell uranium deposits — an example of not so unique unconformity-related uranium mineralization; *in* The Carswell Structure Uranium Deposits, Saskatchewan, ed. by R. Laine, D.Alonso and M.Svab; Geological Association of Canada, Special Paper 29, p. 225-230.

Petruk, W.
1971: General characteristics of the deposits; *in* The Silver-Arsenide Deposits of the Cobalt-Gowganda Region, Ontario, ed. by L.G.Berry; Mineralogical Association of Canada, The Canadian Mineralogist v. 11, part 1, p. 76-107.

Ruzicka, V.
1984: Unconformity-related uranium deposits in the Athabasca Basin region, Saskatchewan; *in* Proterozoic Unconformity and Stratabound Uranium Deposits, ed. J. Ferguson; A Technical Document IAEA-TECDOC-315, International Atomic Energy Agency, Vienna, p.219-267.
1986: Uranium deposits in the Rabbit Lake — Collins Bay area, Saskatchewan; *in* Uranium Deposits of Canada, ed. E.L.Evans; The Canadian Institute of Mining and Metallurgy, Special Volume 33, p. 144-154.
— Conceptual genetic models for important types of uranium deposits and areas favourable for their occurrence in Canada; *in* 'Proceedings of International Atomic Energy Agency Technical Committee Meeting on Uranium Geology and Resources in North America, Saskatoon, 1987' TEC-DOC TI-TC-394 (in press).

Ruzicka,V. and LeCheminant,G.M.,
1987: Uranium and uranium-polymetallic deposits in Canada, 1986; *in* Current Research, Part A, Geological Survey of Canada, Paper 87-1A, p. 249-262.

Ruzicka,V. and Littlejohn,A.L.
1982: Notes on mineralogy of various types of uranium deposits and genetic implications; *in* Current Research, Part A, Geological Survey of Canada, Paper 82-1A, p.341-349.

Thomson, R.
1961: Parts of Coleman Township, concession IV, lots 1 to 5, and Gillies Limit, the Eastern "A" claims, district of Timiscaming; Ontario Department of Mines, Preliminary Report 1961-7.

Voultsidis,V., von Pechmann,E., and Clasen,D.:
1982: Petrography, mineralogy and genesis of the U-Ni deposits, Key Lake, Saskatchewan, Canada; *in* Ore Genesis, the State of the Art, ed. G.C. Amstutz et al.; Springer, p. 469-491.

Whillans, R.T.,
1987: The Canadian Uranium Industry — two perspectives; unpublished paper presented at Atomic Industrial Forum Uranium Seminar, Keystone, Colorado, 26 p.

Some recent developments in geomagnetic activity forecasting at the Geological Survey of Canada

R.L. Coles, J. Hruska and H.-L. Lam
Geophysics Division

Coles, R.L., Hruska, J., and Lam, H.-L., Some recent developments in geomagnetic activity forecasting at the Geological Survey of Canada; in Current Research, Part F, Geological Survey of Canada, Paper 88-1F, p. 31-38, 1988.

Abstract

A recently introduced multizone concept for forecasting magnetic activity at high geomagnetic latitudes (above 55°N), resulting in more definitive medium-term forecasts (for up to 27 days in advance) for the Canadian region, shows good agreement between forecast and observed levels. Recurrent patterns of solar phenomena and their observed interactions with the geomagnetic field form the basis of the forecasting technique. Coronal holes predominate as sources of recurrent magnetic activity. A linear prediction filtering technique has also used past values to predict future activity.

Résumé

Un nouveau concept multizonal de prévision de l'activité magnétique aux hautes latitudes géomagnétiques (au-dessus de 55°N), permettant d'établir des prévisions à moyenne échéance plus définitives (jusqu'à 27 jours d'avance) pour le Canada, a permis de produire des données prévisibles qui correspondaient bien aux données observées. Les configurations récurrentes de phénomènes solaires et leurs interactions avec le champ géomagnétique constituent la base de la technique de prévision. Les trous de couronne sont les principales sources d'activités magnétiques récurrentes. Dans une technique de filtrage des prévisions linéaires, on a aussi utilisé des valeurs antérieures pour prévoir l'activité future.

INTRODUCTION

In recent years, forecasting of geomagnetic activity has been in increasing demand by a variety of user groups, including the exploration industry, telecommunications agencies, electric power utilities, the military, pipeline operators, geodetisists, and other scientific researchers. A number of institutes around the world, concerned with various aspects of solar-terrestrial relations, provide forecasts of solar activity and of related geophysical phenomena. The formed Earth Physics Branch (now part of the Geological Survey of Canada) has provided a geomagnetic activity forecast service since 1974. Initially, only medium-term (27 day) forecasts were issued but since 1976, in addition, short-term forecasts for up to 3 days have been provided. In these forecasts, three levels of magnetic activity were defined (quiet, unsettled, and active) and the daily prediction consisted of one of these levels. It was at that time already recognized that each of these three defined levels required a separate quantitative description for the subauroral, auroral, and polar cap regions (Hruska, 1979). Other formats have been used by other institutes: for example, the Space Environment Services Center (SESC) in Boulder, Colorado, has used a six-level forecast (Space Environment Services Centre, 1985).

The level and character of magnetic activity vary greatly with geomagnetic latitude (e.g. Whitham et al., 1960; Moe and Nebergall, 1969; Campbell, 1973). (Note: Geomagnetic latitude is referenced to the axis of the main geomagnetic dipole which intersects the surface of the earth in northern Greenland.) To incorporate this latitudinal dependence into the geomagnetic activity forecasts, Hruska (1983) recommended the use of a three-zone forecast for the three dominant magnetic zones in Canada.

This paper will include the development of multi-zone forecasts of geomagnetic activity for Canada and their verification for the period 1984 to 1985. One form of the forecasts has been derived manually using a forecaster's skill and judgement. However, as the need develops for increasingly reliable and ongoing forecasts, it is desirable to attempt to place the forecasting process on a more objective basis using all available input data and by applying algorithms that codify previously successful judgemental procedures. To this end, a prediction filter based on Wiener linear prediction theory (Weiner, 1949) has been developed for the medium term (27 days) forecasts and has been tested on data from the Canadian Magnetic Observatory network (Lam, 1987).

THE CHARACTER OF THE MAGNETIC FIELD OVER CANADA

Although magnetic field data of various kinds have been collected in Canada for three centuries, it is only since about the time of the International Geophysical Year (1957-58) that the complexity of the externally-driven time variations and their spatial distribution over Canada, and in fact at high latitudes in general, began to be fully appreciated (e.g., Feldstein,1986). Since then, a network of magnetic observatories has been expanded across the country (Jansen van Beek et al.,1986) and several chains of magnetic variometer stations have existed for special campaigns (e.g. for the International Magnetospheric Study (IMS)). From such networks in Canada and elsewhere, and from satellites, a knowledge of the complex character of the high latitude magnetic field has emerged (for example, Whitham and Loomer, 1957; Akasofu and Kamide, 1980).

In order to characterize the behaviour of the magnetic field over Canada for the purposes of developing a forecast, a simple index was required that provided a measure of the daily activity in each zone and that was readily calculable in a timely fashion. Thus, a daily character index DRX has been defined as the average of the 24 hourly ranges in the northward horizontal (X) component of the geomagnetic field, to be determined from representative observatories for all the zones over Canada (Hruska and Coles, 1987).

Three dominant zones having different magnetic field behaviour (sub-auroral, auroral, and polar cap) exist over Canada, with boundaries defined by physical features in the magnetosphere (Akasofu, 1968). Although the actual positions of the instantaneous boundaries between the zones are continually changing, the approximate undisturbed locations are indicated in Figure 1. As first-order indicators of the levels of activity, we have considered the DRX values from one representative observatory for each zone: Ottawa — subauroral; Fort Churchill - auroral; Resolute Bay — polar cap (Fig. 1).

Figure 2 illustrates the diversity in magnetic activity in these zones. This figure is based on an analysis of the index DRX; the observed DRX levels were sorted into bins, whose sizes are shown in the middle of the figure. The bin sizes were chosen by considering the typical high values of DRX in a zone and subdividing into eight bins. For each season (spring equinox, summer, fall equinox, and winter), the percentage occurrences of the bins are shown in a vertical bargraph. Results from two intervals of time are displayed in this fashion. First, twelve months (1982) near a peak in the 11 year cycle of magnetic activity, and second, twenty three months during 1984-86 in a quieter part of the 11 year cycle. Note the distinct differences in character a) between the 1982 interval and the 1984-86 interval, and b) from zone to zone. In general, the levels of activity are greater in the summer months and lower in the winter, though increased amounts of high level activity during the equinoxes are seen during the quieter part of the solar cycle.

THE BASIS OF THE FORECASTING PROCESS

The external variations of the geomagnetic field are related in a complex way to solar activity. Two types of geomagnetic activity have been recognized (Ol, 1971; Sargent, 1985):

1) Recurrent activity, including both very quiet and disturbed intervals, with a maximum of occurrence during the declining phase of the 11 year solar sunspot cycle;

2) Sporadic activity, of disturbed intervals, with a maximum of occurrence during and around the peak of the solar sunspot cycle.

Coronal holes are currently considered to be recurrent solar sources of the high speed solar wind (Krieger et al., 1973) which often result in geomagnetic storms (Sheeley et

al., 1976). Coronal holes constitute one of the most significant structures in the solar corona (Noyes, 1982). Whereas the corona normally radiates large amounts of X-ray and ultraviolet emissions, coronal holes are large regions conspicuous for the near total absence of these emissions. However, coronal holes are almost undetectable in visible light. They are not permanent features of the solar corona, but wax and wane with lifetimes that may range from a few weeks to months. There are long-lived coronal holes in the polar regions, that sometimes grow in size with equatorward extensions. Other coronal holes form at lower heliolatitudes and over their lifespan often change their latitudinal position significantly. Coronal holes that are closer to the equator of the solar disc tend to produce high-speed solar wind streams that have a greater probability of reaching and coupling with the earth's magnetosphere. The delay between a coronal hole crossing the central meridian of the solar disc and the onset of geomagnetic activity depends on the speed of the solar wind.

Using activity index DRX, described earlier, we examined in more detail the effects of coronal holes (CH), solar flares (SF) and disappearing filaments (DF) on magnetic activity in the three magnetic zones over Canada for the interval December 1984 to August 1986 during the solar activity minimum. In doing this, the magnetic response was characterized by the maximum increase δ in the values of DRX during the interval of five days following a solar event interpreted as a possible causative feature. This differs from the usual approach, in which the magnetic character itself must exceed a certain value to be counted in the analysis. Seven groups were established: Group I — CH; Group II — CH + SF; Group III — CH + DF; Group IV — SF; Group V — DF; Group VI — FL + DF; Group VII — SF + DF + CH.

Table 1 contains the median values of δ for increases in DRX associated with each of the seven Groups, for each zone. Significant increases in δ were considered to be those

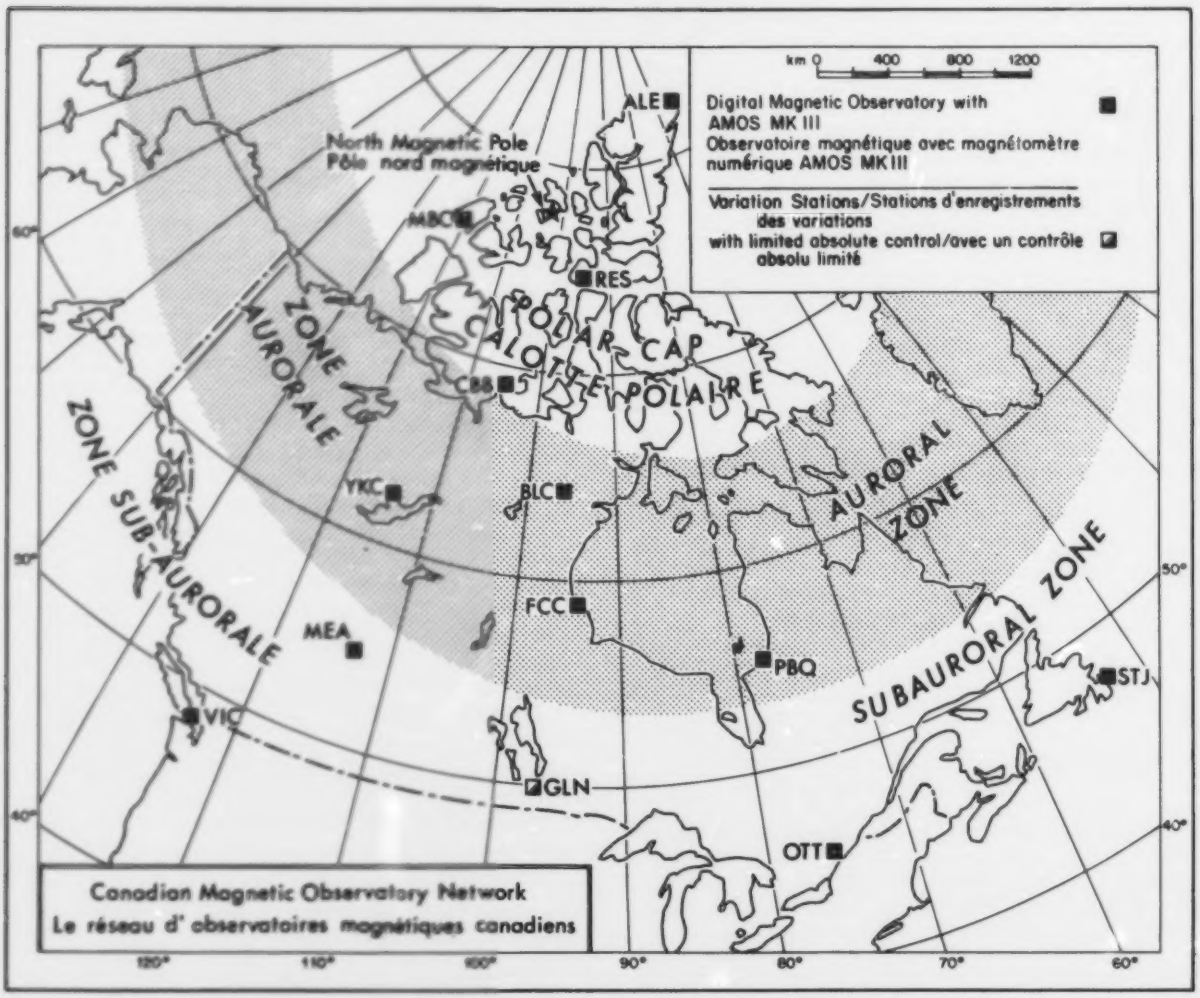

Figure 1. Map showing approximate positions of the three major magnetic zones over Canada, as discused in the text, and also the locations of the Canadian Magnetic Observatories.

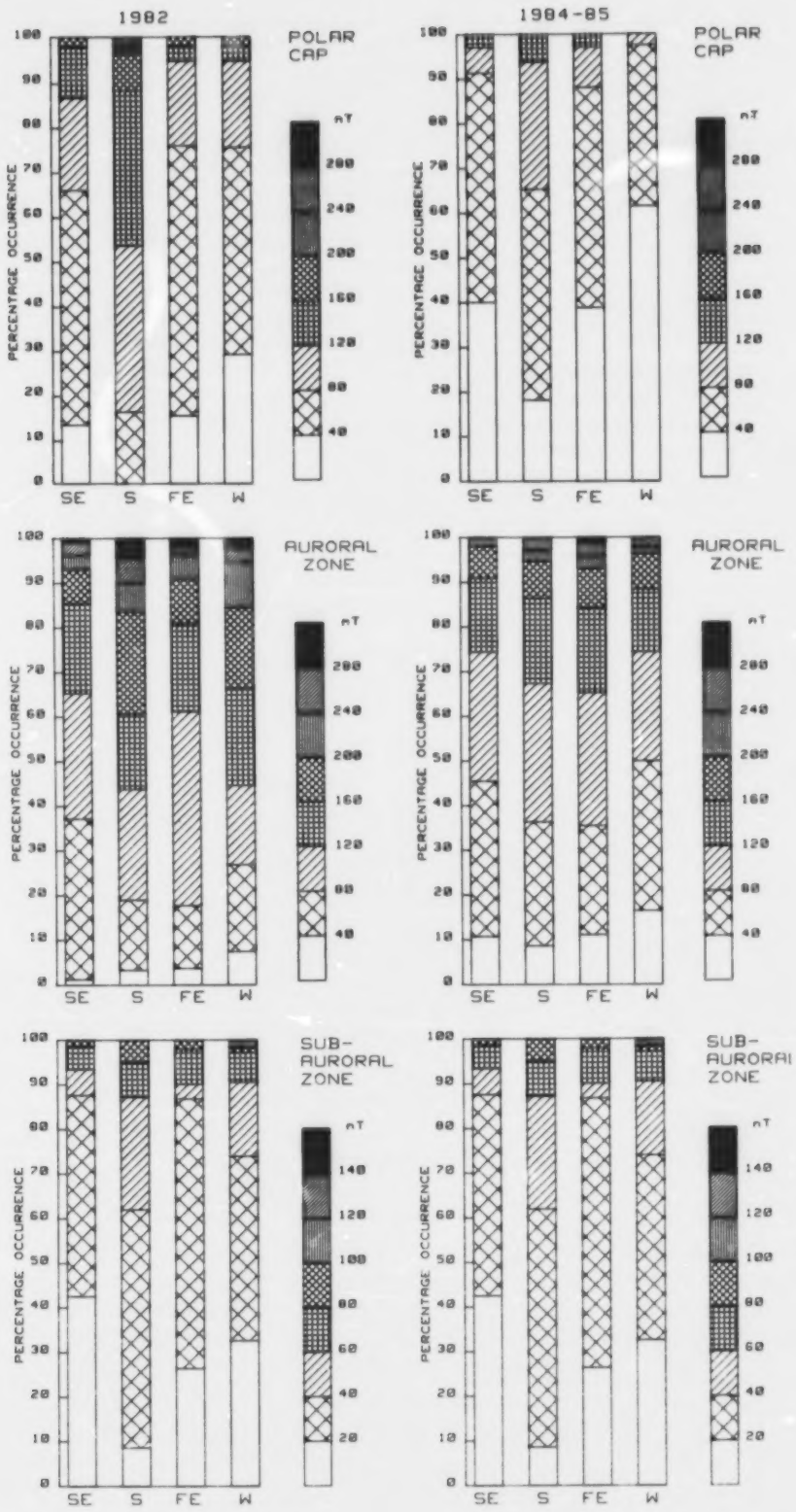

Figure 2. Bar-graphs showing the percentage occurrence of the various binned levels of magnetic activity during spring equinox (SE), summer (S), fall equinox (FE) and winter (W) for each of the three magnetic zones, during an active period (in 1982) and a quiet period (1984-1986) of the 11 year cycle. The data shown are derived from the representative observatories, Ottawa, Fort Churchill and Resolute Bay, from each major zone.

Table 1. Medians of δ

Solar phenomena	Magnetic zone subauroral	auroral	polar cap
		median nT	
Group I CH	17	64	25
Group II CH + FL	13	70	41
Group III CH + DF	8	54	25
Group IV FL	5	43	13
Group V DF	7	31	15
Group VI FL + DF	10	107	14
Group VII CH + FL + DF	15	92	48

Table 2. Percentage occurrence of significant δ associated with types of solar event

	subauroral	auroral	polar cap
	%	%	%
Group I CH	61	84	61
Group II CH + FL	64	100	82
Group III CH + DF	45	100	64
Group IV FL	44	78	44
Group V DF	33	69	33
Group VI FL + DF	50	80	40
Group VII CH + FL + DF	50	100	75

that exceeded half the bin-size for the zone (i.e. 10 nT for sub-auroral, 20 nT for the auroral and polar cap zones). Table 2 shows the percentage of occurrences of a particular Group that resulted in significant increases of δ (by this criterion), for the seven Groups.

The phenomenon 'opposite' to storms, namely, very quiet intervals, also shows a remarkable recurrent tendency. However, a causal link between these intervals and appropriate solar phenomena so far has not yet been established. Very quiet magnetic intervals can occur in spite of concurrent solar activity.

The preparation of a 27 day forecast is based on the recurrent activity. Available data on the solar features, including coronal holes, and on the past behaviour of the geomagnetic field are used. Past geomagnetic events are related where possible to observed solar phenomena. If the solar source is of a recurrent nature, e.g. a coronal hole, then the likelihood of its recurring again during the forecast period is assessed, taking into consideration the previous history of the source feature. In addition, terrestrial seasons are considered, since, as demonstrated in Figure 2, seasonal variations in the level of the geomagnetic response to the solar activity are significant. The position in the 11 year solar cycle is a factor also — not always, however, working in the forecaster's favour. Sargent (1985), for example, has shown how recurrent features predominate during the years around the minimum of solar activity, whereas they become obscured by sporadic activity during the years of solar maximum.

An example of the three zone forecast is shown in Figure 3; also included in the figure are occurrences of coronal holes, disappearing filaments and a solar flare. There is good agreement between forecast and actual values of the index DRX for all three zones. Two persistent coronal holes existed on the sun at this time giving rise to recurrent geomagnetic activity.

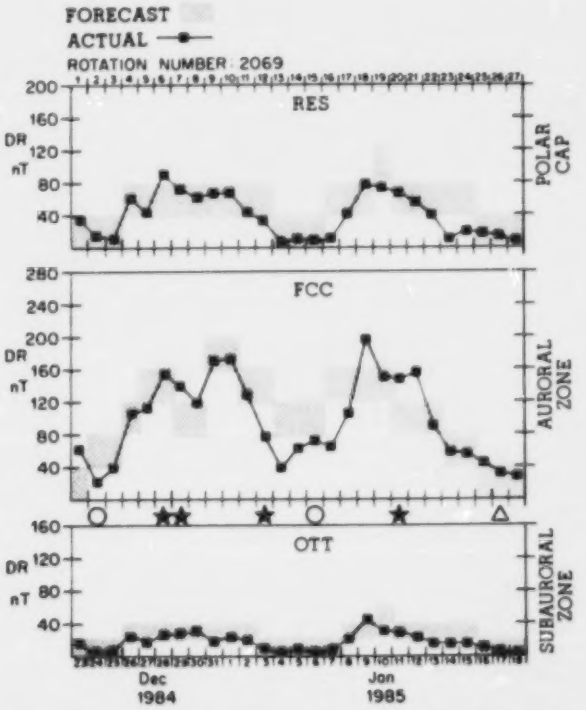

Figure 3. An example of forecasts of the index DRX for the three zones compared with observed values of DRX from the representative observatories in these zones. Coronal hole crossings of the solar central meridian are indicated by open circles; occurrences of disappearing filaments are shown by stars; a solar flare is indicated by an open triangle.

Table 3. Forecast verification statistics

Zone	Bin size nT	R bins	R nT	Mean 'obs' bins	Mean 'obs' nT	Q_N
Polar cap	40	0.72	29	1.64	66	0.10
Auroral	40	1.40	56	2.75	110	0.20
Sub-auroral	20	0.79	16	1.33	27	0.11

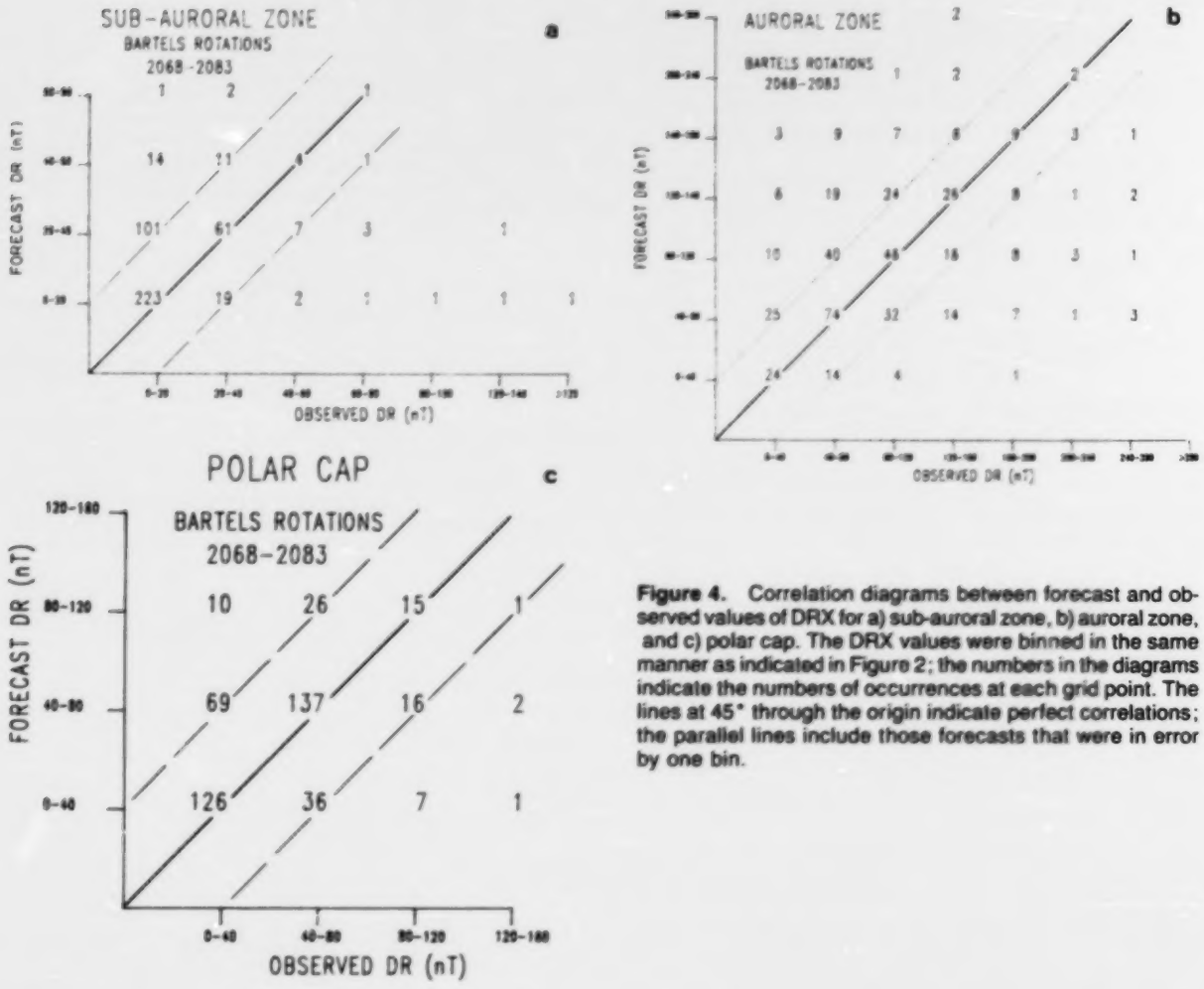

Figure 4. Correlation diagrams between forecast and observed values of DRX for a) sub-auroral zone, b) auroral zone, and c) polar cap. The DRX values were binned in the same manner as indicated in Figure 2; the numbers in the diagrams indicate the numbers of occurrences at each grid point. The lines at 45° through the origin indicate perfect correlations; the parallel lines include those forecasts that were in error by one bin.

FORECAST VERIFICATION

In assessing the validity of the forecasts, we have used the 'root mean square deviation', defined as

$$R^2 = [(\Sigma(\text{for} - \text{obs})^2)/N],$$

where 'for' is the forecasted value, and 'obs' is the observed value.

These statistics have been applied to the complete sequence of medium-term forecasts (up to 27 days in advance) for about 460 days in 1984-86, for each zone. In this case, the forecast and observed DRX values were binned in the same manner as indicated in Figure 2, and the statistics are shown in Table 3.

We have defined a normalized quantity, QN = R/(maxbin − 1), where 'maxbin' is the number of bins, or subdivisions, available. Q_N has a range from 0 to 1, values closer to 0 representing better forecasts. Of course, the choice of the number of bins influences the value of Q_N. In this study, the number of bins (eight) was chosen on the basis of the data shown in Figure 2. So long as we continue to use this system then we have a consistent measure for our forecasts. As an example to show the meaning of Q_N, consider that all forecasts were in error by 1 bin. In that case, R equals 1, and Q_N equals 0.14. Again, consider the case when all but one of 400 forecasts are correct, but the one is in error by 7 bins. Here, R equals 0.35, and Q_N equals 0.05. The values of Q_N for the three zones during the study interval are also given in Table 3.

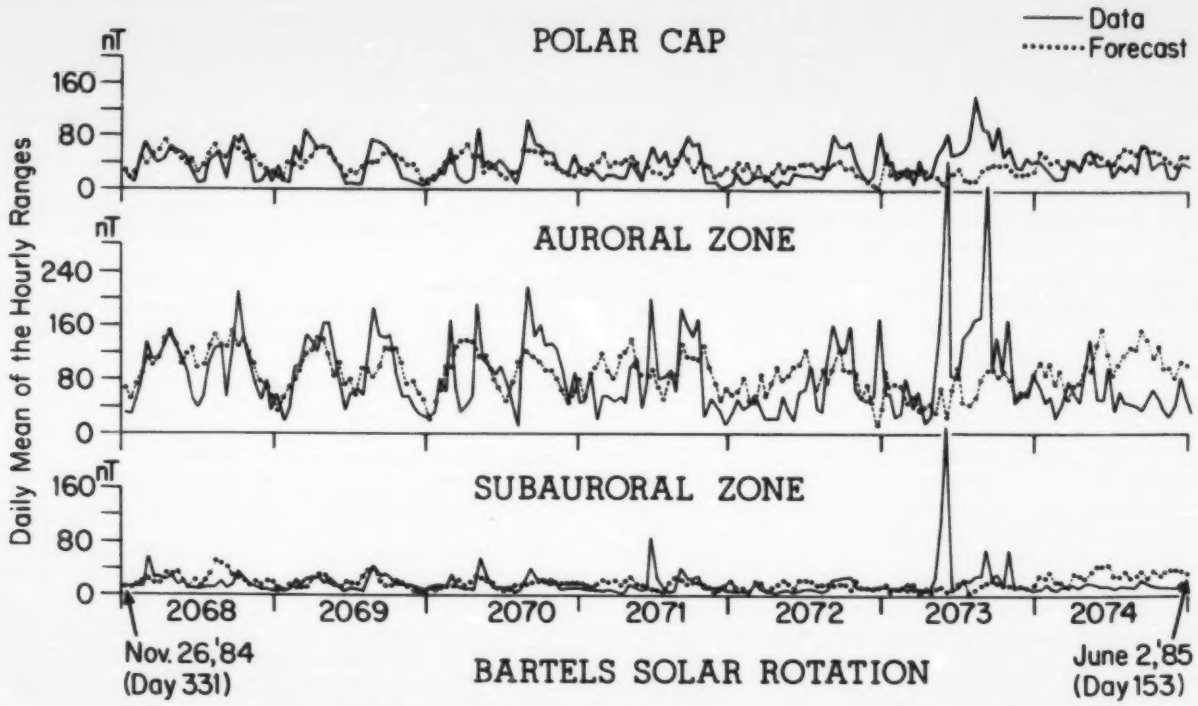

Figure 5. Forecast values (using linear prediction filter - dotted line) and actual data (solid line) for the three zones from 26, November 1984 to 2, June 1985.

Figure 4 shows in a graphical form the extent of correlation between forecasted and observed binned mean ranges DRX. The numbers on the graphs indicate the numbers of occurrences at each grid point. The lines at 45° through the origin indicate perfect correlations; the two parallel lines in each graph indicate those instances where the forecast was in error by only one bin. These displays show the incidence of correct or close forecasts, and also show instances when unforseen high disturbances occurred (when 'obs' > > 'for'; these generally correspond to non-recurrent solar events). Another point to be noted is the number of forecasts that are one bin higher than the observed bin, particularly at the lower levels. This occurs when the forecaster expected an event to recur with a particular intensity but it turned out to be weaker than in the previous solar rotation, or nonexistent.

THE LINEAR PREDICTION FILTER

Figure 5 shows the forecast values (dotted line) from the linear prediction filter and the actual data (solid line) from 26, November 1984 to 2, June 1985. The recurrent high geomagnetic activity, which is mainly due to the long-lived coronal holes co-rotating with the sun, is evident and is punctuated at times by sporadic activity. Except for these very active days due to sporadic activity, the forecasts generally reproduced the trends of the actual activity.

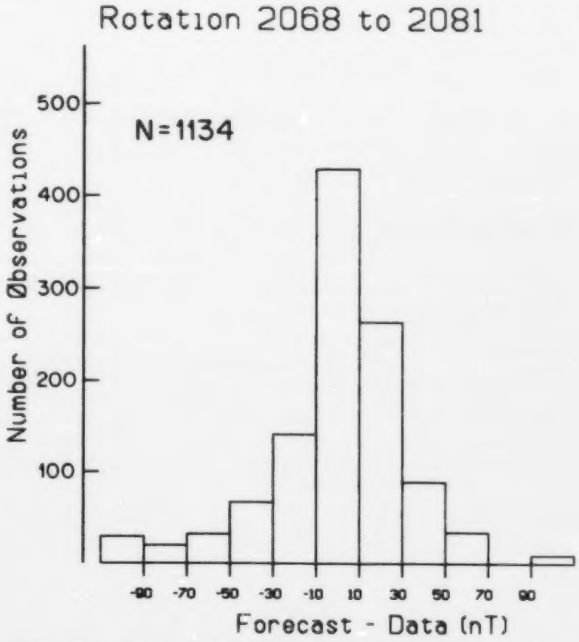

Figure 6. Histogram of differences between values forecast by linear prediction filter and actual data.

Another way to evaluate the deviations of the forecast values from the observed values is to construct a histogram of the difference between the two, as shown for the prediction filter in Figure 6. About 40 % of the observations lie the -10 nT and +10 nT range and 75 % are in the -30 nT to +30 nT range, emphasizing the good agreement between forecast and observed values.

While the filter cannot predict sporadic magnetic activities, the recurrent trends of magnetic activites are well forecast. The filter is therefore particularly useful in times of minimum solar activity when the recurrent tendency is most pronounced. The quantitative forecast values produced by this objective method serve as a useful aid to a forecaster.

CONCLUSIONS

A new forecasting approach has been developed that aims to anticipate the level of magnetic activity in three major magnetic zones over Canada. However, as in earlier formats, the main technique used in producing these new forecasts relies on the recognition of recurrent features in the solar activity and their interactions with the magnetosphere. The new forecast scheme shows good agreement with actual activity, although sporadic, non-recurrent events do cause disagreements on occasion. The forecasts for the sub-auroral and polar cap zones were in the correct bin on 64 % and 62 % of the days, respectively. However, the activity in the auroral zone is more variable, and although only 40 % of the forecasts were in the correct bin, 77 % were within 1 bin of the observed bin.

The concept of multi-zone forecasting is correct, but further adjustments to the technique are required. The use of a linear prediction filter aids in the production of a forecast by establishing recurrent trends.

During the period of development of this new forecast format, coronal holes have been the most reliable source of recurrent enhanced activity.

REFERENCES

Akasofu, S.-I.
1968: Polar and magnetospheric substorms; D. Reidel Publishing Company, Holland, 280 p.

Akasofu, S.-I. and Kamide, Y.
1980: Recent progress in studies of magnetospheric storms and substorms; Journal of Geomagnetism and Geoelectricity, v. 32, p. 585-615.

Campbell, W.H.
1973: Spectral composition of geomagnetic field variations in the period range of 5 min to 2 hr as observed at the earth's surface; Radio Science, v. 8, p. 929-932.

Feldstein, Y.I.
1986: A quarter of a century with the auroral oval; EOS, Transactions of American Geophysical Union, v. 67, no. 40, p. 761.

Hruska, J.
1979: Forecasts of geomagnetic activity by Ottawa magnetic observatory: their reliability and application; *in* Proceedings of International Solar-Terrestrial Predictions Workshop, ed. R.F. Donnelly; Space Environment Laboratory, Boulder, v. 1, p. 398-405.
1983: Forecasts of geomagnetic activity; Division of Seismology and Geomagnetism, Earth Physics Branch, Ottawa, Internal Report 83-4, p. 1-27.

Hruska, J, and Coles, R.L.
1987: A new type of magnetic activity forecast for high geomagnetic latitudes; Journal of Geomagnetism and Geoelectricity, v. 39, p. 521-534.

Jansen van Beek, G., R.L. Coles, and L.R. Newitt
1986: Annual report for magnetic observatories — 1984; Earth Physics Branch, Ottawa, Geomagnetic Series No. 30.

Krieger, A.S., Timothy, A.F., and Roelof, E.C.
1973: A coronal hole and its identification as the source of a high velocity solar wind stream; Solar Physics, v. 29, p. 505-525.

Lam, H.-L.
1987: Forecasts of geomagnetic activity in Canada by linear prediction filtering; Journal of Geomagnetism and Geoelectricity, v. 39, p. 535-542.

Moe, K, and Nebergall, D.
1969: Variation of geomagnetic disturbance with latitude; Journal of Geophysical Research, v. 74, p. 1305-1307.

Noyes, R.W.
1982: The Sun — Our Star; Harvard University Press, Cambridge, Mass., 263 p.

Ol, A.I.
1971: Physics of the 11-year variation of magnetic disturbances; Geomagnetism and Aeronomy, v. 11, p. 549-551.

Sargent III, H.H.
1985: Recurrent geomagnetic activity: evidence for a long-lived stability in the solar wind; Journal of Geophysical Research, v. 90, p. 1425-1428.

Space Environment Services Center
1985: Preliminary report and forecast of solar geophysical data; NOAA-USAF Space Environment Services Center, Boulder, Colorado, Descriptive Text, SESC PRF 511.

Sheeley, Jr., N.R., Harvey, J.W., and Feldman, W.C.
1976: Coronal holes, solar wind streams, and recurrent geomagnetic disturbances: 1973-1976; Solar Physics, v. 49, p. 271-278.

Weiner, N.
1949: Extrapolation, interpolation and smoothing of stationary time series with engineering applications; Technical Press of the Massachusetts Institute of Technology and John Wiley and Sons Inc., New York, 163 p.

Whitham, K., and E.I. Loomer
1957: Characteristics of magnetic disturbance at the Canadian Arctic observatories; Publication of the Dominion Observatory, Ottawa, v. 18, no. 12.

Whitham, K., E.I. Loomer, and E.R. Niblett
1960: The latitudinal distribution of magnetic activity in Canada; Journal of Geophysical Research, v. 65, p. 3961-3974.

A mathematical model for optimization of sample geometry for radiation measurements

K. Nimalasiri De Silva
Mineral Resources Division

De Silva, K.N., A mathematical model for optimization of sample geometry for radiation measurements; in Current Research, Part F, Geological Survey of Canada, Paper 88-1F, p. 39-43, 1988.

Abstract

Sample geometry becomes a critical factor for optimum counting performance during radiation measurements, especially when the distance between the sample and the detector is ralatively small. A mathematical formula was derived to calculate relative counting efficiency as a function of radius of the sample for the most commonly used cylindrical geometry. Underlying principles of the model are applicable to other well defined geometries. Optimum radius of the sample is idependent of surface area of the detector and depends on its total volume and distance between sample and the detector. For a typical case, selection of optimum dimensions is shown to provide a factor of 3 higher counting efficiency than that obtained with dimensions chosen according to the conventional visual judgement.

Résumé

La géométrie de l'échantillon devient un facteur critique pour le rendement optimal du comptage au cours des mesures du rayonnement, en particulier lorsque la distance entre l'échantillon et le détecteur est relativement petite. On a établi une formule mathématique pour calculer l'efficacité relative du comptage qui est une fonction du rayon de l'échantillon à figure géométrique la plus courante, soit cylindrique. Des principes sous-jacents du modèle s'appliquent à d'autres figures géométriques bien définies. Le rayon optimal de l'échantillon ne dépend pas de la surface du détecteur mais de son volume total et de la distance entre l'échantillon et le détecteur. À titre d'exemple, le choix des dimensions optimales doit produire un rendement de comptage supérieur d'un facteur de 3 par rapport à celui obtenu avec des dimensions choisies par simple examen visuel.

INTRODUCTION

In radiation counting many measurements requires that low levels of radionuclides be determined in a wide range of media. Examples of such requirements may be found in monitoring of the environment and effluent discharge of nuclear power plants, monitoring of food products for human uptake, measurement of natural radioactivity in the environment, and quantification of radionuclides in activation analysis, especially when long lived nuclides are monitored. In most cases the total activity may be due to a number of radionuclides. This demands the need not only for measuring the total activity but also to identify and quantify the individual isotopes present. This requires a high resolving power and high efficiency of the detector system.

Optimum measurement conditions depend mainly on (i) resolving power of the detector (ii) signal to noise ratio of the system (iii) counting efficiency of the measurement system including positioning and geometry of the sample. After the highly successful development of high purity silicon and germanium single crystals for transistor technologies, Si and Ge radiation detectors have been developed to achieve most of the above goals (Bertolini and Coche, 1968; Goulding and Pehl, 1974; Knoll, 1979).

In spite of the high performance or sophistication of the detector itself, an important factor that determines the total system performance is the counting geometry (positioning of the sample relative to the detector and its shape) which is at the discretion of the user. This becomes extremely important when the size of the sample is quite large compared to the other relative dimensions such as distance between the sample and the detector. For low level activity measurements it is important to use the largest possible sample size available and also to position the sample "as close as possible" to the detector in order to achieve the maximum detection power.

Studies in exploration geochemistry currently underway at the Geological Survey of Canada require analysis of biogeochemical samples by instrumental neutron activation analyis for a variety of trace elements (Dunn, 1986). It is necessary to use large samples of, for example, powdered vegetation to optimize precision and the detection limits, and to avoid inhomogeneity problems associated with small samples which may provide such poor statistics as to be unsuitable for exploration purposes. Usually, 8 g of sample is pelletized into a cylindrical disc and used for INAA (Dunn et al., 1987). In such a situation one has to decide upon the diameter or the height of the pellet for optimum counting efficiency. This is a general problem even in other situations such as counting a bulk liquid where it would be desirable to estimate the optimum diameter of the beaker/container that should be used for counting. Also, in the case of natural radioactivity measurements, one may want to decide upon the optimum shape of the container to measure the activity of a powdered geological material.

Although the problem is fundamental, little attention has been paid to the optimization of sample geometry. Becker (1974) has experimentally investigated accuracy and precision in activation analysis in relation to positioning a particular sample above the detector. However, no detailed study has been reported regarding optimization of the sample shape, perhaps due to the fact that selection of optimum dimensions by visual judgment might appear to be very straight forward although it may not be the case. This paper describes a simple mathematical model to calculate the optimum dimensions of the sample which can be applied to a wide range of the above discussed situations.

THEORY

It is common practice that solid samples are prepared as pellets or circular discs, or contained in a cylindrical vial. The liquid samples are usually counted in a beaker or a cylindrical vial. Even the paper discs can be considerd as a limiting geometry of a cylinder. Therefore, this discussion is confined to samples of the most commonly used "cylindrical shape", although the principles can be applied to any other well defined geometry.

Consider a cylindrical sample with the radius r and thickness t located at a distance h above the detector as shown in Figure 1. The most commonly used coaxial orientation of the detector and the sample is assumed. For simplicity of the mathematics, thickness of the active area of the detector is assumed to be negligible which will be discussed later.

Consider a point source, P, located at a horizontal distance, x, from the axis and a vertical distance y from the surface of the detector (Fig. 1). The flux of photons or charged particles emanating from point P which falls on the detector surface is proportional to the incident solid angle of point P on the detector surface. The expression for the solid angle S for point P can be written as:

$$S = \frac{A}{d^2} \sin \Theta$$

$$= \frac{A\ y}{(x^2 + y^2)^{3/2}} \quad (1)$$

Where, A is the area of the detector surface and d is the distance between point P and the centre of the detector surface.

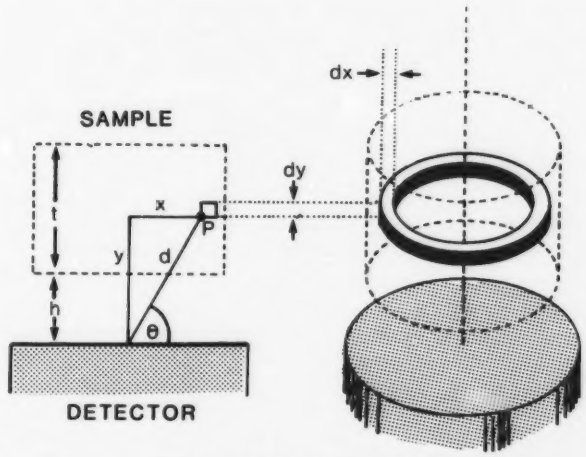

Figure 1. Definition of the mathematical variables

Let us consider, a ring of radius, x, with the horizontal thickness dx and vertical thickness dy, located at a distance y above the detector as shown in Figure 1. If dx and dy are infinitesimally small, the volume of the ring, dV, can be written as:

$$dV = 2\pi x \, dx \, dy \quad (2)$$

If the concentration of the radioactive nuclide in the sample is p, then the photon flux, dQ, emanating from volume dV and falling on the detector can be written as:

$$dQ = C \, p \, S \, dV \quad (3)$$

Where C is a proportionality constant which depends on factors such as the rate of radioactive decay. By combining the above equations,

$$dQ = C \, p \, \frac{A \, y}{(x^2 + y^2)^{3/2}} \, 2\pi x \, dx \, dy \quad (4)$$

Therefore, the portion of the total flux falling on the detector surface, Q(r,t,h), that emanates from the whole sample of radius, r and the thickness, t which is positioned at a height, h above the detector, can be written as

$$Q(r,t,h) = K \int_{x=0}^{r} \int_{y=h}^{h+t} \frac{x \, y}{(x^2 + y^2)^{3/2}} \, dx \, dy \quad (5)$$

Where,

$$K = 2\pi \, C \, p \, A \quad (6)$$

By integrating equation (5),

$$Q(r,t,h) = K \{t - [r^2 + (h+t)^2]^{1/2} + [r^2+h^2]^{1/2}\} \quad (7)$$

$$= K \, . \, F(r,t,h) \quad (8)$$

This gives the expression for integrated flux, Q(r,t,h) of photons or charged particles falling on the detector surface emitted by the whole sample. It is assumed that the sample is a "soft material" and therefore, the attenuation of the photon flux through the sample is negligible.

For selecting the optimum value of r for a given t and h, the above equation can be used to find the value of r that gives the maximum F(r,t,h) and therefore the maximum counting efficiency. However, in practice, what one would need to know is the optimum radius, r_o for a given volume of sample; i.e. r and t in the above equation would be dependent variables. If t is substituted in terms of r and volume, V the F(r,t,h) term (from equations (7) and (8) can be converted to F(r,V,h) as

$$F(r,V,h) = V/\pi r^2 - [r^2 + (h + V/\pi r^2)^2]^{1/2} + [r^2+h^2]^{1/2} \quad (9)$$

In order to determine the optimum radius, r_o using the above equation, we can take one of two approaches. The mathematical approach is to differentiate the above equation and find the value of r that satisfies the condition, $dF/dr = 0$. However, this would result in a relatively complex mathematical expression for r_o.

The second approach would be to use a simple computer program to compute F(r,V,h) using equation (9) for different numerical values of r and find the value of r that gives maximum F(r,V,h) for the desired accuracy. Since the second approach can also be used to obtain more information about the numerical values of F, which is a measure of relative counting efficiency, it is preferable and simpler to use the numerical method to calculate r_o.

DISCUSSION

Figure 2 shows plots of F(r,V,h) versus r at several h values (0 — 2 cm) away from the detector calculated assuming a sample volume of 10 cm^3. As one would expect, the value of F(r,V,h) passes through a maximum and it approaches 0 when the value of r reaches its extreme values 0 or oo. Equation (7) has other important ramifications, some of which may appear to be contrary to intuition.

Since the term A, the area of the detector surface, does not appear in the variable portion of the equation (8), F(r,V,h), it is apparent that the optimum geometry for a sample of a given volume is independent of the actual surface area of the detector, although a larger A can give us a better absolute efficiency as the value of K in equation (8) is directly proportional to A. This means that the optimum dimensions for a given sample remain constant whether the relative size of the detector is significantly smaller or larger than the sample. Since the actual physical size of the detector surface is immaterial, the optimum sample shape does not vary from one detector to the other.

It can be seen from Figure 2 that, as the distance between the sample and the detector, h, increases the maximum attainable counting efficiency gradually decreases, as expected. The shift in the peak position of the curves to the right as h increases , shows that the optimum radius, r_o increases with h. Numerically calculated r_o, at different heights using equation (9 are given in Table 1. It is evident from Figure 2 and Table 1 that the variation of r_o within a practical range of h (eg. 0 — 2 cm) is relatively small indicating that the optimum dimensions selected for a certain height above the detector is also applicable to the other heights with only a small sacrifice in the maximum efficiency. For example, counting a sample at h=1.0 cm with the optimum geometry calculated for h=0.2 cm (r_o = 1.32 cm) would enable us to achieve 96 % of the maximum attainable efficiency for that height, sacrificing only 4 % of the efficiency. This also relieves the constraint of knowing the exact distance to the active surface area of the detector from the sample for the calculation. In deriving equations (7) and (9) it was assumed (Fig. 1) that the thickness of the active region of the detector is small. The relatively small dependency of r_o on h also validates the above assumption.

It can be seen from the plots in Figure 2 that selection of the optimum radius becomes more and more critical as the sample gets closer to the detector. Conversely, the significance of optimum dimensions diminishes as the sample is positioned farther from the detector. Therefore, in situations where one is uncertain about the height that is going to be used for the measurement, it is advisable to optimize the dimensions according to the shortest distance that is anticipated. For example, this situation may arise in activation analysis where the same sample may be counted more than once in order to cover a series of radionuclides with a wide range of half-lives. Then the measurement of the short lived

nuclides may be performed at a finite distance from the detector to avoid problems related to analyser dead-time caused by high activity. After a longer decay period, the second counting can be done for long lived nuclides with the sample being kept as close as possible to the detector since the total activity is usually very low.

It was mentioned that the optimum radii (r_o) for a given sample size do not vary significantly within a range of h values. However, improper selection of sample geometry can have a significant detrimental effect for the counting efficiency attainable at a particular height. This can best be illustrated visually by taking a typical example. Figure 3 shows three sets of dimensions (drawn to scale) that one may select for counting a sample which has a volume of 5 cm^3. Although it is immaterial for the optimum dimensions, let us assume the radius of the detector surface is 2.5 cm. Assuming the height, h, as 0.2 cm the calculated relative counting efficiencies (normalized to the optimum) are 0.56, 1.00 and 0.39 for the sample radii 0.50, 1.06 and 2.5 cm, respectively (Fig. 3a-c.). In order to bring as much sample material to the closest vicinity of the detector surface, one may intuitively decide to prepare the sample with a diameter to match that of the detector as shown in Fig 3c. It can be seen that such a selection of sample shape can result in a sensitivity loss, therefore a poorer detection limit, by about a factor of 3 as compared to the sensitivity that can be obtained with the optimum geometry. This factor would increase higher as the sample volume decreases for the above values of radii.

Table 1. Optimum sample radii (r_o) calculated for different distances (h_o) between the sample and the detector. (Sample volume = 10 cm^3)

h_o (cm)	r_o (cm)
0.0	1.25
0.2	1.32
0.4	1.38
0.6	1.44
0.8	1.49
1.0	1.55
1.2	1.59
1.4	1.64
1.6	1.68
1.8	1.72
2.0	1.76

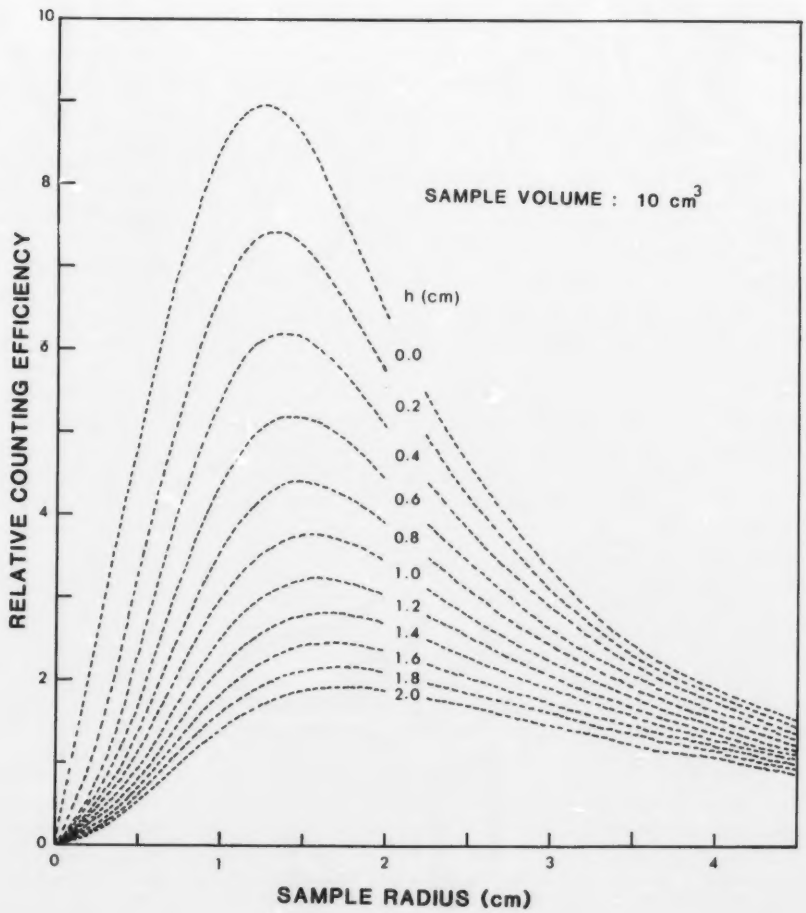

Figure 2. Variation of the relative counting efficiency as a function of the sample radius, r. (h = distance between the sample and the detector, sample volume = 10 cm^3)

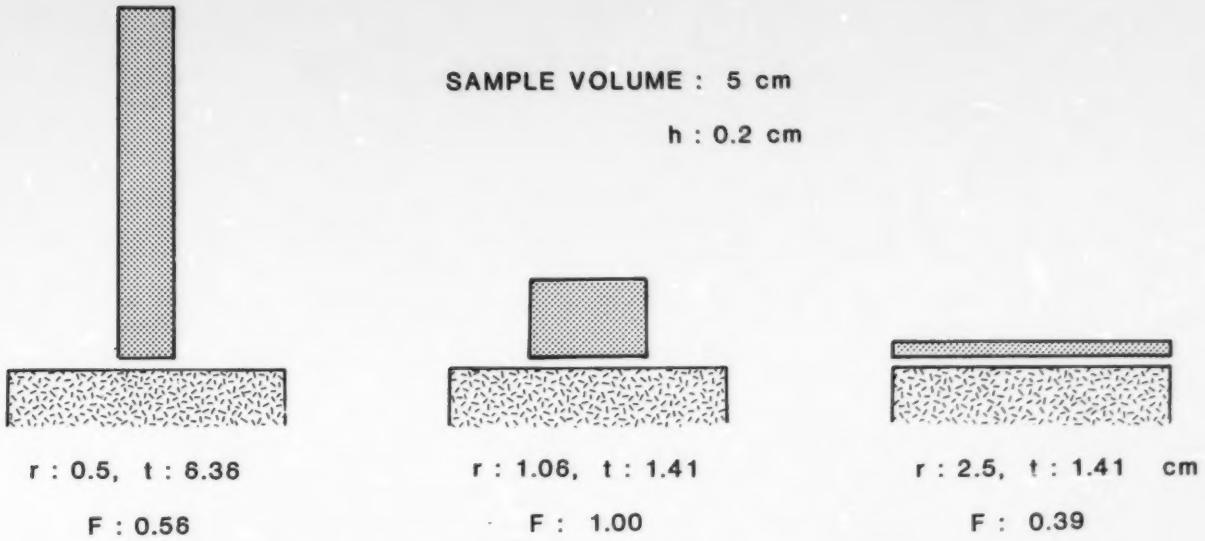

Figure 3. Relative counting efficiencies for a typical set of sample geometry. (sample volume = 5 cm^3, h = 0.2 cm, detector diameter = 2.5 cm)

SUMMARY AND CONCLUSIONS

The mathematical model provides a simple and effective way to select the optimum dimensions of a sample for maximum counting efficiency. Furthermore, some important inferences can be made that may not be obvious upon visual judgement. For a sample of a given volume, the optimum dimensions are independent of the actual size of the detector. Selection of optimum dimensions becomes more critical as the sample approaches to the detector. Within a reasonable range of distances between the detector and the sample, the optimum geometry does not vary significantly, indicating that the dimensions calculated for one height can be used for another with only a small sacrifice in the maximum possible counting efficiency. However, in selecting optimum dimensions suitable for a range of distances between the sample and the detector, it is more appropriate to calculate the optimum dimensions according to the anticipated minimum distance from the detector than otherwise.

For simplifying the model, the attenuation of the radiation flux during the passage through the sample itself was not considered here. However, for common matrices which can be considered as "soft matrices", especially for photon counting, this can be neglected. Should there be any need, an attenuation factor also can be incorporated in the model with an added complexity to the mathematical derivation which may not have a significant effect on the final result for the optimum dimensions.

Although the principles behind the model are fundamental it permits us to make important deductions about the counting geometry in radiation measurements in general. While this discussion was limited to the most commonly used geometry "the cylindrical shape", the principles can be applied to any geometry provided the shape of the sample can be defined mathematically.

ACKNOWLEDGMENTS

The author thanks G.E.M. Hall, A.G. Plant, D.C. Gregoire and C.E. Dunn for reviewing the manuscript and for their comments. U. Mampitiya is thanked for his helpful discussions.

REFERENCES

Becker, D.A.
1974: Proceedings of the International Conference on Nuclear Methods in Environmental Research, University of Missouri, USA, p. 69-74.

Bertolini G. and Coche, A.
1968: Semiconductor Detectors; North Holland Publishing Co., New York City.

Dunn, C.E.
1986: "Gold Exploration in Nothern Saskatchewan by Biogeochemical methods" *in* "Gold in Western Shield, ed. L. Clark; Canadian Institue of Mining and Metallurgy, Special Volume 38, p. 418-434.

Dunn, C.E., Hall, G.E.M., and Hoffman, E.L.
1987: Platinum Group Metals in Common Plants of Nothern Forrests: Developments in Analytical Methods, and the Application of Biogeochemistry to Exploration Strategies, Journal of Geochemical Exploration.

Goulding F.S. and Pehl R.S.
1974: "Semiconductor Detectors", Section IIIA, Nuclear Spectroscopy and Reactions, ed. J. Cerny; Academic Press.

Knoll, G.F.
1979: Radiation Detection and Measurement; John Wiley and Sons.

Forecasts of Pc5 magnetic pulsations

H.-L. Lam
Geophysics Division

Lam, H.-L., Forecasts of Pc5 magnetic pulsations; in Current Research, Part F, Geological Survey of Canada, Paper 88-1F, p. 45-51, 1988.

Abstract

Pc5 magnetic pulsations are the ambient fluctuations of the earth's magnetic field with periods in the 2 to 10 minutes range. While they are sensitive indicators of the dynamic changes of the magnetosphere and can be used for geomagnetic sounding for the study of conductive structures of the earth, they are the unwanted background noise for magnetic exploration surveys. A prior knowledge of the levels of Pc5 activities is therefore useful. By using the results in this study, it is possible to infer the future levels of Pc5 pulsational activity. This study also indicates that during the course of a day, morning would be appropriate for using Pc5 pulsations to probe buried conductive targets, while afternoon would be optimal for conducting magnetic surveys.

Résumé

Les impulsions magnétiques Pc5 sont les fluctuations ambiantes du champ magnétique terrestre dont les périodes varient de 2 à 10 minutes. Bien qu'ils constituent des indicateurs sensibles des changements dynamiques de la magnétosphère et qu'ils peuvent être utilisés dans le sondage géomagnétique visant à étudier les structures conductrices de la Terre, ils correspondent aux bruits de fond non voulus des levés d'exploration magnétique. C'est pourquoi une connaissance préalable des niveaux d'activités Pc5 est utile. En utilisant les résultats de cette étude, il est possible de déduire les niveaux futurs de l'activité pulsationnelle Pc5. Cette étude indique en outre que le matin serait la période du jour la plus appropriée pour l'utilisation des impulsions Pc5 dans le sondage des cibles conductrices enfouies tandis que l'après-midi serait la meilleure période pour réaliser des levés magnétiques.

INTRODUCTION

The earth's magnetic field is not constant but fluctuates with time with periods ranging from small fractions of a second to millions of years. Oscillations with a period range from 0.2 to 10 min. (corresponding frequency range from 1.7 to 5000 mHz) are generally referred to as magnetic pulsations. The pulsations are further classified by period and character into Pi1, Pi2 (for irregular pulsations) and Pc1, Pc2, Pc3, Pc4 and Pc5 (for continuous pulsations). Details of the nomenclatures and general information on pulsations are given by Jacobs (1970). Among the different classes of pulsations, Pc5 has the longest period (150 to 600s, with the corresponding frequency range of 1.7 to 6.7 mHz) and largest amplitudes which can reach several hundred nT. Therefore, this class of pulsations produces the most severe effects on geomagnetic surveys. Unfortunately, as lamented by Reford (1979), the application of pulsation studies to magnetic exploration surveys seems to have been largely neglected. This paper is an attempt to address this concern.

An example of Pc5 recorded at high latitudes in Fort Churchill, Manitoba (67.8 deg N and 323.0 deg E, measured in geomagnetic co-ordinates) in the auroral zone is shown in Figure 1. Universal Time (UT) is used as the time scale in this plot. A conversion to Local Time (LT) is to subtract UT by 6 h. It can be seen that the oscillations are rather continuous, with a wave train consisting of a series of damped fluctuations lasting about an hour or more. The large amplitude oscillations of Pc5 can be noted from this plot. Pc5 pulsations are basically a daytime phenomena. A compressed plot of the bandpass filtered data showing pulsational activities in Fort Churchill for the entire daytime sector is shown in Figure 2. 18 UT is local noon. It can be seen that the oscillations tend to occur in bursts and the difference in the levels of pulsational activity between morning and afternoon is clearly discernible. It is now well established that the occurrence frequencies and amplitudes of Pc5 maximize in the auroral zone (65 deg — 70 deg geomagnetic latitude) (e.g. Jacobs and Sinno, 1960; Hirasawa, 1970; Gupta, 1974). In particular, Pc5 pulsations are localized in latitude and colocated with the auroral electrojets, the activity being enhanced in conjunction with a recovery of the auroral electrojet from a period of prior activity (Lam and Rostoker, 1978). The localized nature of Pc5 activity in longitude has also been established (Lam, 1980). However, the generation mechanisms of these pulsations are still uncertain (see Southwood and Hughes, 1983 for review).

In space physics geomagnetic pulsations are topics of challenging studies for solar-terrestrial interactions with a real possibility of using them as natural probes for remote sensing of the magnetosphere. In solid earth physics they are used for carrying out induction studies of earth's conductive structures. Magnetic pulsations are useful mainly in magnetotelluric studies of the sedimentary rocks of the crust to depths of a few kilometres Lam et al. (1982) have modelled the induction responses of buried 3D-conductive anomalies to source fields with Pc5 frequencies. Despite these virtues, magnetic pulsations are the unwanted ambient noise for geomagnetic surveys (Reford, 1979) which are concerned with the spatial variations of the geomagnetic field. But, whatever the undertaking on which pulsations have influence it is desirable to have a prior knowledge of the levels of the pulsational activity so that proper planning can be made.

APPROACH

Despite advances in the study of the characteristics of Pc5 pulsations, their origins and generation mechanisms are still not fully understood. It would thus seem that prediction of Pc5 pulsations is an improbable task. Moreover, satellite data such as solar wind velocities, interplanetary magneric field

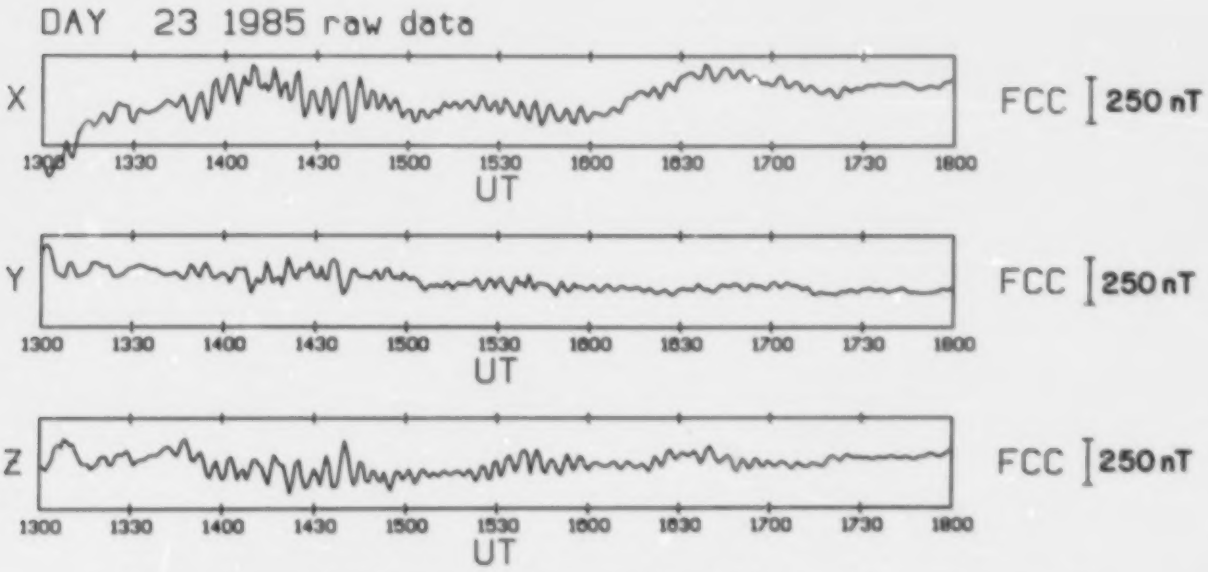

Figure 1. An example of Pc5 magnetic pulsations recorded at high latitudes in the auroral zone station of Fort Churchill, Manitoba. Note the large amplitude of pulsations.

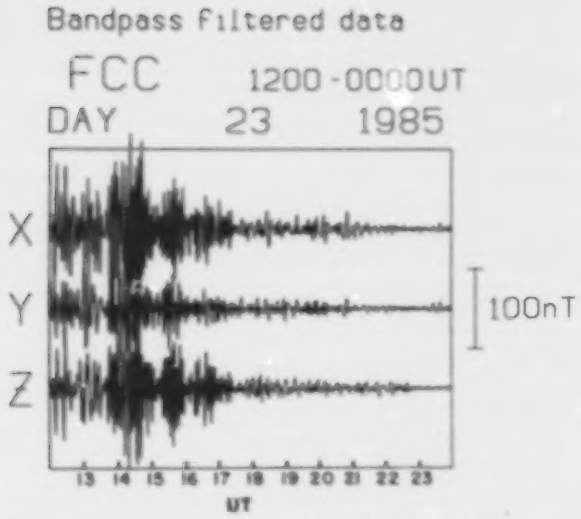

Figure 2. A compressed plot of Pc5 pulsations for the entire daytime sector. Note the intense pulsational activities in the morning and reduced activities in the afternoon. The data were bandpass filtered. 18 UT is local noon.

variations, magnetospheric field and particle changes that can be compared with ground pulsations are not readily available for routine use to predict pulsations even if forecasting techniques based on their empirical relations could be established. On the other hand, since Pc5 pulsations tend to intensify during intervals of recovery from previous higher levels of magnetospheric activity (Lam and Rostoker, 1978), it may not be unreasonable to relate Pc5 pulsations to a parameter that is a manifestation of such levels of activity. Since disturbed geomagnetic fields correspond to enhanced magnetospheric activity which has the effect of intensifying preexisting current systems, I therefore adopt a practical and pragmatic approach by relating Pc5 activities to the daily mean of the hourly ranges in the X component of the geomagnetic field in the auroral zone. This particular parameter is also referred to as the DRX index (Hruska and Coles, 1987; Lam, 1987). The DRX indices are routinely forecast for 27 day every 3 weeks by the Geophysics Division, Geological Survey of Canada, and give an indication of the general "magnetic weather" condition which is a manifestation of the levels of magnetospheric activity. As DRX is a predictable parameter and Pc5 activities can be related to it, as will be shown later in this paper, we can speak of the forecasts of Pc5 magnetic pulsations in this sense.

In this study, an entire year (1985) of digital magnetic data recorded in Fort Churchill, (67.8 deg N and 323.0 deg E, measured in geomagnetic co-ordinates) in the auroral zone have been spectrally analyzed day by day and hour by hour for the entire daytime sector for Pc5 pulsation activity for comparison with the auroral zone DRX. It is worth noting that the year 1985 is at a period of minimum solar activity. Power spectral estimates were computed by means of the Fast Fourier Transform algorithm after the data had been detrended by a band pass filter and tapered by a cosine-bell data window. The temporal length of the data window was set at 1 h which is appropriate for studying Pc5 pulsations that have stationary spectral characteristics over periods of an hour or more. The Pc5 powers seem to group into two bands: the 1-3 mHz band (period of 333 to 1000s) and the 3-6 mHz band (period of 166 to 333s). It is therefore more appropriate to separate the Pc5 activities into ghese 2 spectral bands and examine them separately.

RESULTS

Figure 3 shows plots of the sum of the hourly Pc5 powers vs DRX for the two spectral bands. Here the Pc5 powers refer to the power of the largest spectral peak within the 1-3 mHz or 3-6 mHz bands. The sums were calculated separately for the entire day, morning and afternoon. A regression line was fitted through the data in each plot. The data do not suggest that the relation between Pc5 power and DRX is other than linear. In every case, the regression line gives a positive intercept in the DRX axis, indicating that there is a threshold for Pc5 activities. The correlation coefficients R are also shown on the diagram. The higher R values for the 1-3 mHz band than the 3-6 mHz band implies a stronger linear trend between Pc5 power and DRX values for the lower frequency band. The powers in the afternoon sector are lower than those in the morning sector particularly in the 3-6 mHz frequency band. One could use the plots in Figure 3 to infer Pc5 powers from the forecast DRX. The regression equations for predicting Pc5 powers from DRX are given as follows:

Y = 13.3DRX-500 (to predict daily sum of Pc5 power in 1-3 mHz band)

Y = 10.4DRX-470 (to predict morning sum of Pc5 power in 1-3 mHz band)

Y = 4DRX-100 (to predict afternoon sum of Pc5 power in 1-3 mHz band)

Y = 8DRX-350 (to predict daily sum of Pc5 power in 3-6 mHz band)

Y = 7.3DRX-330 (to predict morning sum of Pc5 power in 3-6 mHz band)

Y = 1.2DRX-50 (to predict afternoon sum of Pc5 power in 3-6 mHz band)

Figure 4 shows variations of Pc5 powers in the two spectral bands as a function of UT (local noon being at 18UT) for three different ranges of DRX values. The three different ranges of DRX values correspond to geomagnetic conditions that are quiet (for DRX between 0 and 60nT), unsettled (for DRX between 60 and 160nT) and active (for DRX greater than 160nT). To produce these plots, Pc5 powers were sorted according to the corresponding DRX values. Powers were plotted on a linear scale up to 1000 and log scale above as shown on the right of the plot. On the left is a scale for DRX. Th average DRX for the events in a given DRX range is shown by the top of the rectangle at the left of each plot. It can be seen that Pc5 powers are generally low, particular in the 3-6 mHz band, throughout the day for quiet conditions. In the 1-3 mHz band, Pc5 powers are more enhanced for both the unsettled and active conditions throughout the day although there is a greater tendency for larger

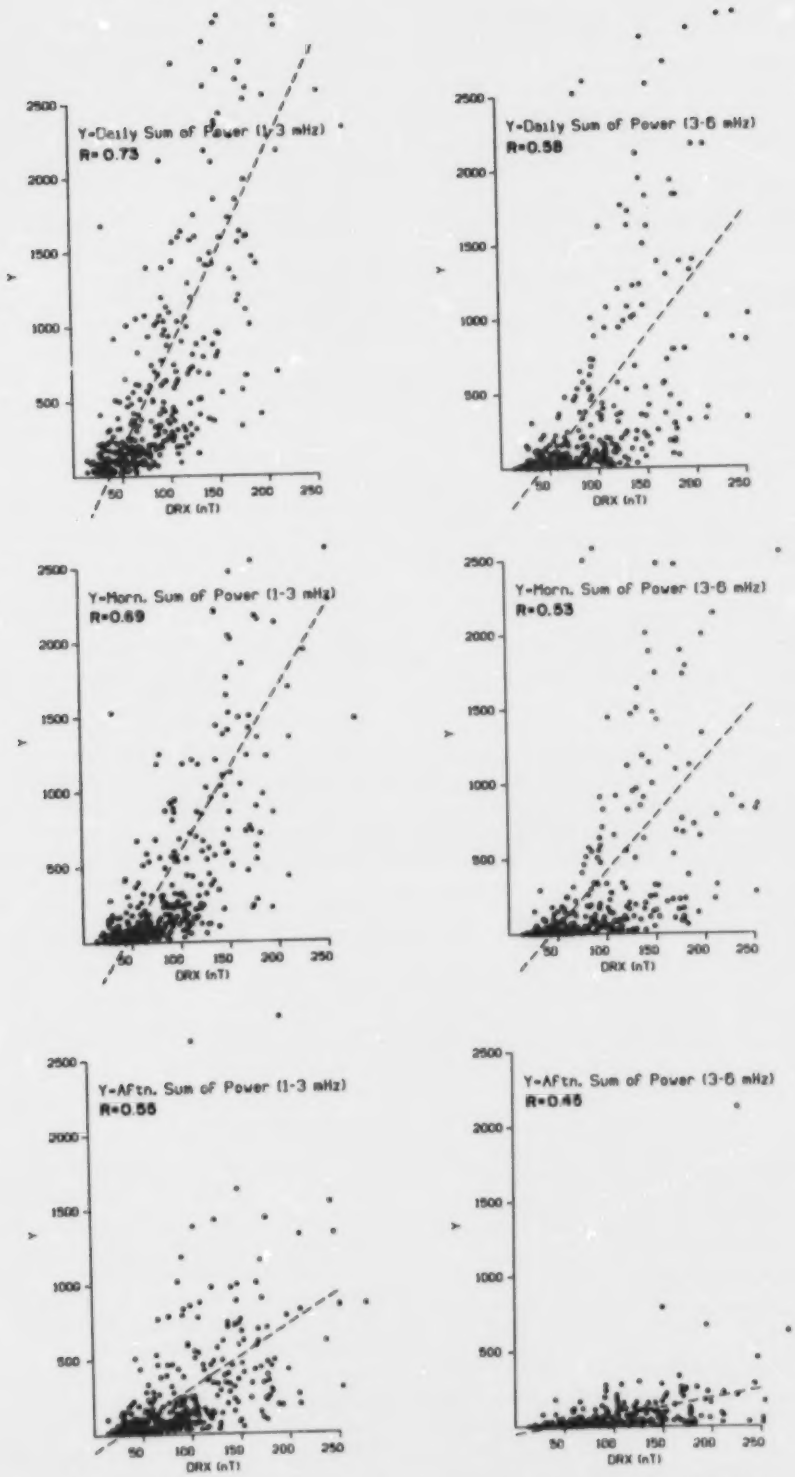

Figure 3. Sums of Pc5 powers vs DRX values for the 1-3 mHz and 3-6 mHz bands. The values of the correlation coefficients R are shown for each plot. The unit for Y is nT^2/mHz.

powers to concentrate in the morning sector (12-18 UT). In the 3-6 mHz band, there is a virtual absence of large powers in the afternoon sector (18-24 UT) for both the unsettled and active conditions. This is in contrast to the findings for the 1-3 mHz band. This particular result should be of interest to the magnetic explorationists as will be discussed later.

From a casual comparison of the DRX and Pc5 power data, it appears that intensive Pc5 pulsational activity sometimes 'reverberates' following an 'impulse' in DRX. Figure 5 illustrates this point. On the top panel is a plot of DRX vs days. Below it is a plot of the total Pc5 powers summed over the entire daytime sector for each individual day in the 1-3 mHz band. The bottom two panels are similar plots for different days. It can be seen that a sudden increase in DRX not only caused an enhancement in the Pc5 power on the same day but also several days later. There appears to be some recurrence of enhanced Pc5 activity in the 1-3 mHz band after the initial 'pulse' as can be clearly seen in days 12, 15 and 17 in the second panel and days 32, 41 and 44 in the bottom panel. It would be interesting to generalize this recurrence tendency and also to see if it holds true for activities in both the morning and afternoon sector as well as for the 3-6 mHz band. Thus, the linear prediction filtering technique due to Wiener (1949) was employed to model the most general linear relationship between DRX and Pc5 powers. This technique has also been used to produce the forecasts of geomagnetic activity in Canada (Lam, 1987).

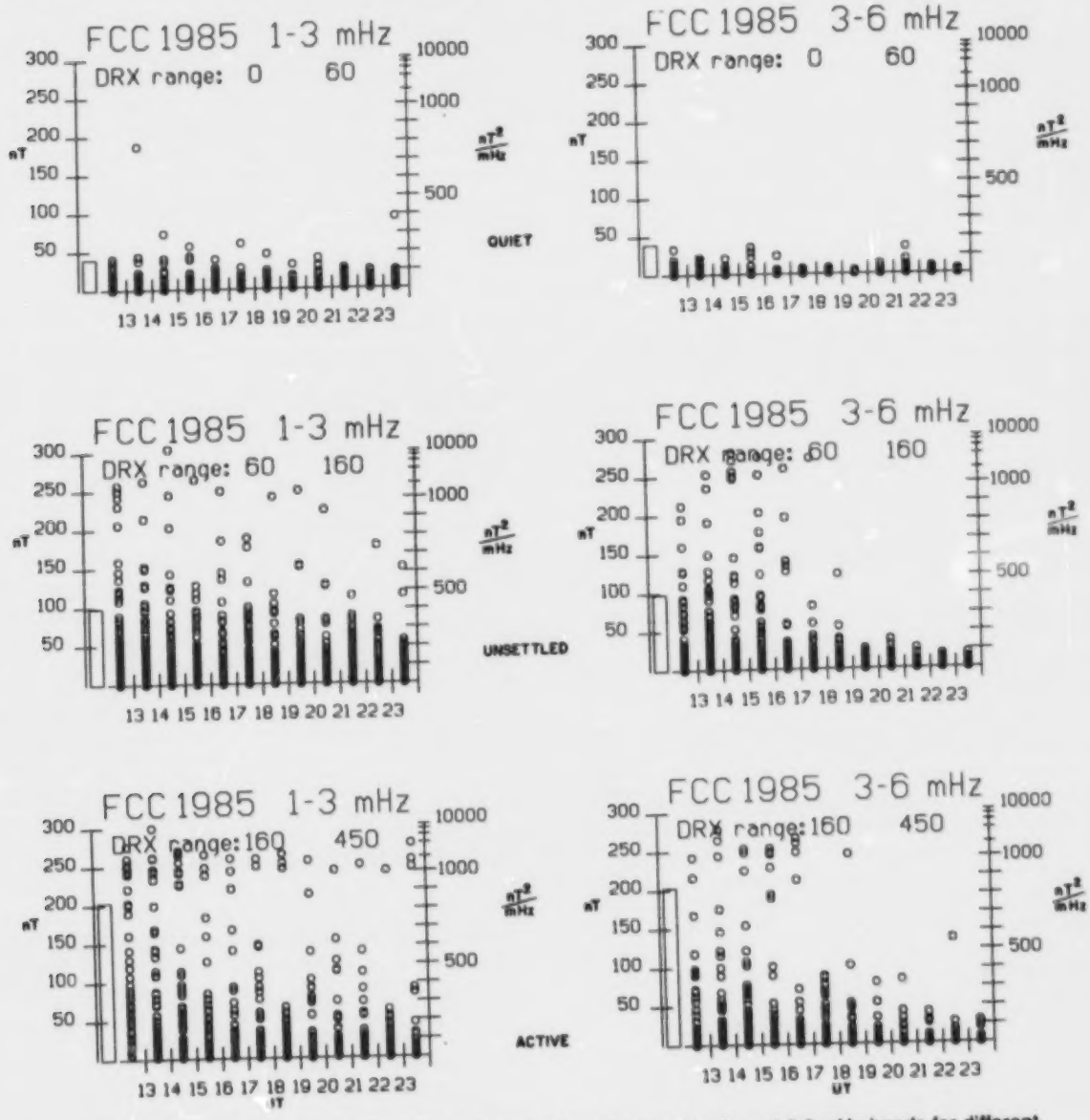

Figure 4. Variations of Pc5 powers as a funtion of UT in the 1-3 mHz and 3-6 mHz bands for different ranges of DRX values corresponding to different levels of geomagnetic activity.

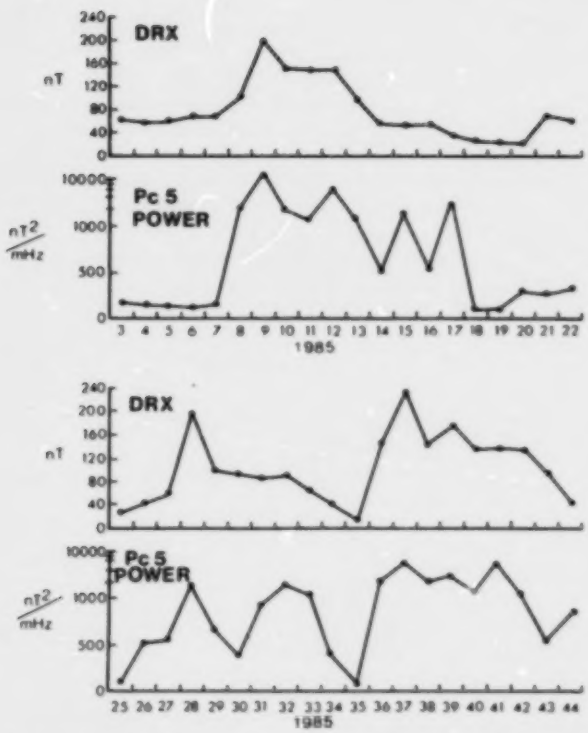

Figure 5. Plot of DRX and Pc5 powers in the 1-3 mHz band vs days. Note the recurrence of Pc5 activities.

Pc5 power (y) is assumed to be related to DRX (x) by a specification of an impulse response function (f)

$$Y_t = \sum_{s=0}^{m} {}_f x_{t-s}$$

where the values of ${}_f$ are the filter elements of the Wiener linear prediction filter. The impulse response function consists of values of time lagged response coefficients and would thus shed some light on the response of Pc5 to changes in DRX.

The impulse responses of the maximum Pc5 powers in the morning and afternoon sector for 1-3 and 3-6 mHz bands are shown in Figure 6. There is a large peak at 'zero-lag' on all of the 4 plots. The amplitude of fluctuations in the coefficients are relatively small in all plots except the one which shows the impulse response of the maximum Pc5 power in the 1-3 mHz band in the morning (top panel on the left). This particular panel shows that the fluctuations are of significant magnitude up to day 9 after which the general amplitude level is reduced. The 'zero-lag' peak on all 4 plots implies that Pc5 powers are enhanced both in the morning and afternoon for both spectral bands on the same day that the DRX is increased. For the 1-3 mHz band, intensive Pc5 activities would recur a few times up to 9 days after the initial enhancement in Pc5 activity. This recurrent tendency is not so evident in the afternoon sector and for the 3-6 mHz band. These findings are consistent with previous studies which indicate that Pc5 activities in the morning sector are different from those in the afternoon sector (e.g. Lam, 1980). The results presented here suggest different source mechanisms for Pc5 activities in the morning and afternoon sector and for the two different spectral bands. Further perusal on this may be fruitful in discerning the source mechanims for Pc5 activities. Impulse response functions were also calculated for the sum and mean of Pc5 powers in the two spectral bands for the morning and afternoon activities and the results are similar to those of the maximum powers as shown in Figure 6.

SUMMARY AND CONCLUSION

While it is not possible to predict precisely the occurrence and the intensity of Pc5 pulsations, it is plausible to use the results presented in this study to infer its future level of activity by relating it to the DRX index, a parameter that is predictable and routinely forecast in Canada. In the present investigation, pulsational activities as a function of time throughout the day were related to the quiet, unsettled and active levels of geomagnetic activities and formulae for Pc5 power were derived as a function of DRX. These formulae are suitable for predicting the sum of Pc5 powers taken over all hours of the day, morning or afternoon. For a given value of DRX, Pc5 activities in the afternoon sector are less intense than those in the morning sector (a dramatic illustration of this statement can be seen in Figure 2 which shows a remarkably reduced pulsational activity in the afternoon) and the amplitude of shorter period pulsations in the 3-6 mHz band are generally less than those in the 1-3 mHz band. This study also shows that there is a virtual absence of any intensive shorter period Pc5 pulsations in the 3-6 mHz band in the afternoon sector. The impulse response functions suggest that after an initial enhancement of longer period pulsational activity in the 1-3 mHz band in the morning sector due to a sudden increase in DRX, the intense longer period Pc5 activity might recur again for several days even when DRX has returned to low values.

The results presented in this study as summarized above should be of interest to the explorationists concerned in carrying out magnetic surveys during times of low pulsational activity and the inductionists interested in using Pc5 frequency to probe the earth for buried targets during times of high pulsational activity. From the forecast DRX, they can interpolate the levels of pulsational activity by using the relations established in this study. Thus, intervals with optimal pulsational activities suitable to their particular endeavour could be selected. In high resolution magnetic surveys, the stringent requirement that the ground magnetic trace's deviations not exceed 2 nT from any chord two minutes long (Reford, 1979) is more likely to be met in the afternoon sector because of the virtual absence of intensive shorter period pulsations in the 3-6 mHz range. The general level of the longer period pulsational activity in the afternoon is also low. It would therefore appear that in the course of a day, afternon would be favourable for carrying out magnetic surveys by the explorationists. On the other hand, the inductionists might want to conduct magnetic sounding work in the morning because of more intensive pulsational activities in that sector and the recurrent tendency of enhanced longer period pulsations in the 1-3 mHz range in the morning.

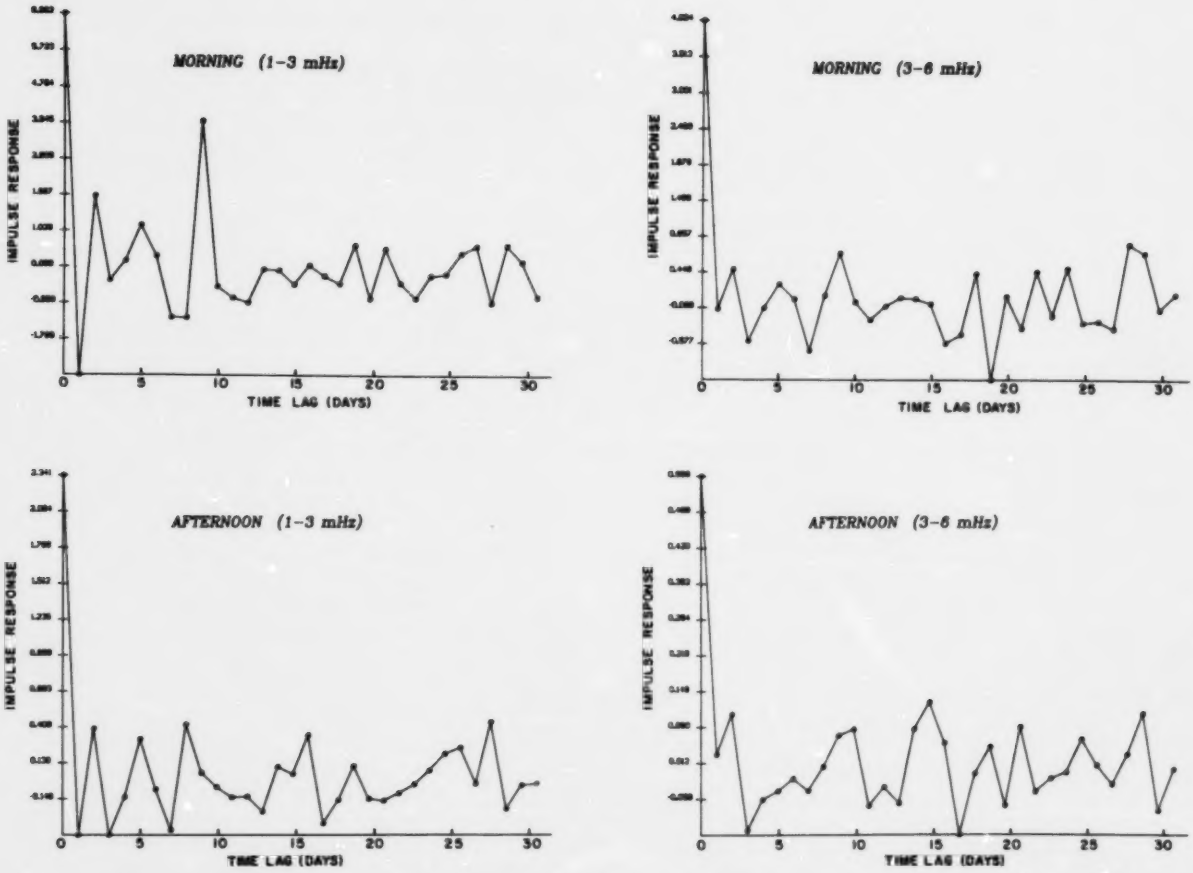

Figure 6. Impulse responses of the maximum Pc5 powers in the morning and afternoon for 1-3 mHz and 3-6 mHz bands.

Using the results presented in this study, a magnetic explorationist or inductionist is able to infer the future levels of Pc5 activity from the forecast DRX and choose the appropriate local time for carrying out the measurement. A full understanding of the origins and generation mechanisms of Pc5 pulsations in the future would inevitably render a better prediction scheme to be developed. But, at the moment, the approach adopted in this study seems most practical.

ACKNOWLEDGMENT

I thank G. Jansen van Beek for providing a tape containing the Churchill data, and R.L. Coles and J. Hruska for discussions.

REFERENCES

Gupta, J.C.
1974: Amplitude variation of Pc5 pulsations at high latitudes; Radio Science, v. 9, p. 757-768.

Hirasawa, T.
1970: Long period geomagnetic pulsations (Pc5) with typical sinusoidal waveforms; Report of Ionosphere and Space Research in Japan, v. 24, p. 66-79.

Hruska, J. and Coles, R.L.
1978: A new type of magnetic activity forecast for high geomagnetic latitudes; Journal of Geomagnetism and Geoelectricity.

Jacobs, J.A.
1970: Geomagnetic Micropulsations; 179 p., Springer-Verlag, New York.

Jacobs, J.A. and Sinno, K.
1960: World-wide characteristics of geomagnetic micropulsations; Geophysical Journal, v. 3, p. 333-353.

Lamb, H.-L.
1980: Longitudinal characteristics of Pc5 magnetic pulsations; Planetary and Space Science, v. 28, p. 1035-1050.
1987: Forecasts of geomagnetic activity in Canada by linear prediction filtering; Journal of Geomagnetism and Geoelectricity.

Lam, H.-L. and Rostoker, G.
1978: The relationship of Pc5 micropulsation activity in the morning sector to the auroral westward electrojet; Planetary and Space Science, v. 26, p. 473-492.

Lam, H.-L., Jones, F.W., and Hibbs, R.D.
1982: The response of perturbation and induction arrows to a three-dimensional buried anomaly; Geophysics, v. 47, p. 51-59.

Reford, M.S.
1979: Problems of magnetic fluctuations in geophysical exploration, in Solar System Plasma Physics, v. 3, ed. L.J. Lanzerotti, C.F. Kennel and E.N. Parker; p. 356-363; North-Holland, Amsterdam, Holland.

Southwood, D.J. and Hughes, W.J.
1983: Theory of hydromagnetic waves in the magnetosphere; Space Science Review, v. 35, p. 301-366.

Wiener, N.
1949: Extrapolation, Interpolation and Smoothing of Stationary Time Series with Engineering Applications; 163 p., Tech. Press of the M.I.T. and John Wiley and Sons, Inc., New York.

Mining induced seismicity

H.S. Hasegawa
Geophysics Division

Hasegawa, H.S., Mining induced seismicity; in Current Research, Part F, Geological Survey of Canada, Paper 88-1F, p. 53-58, 1988.

Abstract

Besides depth of mining, there are other factors affecting the nature of mine-induced tremors in metalliferous, potash and coal mines in Canada. These factors are the method of mining, the rate of volume extraction and associated rate of volume closure, the geology of the host rocks, pre-existing faults near the mine, and the reaction of mine-related stresses with the ambient tectonic stress. At present, mine-induced tremors are studied by deploying a network of geophones on the surface and underground at mines that are experiencing a high level of mine-induced seismic tremors. Analysis of the resulting measurements, in both the time and frequency domains, should lead to a better understanding of the causative factors of these tremors and may lead to pattern recognition of precursors in potentially hazardous situations.

Résumé

Plusieurs facteurs, outre la profondeur de l'exploitation, influent sur la nature des séismes miniers induits dans des mines métalliques et des mines de potasse et de charbon au Canada. Il s'agit des facteurs suivants: la méthode d'exploitation minière, le taux d'extraction volumétrique et le taux associé de fermeture volumétrique, la géologie des roches encaissantes, les failles pré-existantes près de la mine, et la réaction des contraintes minières sous la contrainte ambiante de nature tectonique. Actuellement, les séismes miniers induits sont étudiés au moyen d'un réseau de géophones déployé en surface et sous terre à des mines où se produit un taux élevé de séismes miniers induits. Une analyse des mesures qui en résultent, dans les domaines du temps et de la fréquence, devrait mener à une meilleure compréhension des facteurs produisant ces séismes induits et pourrait permettre une reconnaissance de configurations des précurseurs qui indiqueraient une condition périlleuse.

INTRODUCTION

Initial attempts to identify mine-related seismic signals were hampered for several reasons. Many mines are located in regions of moderate seismic activity, as shown in Figure 1 (cf. Milne and Berry, 1976). In general the spacing between seismograph stations spanning the Canadian landmass is too large for a definitive location of mine-related tremors. However, with the deployment of specialized networks such as telemetered seismograph networks (Shannon et al., 1983) and geophone networks around some of the more seismically active mines (Gendzwill et al., 1982), the location accuracy of mine-induced tremors has improved considerably and the magnitude detection threshold has been lowered significantly (Hasegawa et al., in press).

An understanding of the salient features causing mine-induced tremors is necessary to mitigate hazards associated with mining. Mine-induced tremors, as used in this text, include the following mechanisms: (i) rockburst, which is a violent expulsion of a large volume of rock into the mine opening; (ii) pillar burst; (iii) large rock fall from the mine roof; (iv) shear or tensile failure of the intact rock near the mine opening; (v) shear failure along a pre-existing (weakened) fault farther away from the mine opening; and (vi) coal outburst. Other types of mine-induced tremors that are not discussed explicitly in the text are a strain burst, which generates a sharp tremor but does not result in observable damage to the mine walls, and a coal bump, which is due to sudden slip between the coal seam and the adjacent strata (Obert and Duvall, 1967; Osterwald, 1970). In this review significant features of mine-induced tremors in metalliferous, potash and coal mines are summarized briefly.

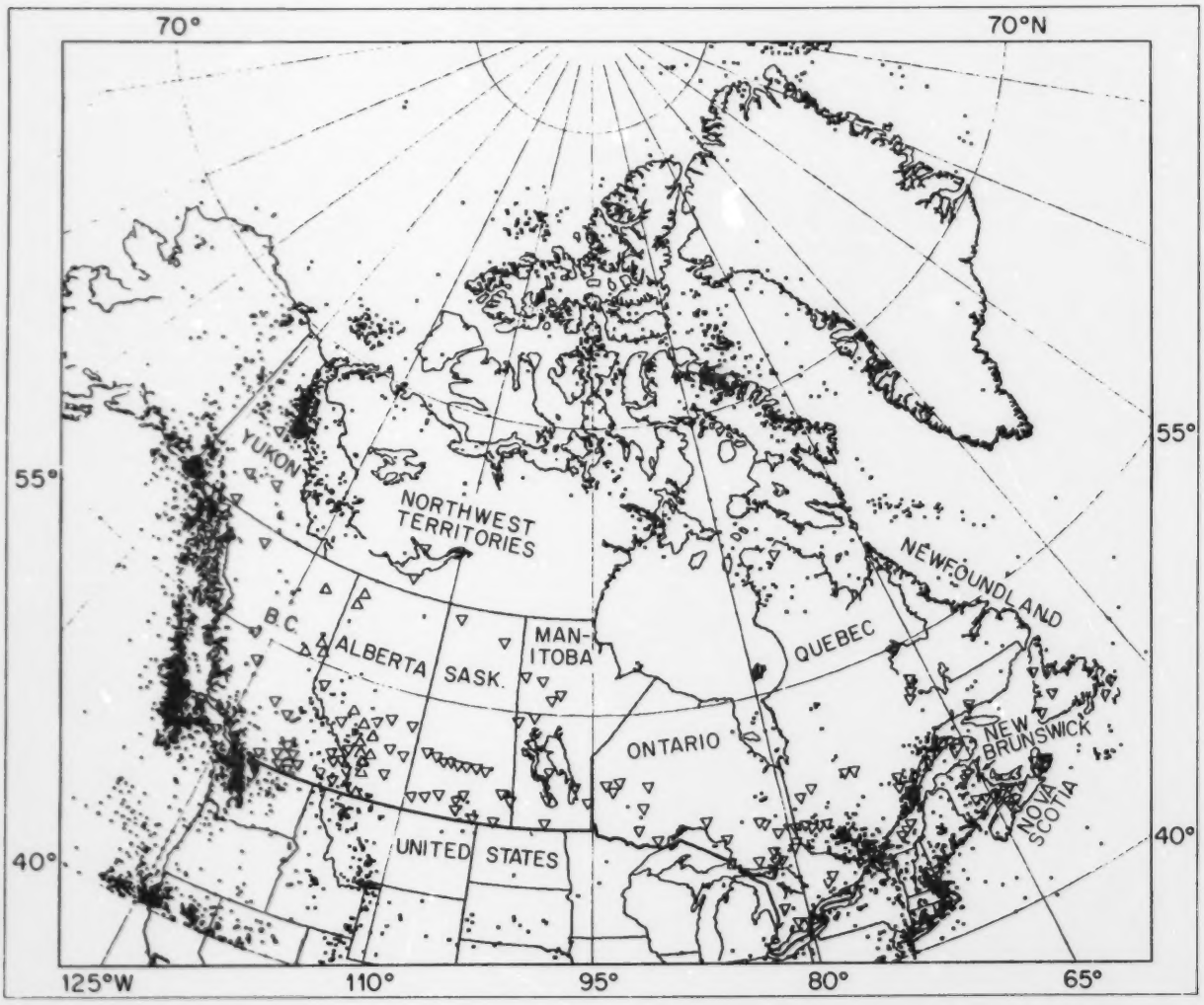

Figure 1. Earthquake epicentres (dots) to 1986 and mine locations (open triangles) in Canada (from Hasegawa et al., in press).

MINE-INDUCED SEISMIC TREMORS

The metalliferous mines in northern Ontario and southwestern Quebec are in a region of low-to-moderate tectonic seismic activity. Figure 2 shows the location of mines that are discussed later, superimposed on the regional tectonic seismicity pattern (from Basham and Cajka, 1984).

A noteworthy feature of induced tremors from mines in Ontario is that the frequency of these tremors dos not manifest an increasing trend with depth, despite the fact that potential for mine-induced tremors tends to increase with depth (Herget, 1980). Figure 3 shows that the reported "rockburst" occurrences in Ontario mines manifest a peak around 1940 (from Hedley and Wetmiller, 1985); in this figure "rockburst" is used in the same sense as mine-induced tremors, as defined previously. According to Herget (1980), the cause of the dramatic increase in mine-induced tremors at Kirkland Lake is that mining at that time was through a competent layer (depth around 500 m) that could store a high level of stress, much of which was released by mining. The cause of the increase in mine-induced tremors in the Sudbury basin is uncertain because of the complex geology in this region, but a possibility is an increase in rate of volume extraction. Whereas the smaller tremors are likely occurring in intact rock near the mine (see McGarr, 1971), the larger (magnitude 3 1/2 to 4) events are probably occurring on pre-existing faults farther away (above) from the mine (Hedley and Wetmiller, 1985) and are probably triggered by mine-induced stress migrating upwards from the mine opening (e.g. the unclamping effect of roof subsidence).

Prior to the mid-1970s, there were no reports of induced tremors in potash mines in Saskatchewan. Figure 4 shows that there is a low level of tectonic earthquake activity in this region (Horner and Hasegawa, 1978). However since that time the number of reported mine-related tremors exceeded the number of tectonic earthquakes (Hasegawa et al., in press). The larger of the mine-induced tremors are apparently originating in the competent limestone layer above the mine because this is the only layer that is strong enough to store a sufficiently high stress level. A normal-fault mechanism (Gendzwill et al., 1982) and also a horizontal shear mechanism (Gendzwill, 1983) have been proposed for the larger tremors. More seismograms of the larger tremors from geophone networks around the mines are required to resolve this dicothomy.

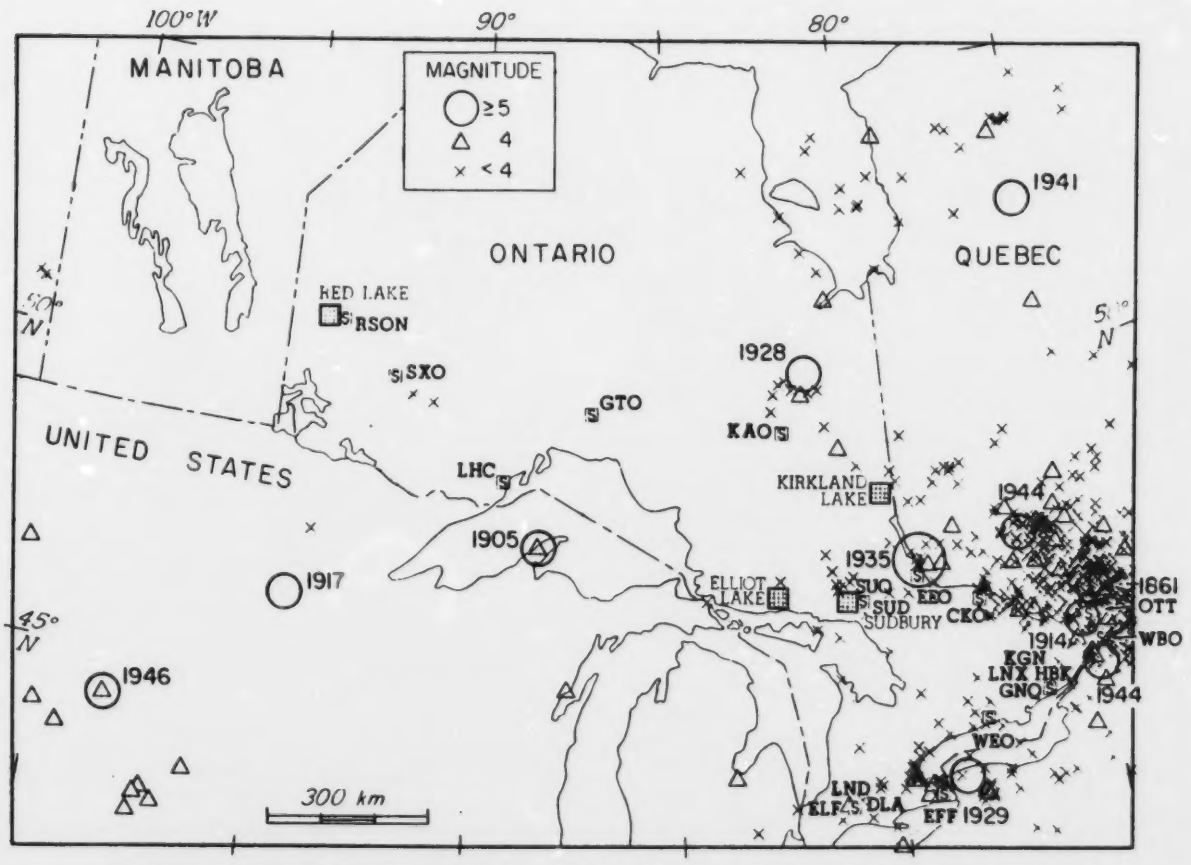

Figure 2. Known seismicity in Ontario and peripheral regions to 1980, regional seismograph stations (small square enclosing letter s) and four mines (checkered squares) in Ontario (from Basham and Cajka, 1984).

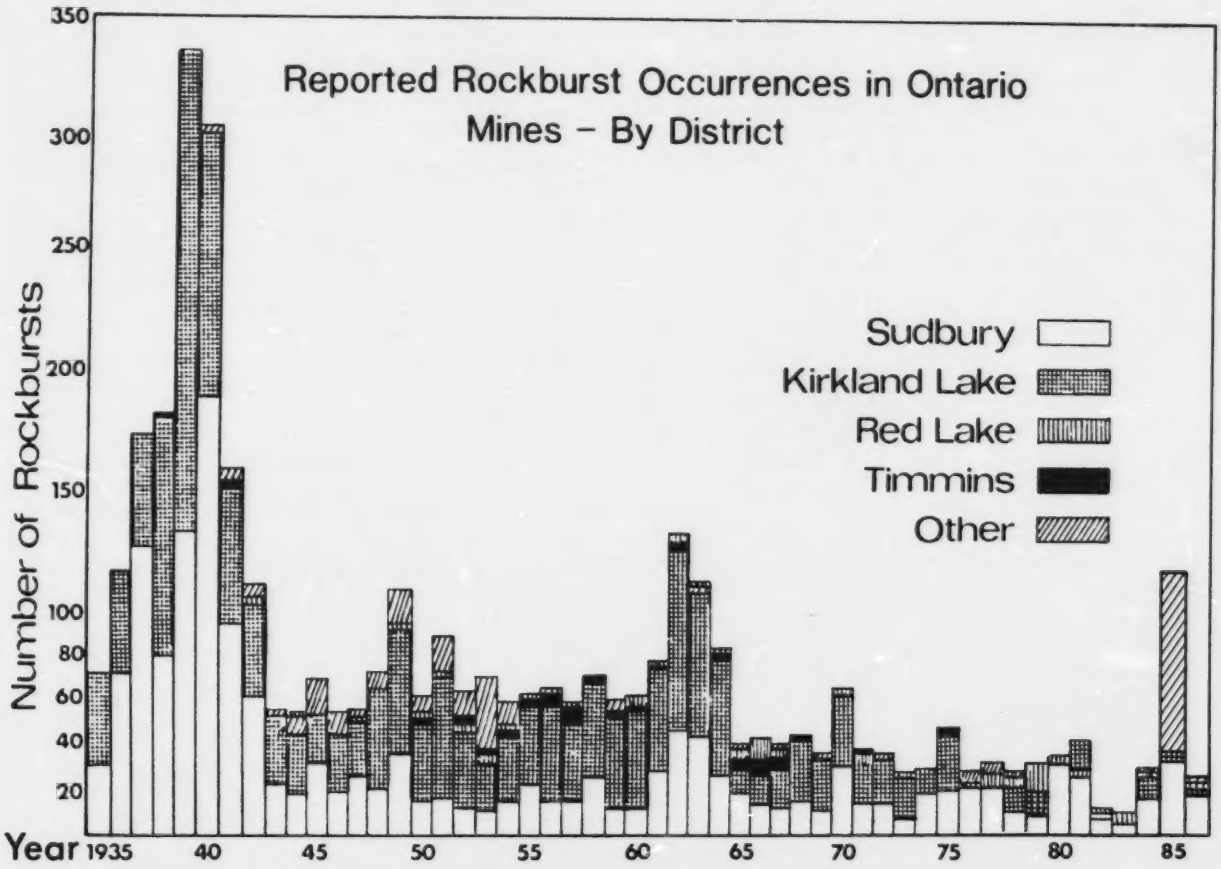

Figure 3. Histogram of reported rockburst occurrences in Ontario mines (after Hedley and Wetmiller, 1985). "Other" refers to Elliot Lake.

The Springhill coal mine in the Cumberland basin of Nova Scotia has a lengthy history of mine-induced tremors and consequently will be used as an example to illustrate causative factors of induced tremors at great depth in a coal mine. When the depth of overburden reached 1200 m, there was a dramatic increase in the rate of mine tremors. This sudden surge in mine tremors was followed by a massive outburst of coal into the seam opening. The high pressure at this depth (1200 m) caused the host rock to exert an intensive squeezing action on the coal seam. The extrusive force on the coal seam resulting from this squeezing action exceeded the resistive forces, which consisted of the frictional force between coal and adjoining host rock and the effective force on the coal face. As a consequence, coal was ejected violently into the mine opening (Notley, 1984).

Six different ways in which mine-induced tremors can occur are shown schematically in Figure 5 (from Hasegawa et al., in press). Rockburst downwards from the mine roof or sudden detachment of a large portion of the foot wall of an inclined fracture in the roof imparts a vertical impulse to the overlying host rock. Pillar burst is equivalent to a vertical dipole (implosion). Tensile failure in a cap rock above

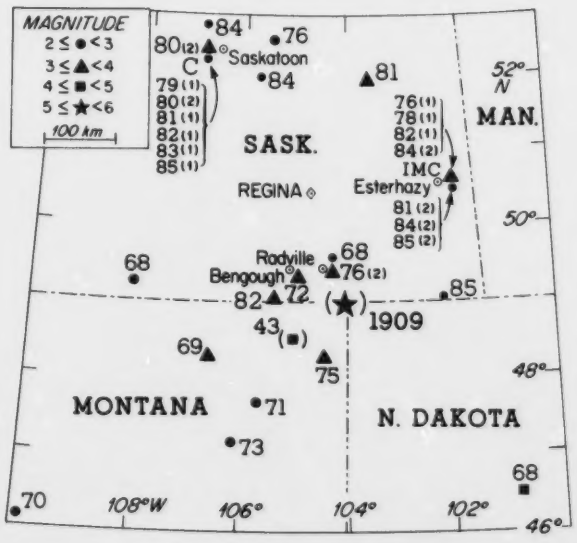

Figure 4. Known seismicity in southern Saskatchewan and adjoining areas in north-central United States to 1985. Mine-induced tremors at Cory (C) and International Mining Company (IMC) are labeled with year and number of occurrences (in brackets) (after Gendzwill et al., 1982).

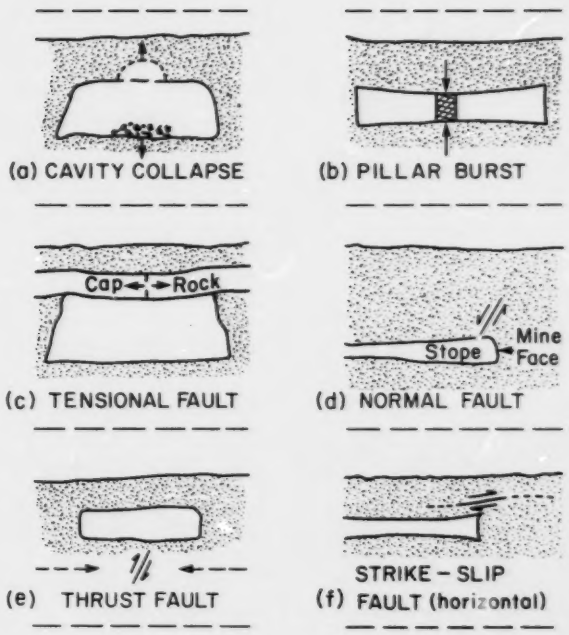

Figure 5. Schematic diagram of six types of mine-induced tremors. Single arrow represents force, co-linear pair of arrows a dipole, parallel pair of oppositely pointing offset arrows a double couple. Dashed arrows represent tectonic stress (from Hasegawa et al., in press).

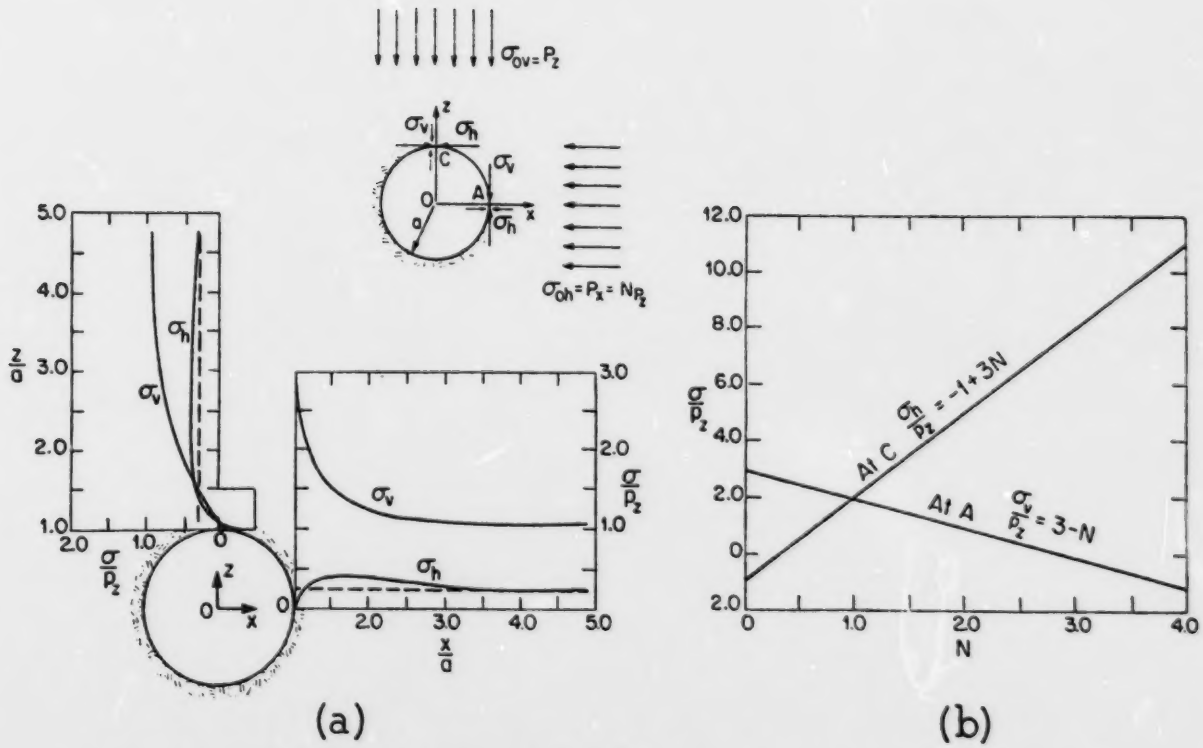

Figure 6. (a) Tangential and normal stress at points A and C (see top right figure) on periphery of horizontal, cylindrical opening in ambient stress field consisting of horizontal (P_x) and vertical (P_z) components. Induced horizontal (σ_h) and vertical (σ_v) stress is plotted against x/a and z/a, respectively, where x and z are radial distances from edge of open cylinder and a is radius of opening. In (b) ratio of induced-to-applied stress is plotted against N, which is ratio of P_x to P_z (from Terzaghi and Richart, 1952.)

the mine can be simulated with a horizontal dipole. Faulting can be initiated in intact rock near the stope face due to a combination of blasting and volume closure (McGarr, 1971). Faulting can also be triggered on pre-existing faults (in many cases steeply dipping and in some cases, horizontal) farther away from the mine excavation by a migrating stress-strain field due to on-going volume closure. (Hedley and Wetmiller, 1985; Gendzwill et al., 1982; Genndzwill, 1983).

THE STRESS FIELD

Figure 6 shows the perturbing effects of a horizontal cylindrical opening on a uniform tectonic stress field with two components (from Terzaghi and Richart, 1952). As the ratio (N) of the horizontal-to-vertical applied (tectonic) stress increases, the tangential stress at point A becomes more extensional and at C, more compressional. The value of N will influence the type of slip on nearby pre-existing faults that are prone to triggering by a migrating stress-strain field due to on-going volume closure. The larger magnitude events appear to be occurring on pre-existing faults near the mine. (Hedley and Wetmiller, 1985).

MITIGATION OF MINE-INDUCED HAZARDS

At present a feasible approach to mitigate hazards associated with mine-induced tremors is to deploy a network of geophones around mines experiencing a conspicuous level of these tremors (Prugger and Gendzwill, 1983; Notley, 1984; Brehaut and Hedley, 1986). Analysis of the corresponding seismograms in both the time and frequency domains should lead to a better understanding of the potential modes of failure. Pattern recognition of rockburst activity (Brady, 1977) and also geotomographic imagery (Young et al., 1987) may be useful to delineate zones that are undergoing a high rate of change in stress and strain and, consequently, are potentially dangerous zones.

ACKNOWLEDGMENTS

The author is grateful to the following for helpful comments: M.J. Berry, P.W. Basham, F.M. Anglin, G.G. Buchbinder and A.E. Stevens.

REFERENCES

Basham, P.W., and Cajka, M.
1984: Contemporary seismicity in northwestern Ontario; *in* Proceedings of the Seventeenth Information Meeting of the Nuclear Fuel Waste Management Program, Atomic Energy of Canada Ltd., Technical Record TR-299, p. 367-374.

Brady, B.T.
1977: Anomalous seismicity prior to rock bursts: implications for earthquake prediction; *in* Stress in the Earth, M. Wyss, ed., Pure and Applied Geophysics, v. 115, p. 357-374.

Brehaut, C.H., and Hedley, D.G.F.
1986: 1985-1986 annual report of the Canada-Ontario-Industry rockburst project; CANMET Special Publication, SP86-3E, 13p.

Gendzwill, D.J.
1983: A theory for the source mechanism of the Cory Mine earthquakes; *in* Potash Technology, R.M. McKercher, ed., Pergammon Press, p. 197-202.

Gendzwill, D.J., Horner, R.B. and Hasegawa, H.S.
1982: Induced earthquakes at a potash mine near Saskatoon, Canada; Canadian Journal of Earth Sciences, v. 19, p. 466-475.

Hasegawa, H.S., Wetmiller, R.J., and Gendzwill, D.J.
— Induced seismicity in mines in Canada — an overview; (Submitted to Pure and Applied Geophysics) (in press).

Hedley, D.G.F., and Wetmiller, R.J.
1985: Rockbursts in Ontario mines during 1984; CANMET, Energy, Mines and Resources Canada, Report No. SP85-5, 36 p.

Herget, G.
1980: Regional stresses in the Canadian Shield; *in* Proceedings of the 13th Canadian Rock Mechanics Symposium, CANMET, Energy, Mines and Resources, Canada, Division Report MRP/MRL 80-8 (OP): 9-16.

Horner, R.B., and Hasegawa, H.S.
1978: The seismotectonics of southern Saskatchewan; Canadian Journal of Earth Sciences, v. 15, p. 1341-1355.

McGarr, A.
1971: Violent deformation or rock near deep-level, tabular excavations seismic events; Bulletin of the Seismological Society of America, v. 61, p. 1453-1466.

Milne, W.G. and Berry, M.J.
1976: Induced seismicity in Canada; Engineering Geology, v. 10, p. 219-226.

Notley, K.R.
1984: Rock mechanics analysis of the Springhill mine disaster (October 23, 1958); Mining Science and Technology, v. 1, p. 149-163.

Obert, L. and Duvall, W.I.
1967: Rock mechanics and the design of structures in rock. J. Wiley and Sons, New York, 650 p.

Osterwald, F.W.
1970: Comments on rockbursts, outbursts and earthquake prediction; Bulletin of the Seismological Society of America, v. 60, p. 2083-2085.

Prugger, A.F. and Gendzwill, D.J.
1983: Earthquake monitoring system used at the PCS Mining, Cory Division potash mine near Saskatoon, Canada; *in* Potash Technology, R.M. McKercher, ed., Pergammon Press, Toronto, p. 191-196.

Shannon, W.E., Munroe P.S., Schieman, D.R.J., and Halliday, R.J.
1983: Canadian Seismograph Operations- 1982; Energy, Mines and Resources Canada, Earth Physics Branch, Seismological Series Number 89, 111 p.

Terzaghi, K., and Richart, F.E.
1952: Stresses in rock above cavities. Geotechnique, v. 3, p. 57-90.

Young, R.P., Hutchins, D.A., McGaughey, J., Towers, J., Jansen, D., and Bostock, M.
1987: Geotomographic imaging in the study of mining induced seismicity; *in* Fred Leighton Memorial Workshop in Mining Induced Seismicity, International Rock Mechanics Congress, August 30-September 3, 1987, Montreal Canada, p. 41-67.

National gravity survey program, 1987-1988

R.A. Gibb and J.B. Boyd
Geophysics Division

Gibb, R.A. and Boyd, J.B., National gravity survey program, 1978-1988; in Current Research, Part F, Geological Survey of Canada, Paper 88-1F, p. 59-62, 1988.

Abstract

In 1987, seven gravity surveys were completed under the national gravity survey program: they were located in the high Arctic (2), in the Yukon Territory, in southern British Columbia (2) and in Ontario (2). More than 3800 new gravity stations were added to the national gravity data base as a result of these surveys.

Résumé

En 1987, sept levés gravimétriques ont été faits dans le cadre du programme national de levés gravimétriques: ils ont eu lieu dans le haut-Arctique (2), au Yukon, dans le sud de la Colombie-Britannique (2) et en Ontario (2). Plus de 3800 nouvelles stations de gravité ont été ajoutées à la base nationale de données gravimétriques suite à ces levés.

INTRODUCTION

Completion of the regional gravity survey of Canada's landmass and offshore areas by the year 2005 is a major objective of the GSC's gravity program (Gibb and Thomas, 1976). Major areas that remain to be surveyed include parts of the Cordillera of northern British Columbia and Yukon Territory, parts of the Arctic Islands and Arctic Channels, and parts of the Arctic Ocean (Fig. 1). These regions all pose special problems with respect to horizontal and vertical positioning of gravity stations and logistic difficulties of terrain, ice and climate.

Gravity surveys completed in 1987-88 are numbered 1 to 6 in Figure 1. Figure 2 shows Open File gravity maps.

POLAR SHELF SURVEY (AREA 1, FIG. 1)

A gravity and bathymetry survey of the polar continental shelf was completed during March and April 1987 in co-operation with the Canadian Hydrographic Service, Department of Fisheries and Oceans and the Polar Continental Shelf Project (PCSP). Using the Canadian Ice Island as a base for operations more than 1900 gravity and bathymetry stations were established from the frozen surface of the Arctic Ocean at a 6 to 10 km grid spacing in the area west of Axel Heiberg Island. The survey was linked to the CESAR(83) survey of the Alpha Ridge to the north and closed the last remaining gap in the gravity coverage of the polar shelf extending from the Beaufort Sea to the Lincoln Sea, representing 25 years of surveying.

AXEL HEIBERG AND ELLESMERE ISLAND SURVEY (AREA 2, FIG. 1)

A gravity survey of Axel Heiberg and Ellesmere Island was completed during the late summer of 1987 in response to a request from the Institute of Sedimentary and Petroleum Geology (GSC) in Calgary for the Frontier Geoscience Program. More than 650 land and on-ice gravity stations were observed at a grid spacing of 10 km. Two traverses across Axel Heiberg Island and the northwestern part of Ellesmere Island were completed with stations 3 km apart. Data reduction and terrain corrections are in progress. Logistic support, including fixed-wing and helicopter support, was provided by PCSP. A highlight of the survey was the first use of a Litton Inertial Survey System (LASS II) north of latitude 72°N to provide elevations for the gravity stations. The system was operated by the Geodetic Survey of Canada, Surveys, Mapping and Remote Sensing Sector.

YUKON TERRITORY (AREA 3, FIG. 1)

A regional gravity survey of the Yukon Territory, north of 64°N, and adjacent parts of the Northwest Territories was

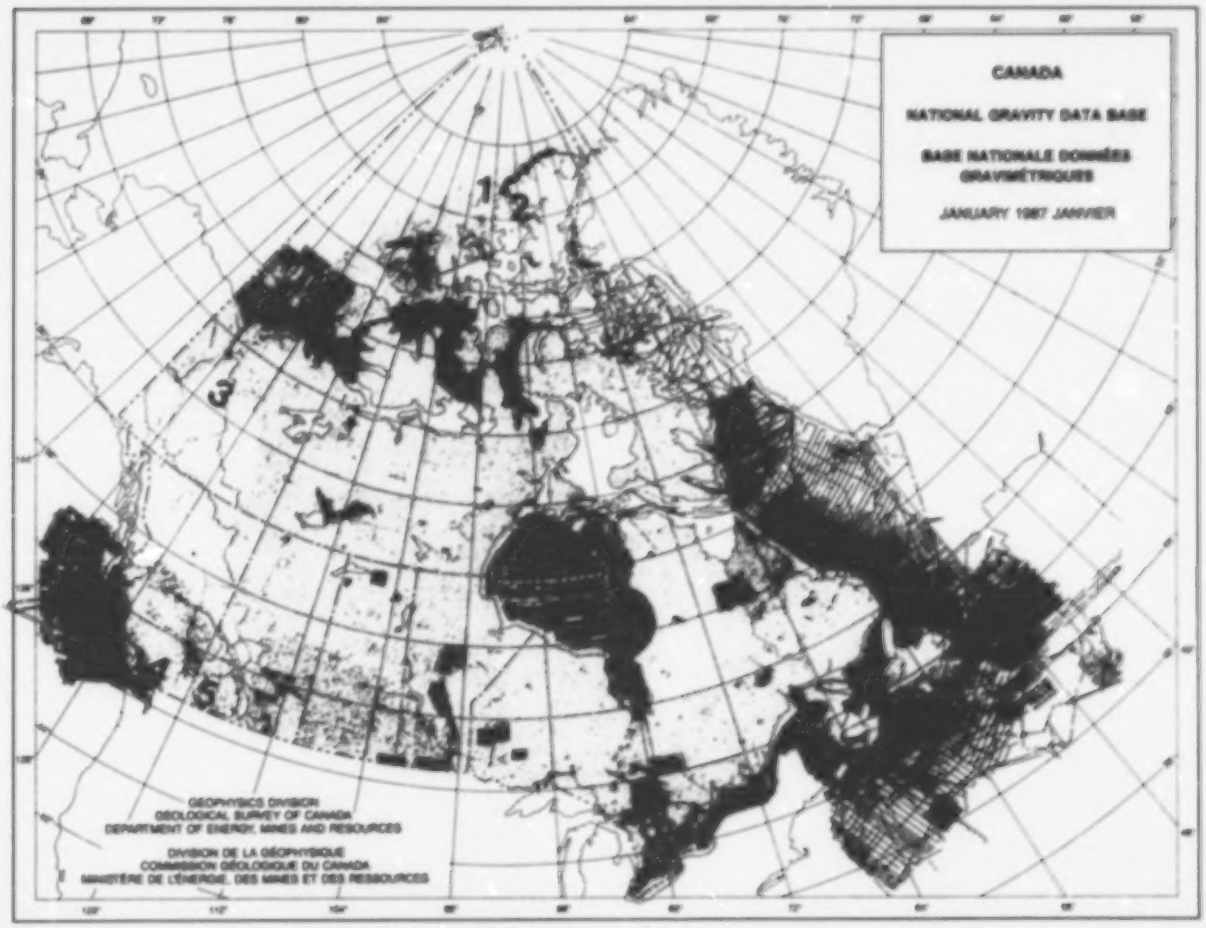

Figure 1. Distribution of gravity stations in Canada. Numbers refer to gravity surveys completed in 1987/88.

completed in the summer of 1987 under a two-year contract issued by the Pacific Geoscience Centre in 1986. The contract was partly funded by the Frontier Geoscience Program. Approximately 1500 new gravity observations, at a grid spacing of 10 to 12 km, have been added to the National Gravity Data Base. A highlight of this survey was the first production-oriented application of the satellite-based Global Positioning System (GPS) for horizontal positioning (latitude and longitude) and vertical positioning (elevation) of land-based gravity stations.

SOUTHWESTERN BRITISH COLUMBIA (AREA 4, FIG. 1)

The Department of National Defence (DND) has a continuing requirement for gravity data to support navigation systems in selected areas of Canada. In the past this requirement has been met by the Gravity Section, Geophysics Division. In the summer of 1987, the Section provided DND staff training, instrumentation, data processing software and assistance, and local extensions to the National Gravity Net of gravity control stations for a gravity densification survey in southwestern British Columbia. More than 230 new stations were added to augment existing regional gravity coverage. The new data have been added to the National Gravity Data Base.

SOUTHERN BRITISH COLUMBIA (AREA 5, FIG. 1)

A gravity survey along Lithoprobe seismic lines was completed in response to a request from the Lithosphere and Canadian Shield Division. More than 250 gravity observations were made along four profiles. Data reduction and terrain corrections are in progress.

GEORGIAN BAY, LAKE HURON (AREA 6, FIG. 1)

A gravity traverse on the east and north shores of Georgian Bay was completed in response to a request from the Lithosphere and Canadian Shield Division. About 140 observations were made by boat at 2 km spacing. Data have been processed and more details on this project are reported by (McGrath et al., 1988).

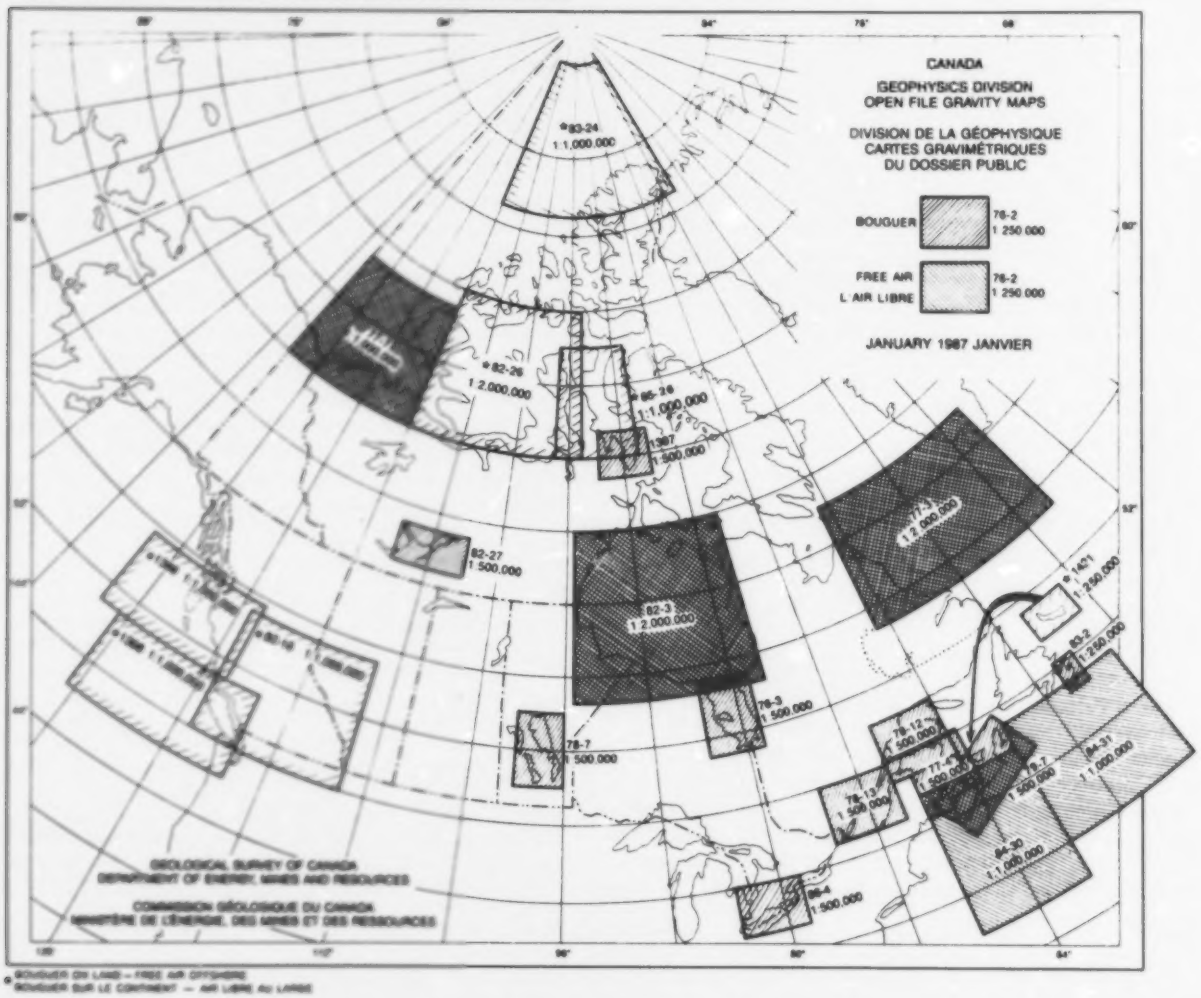

Figure 2. Index to open file gravity maps released by the Geological Survey and the former Earth Physics Branch.

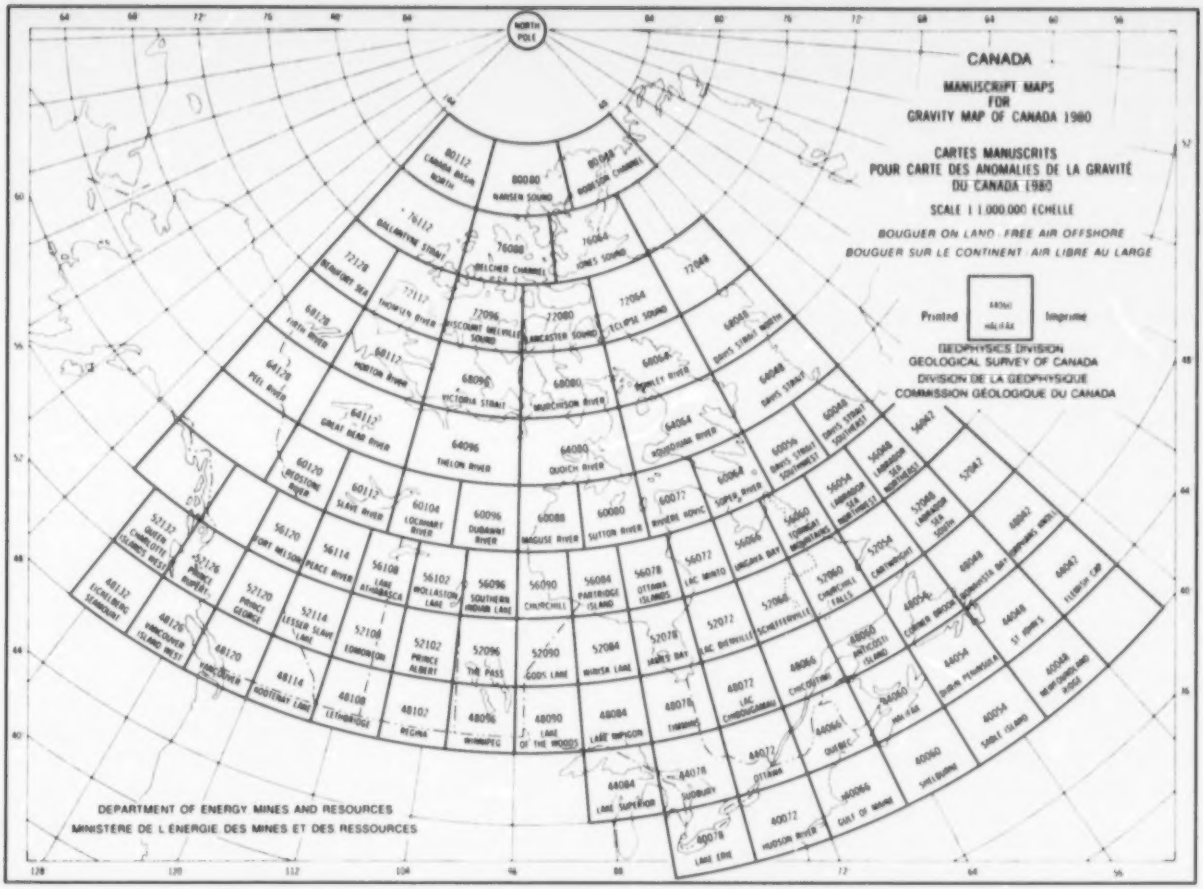

Figure 3. Index to manuscript gravity maps (scale 1:1 000 000).

ALGONQUIN PARK

During February a local gravity survey, requested by the Mineral Resources Division, was completed at Allan Lake in Algonquin Park. About 100 gravity stations were observed at a spacing of 50 m along three cutlines across an carbonatite body. Data reduction has been completed.

GRAVITY DATA BASE AND MAPS

All GSC gravity data are maintained in the National Gravity Data Base of the Geophysical Data Centre (McConnell, 1976). It currently contains about 600 000 data points. The Geophysical Data Centre provides a variety of gravity data products to users both inside and outside the Survey. The major products include anomaly and control station data in the form of plots, tapes or listings; digital terrain data; open file-, manuscript- and applicon-type maps; contour overlays; derived maps; gridded gravity values; calibration line data; earth tide values; and certain computer programs.

Gravity data for Canada have been released in a manuscript map series at a scale of 1:1 000 000 (Fig. 3). Several new gravity maps of Canada (scale 1:10 000 000) are in preparation; these include Bouguer, free air, isostatic and horizontal gradient maps.

REFERENCES

Gibb, R.A. and Thoms, M.D.
1976: Gravity Mapping in Canada; *in* Geophysics in the Americas, J.G. Tanner and M.R. Dence, ed., Publications of the Earth Physics Branch, Ottawa, v. 46(3), p. 48-57.

McConnell, R.K.
1976: The Management of the Canadian National Gravity Data Base; *in* Geophysics in the Americas, J.G. Tanner and M.R. Dence (eds), Publications of the Earth Physics Branch, Ottawa, v. 46(3), p. 107-112.

McGrath, P.H., Halliday, D.W., and Felix, B.
1988: An extension of the Killarney complex into the Grenville Province based on a preliminary intepretation of a new gravity survey, Georgian Bay, Ontario; in Current Research, Part C, Geological Survey of Canada, Paper 88-1C

Aeromagnetic survey program of the Geological Survey of Canada 1987-1988

E.E. Ready, W.A. Knappers, P.E. Stone, D.J. Teskey, and R.A. Gibb
Geophysics Division

Ready, E.E., Knappers, W.A., Stone, P.E., Teskey, D.J., and Gibb, R.A., Aeromagnetic survey program of the Geological Survey of Canada 1987-1988; in Current Research, Part F, Geological Survey of Canada, Paper 88-1F, p. 63-66, 1988.

Abstract

During 1987-88 the Geological Survey of Canada was involved in the collection and processing of approximately 314 000 km of aeromagnetic data. In addition to the 'A' base programs, this work was carried out in support of Mineral Development Agreements with six provinces (British Columbia, Manitoba, Ontario, New Brunswick, Nova Scotia and Newfoundland) and the Canada Initiatives-Lower St. Lawrence Gaspé in Quebec, the Frontier Geoscience program (Grand Banks) and the Great Lake Multidisciplinary International Crustal Evolution (GLIMPCE) program (Lake Superior). Contracts were let and supervised with six airborne geophysical contractors in addition to the GSCs Queenair crew which conducted the Lake Superior survey.

Résumé

En 1987-88, la Commission géologique du Canada a participé à la collecte et au traitement de données aéromagnétiques sur environ 314 000 km. En plus des programmes de base « A », ce travail a été fait dans le cadre des ententes sur l'exploitation minérale avec six provinces (Colombie-Britannique, Manitoba, Ontario, Nouveau-Brunswick, Nouvelle-Écosse et Terre-Neuve) et du plan de développement économique Canada-Gaspésie et Bas Saint-Laurent au Québec, le programme géoscientifique des régions pionnières (Grands Bancs) et le programme multidisciplinaire intégré sur l'évolution crustale des Grands Lacs (GLIMPCE) (lac Supérieur). Des contrats ont été passés avec six compagnies de géophysique aérienne en plus de l'équipe de Queenair de la CGC qui dirigeait le levé du lac Supérieur.

INTRODUCTION

During the fiscal year four detailed total field/gradiometer/VLF-EM surveys, and three regional total field surveys were initiated for a total of 203 365 km. In addition four total field/gradiometer/VLF surveys and one regional survey initiated in 1986/87 were completed in 1987/88 for an additional 110 628 km. The survey parameters are given in Table 1, while the areas are shown in Figure 1. Note that the three areas in central and southeast British Columbia were flown under one contract and thus are considered to be one survey as are the three areas in Manitoba and the two in Gaspé area of Quebec.

REGIONAL SURVEYS

The areas in southeastern and southwestern British Columbia were flown as part of the ongoing mapping program of the Geological Survey of Canada and will complement the recent Lithoprobe transects of Vancouver Island and the southern mainland. The central B.C. area while extending the regional coverage will also assist and stimulate mineral exploration.

The Lake Superior survey was flown with the GSC's Queenair aircraft as part of the Great Lakes Multidisciplinary International Program on Crustal Evolution (GLIMPCE). These data, along with the deep seismic profiles recorded in 1986 will help to unravel the complex; geology of this area. Navigation and flight path recovery for this survey, as with the previous Great Lakes surveys flown by the Queenair were by Loran-'C', which when tied to known land; points has proved to be highly reliable. The Grand Banks survey, funded under the Frontier Geoscience Program was flown as part of a detailed mapping program of the Grand Banks to complement the 1985 Laurentian Channel and Orphan Knoll surveys to the west and north-east respectively. This survey area has significant economic potential and was the site of deep seismic reflection profiles in 1985. Navigation for this survey was by an integrated on-

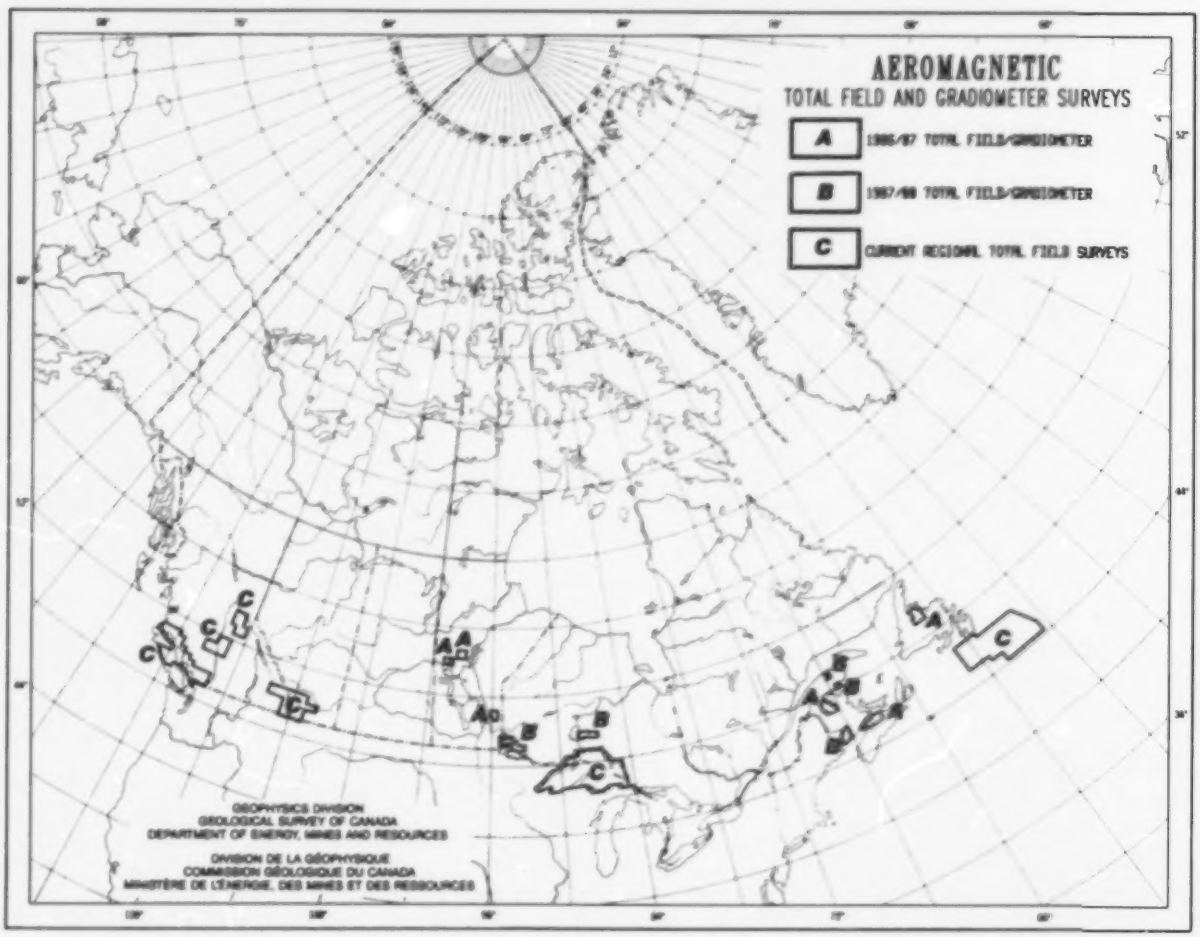

Figure 1. Location of aeromagnetic total field and gradiometer survey 1987/88 and 1986/87 carried over to 1987/88.

Table 1. Aeromagnetic surveys - 1987

Survey	Type	Km	Line Spacing	Altitude (m)
Newfoundland (1986-87)	Aeromagnetic Total Field Gradiometer VLF	18,686	300 m	150 Radar
Nova Scotia (1986-87)	Aeromagnetic Total Field Gradiometer VLF	17,150	300 m	150 Radar
New Brunswick (1986-87)	Aeromagnetic Total Field Gradiometer VLF	17,985	300 m	150 Radar
New Brunswick (1987-88)	Aeromagnetic Total Field Gradiometer VLF	13,524	300 m	150 Radar
Gaspé (1987-88)	Aeromagnetic Total Field Gradiometer EM	4,060	Murdochville (North) 100 m Port Daniel (South) 200 m	50 Radar
Ontario (Kenora-Ft. Francis) (1987-88)	Aeromagnetic Total Field Gradiometer VLF	21,288	300 m	150 Radar
Ontario (Geraldton-Beardmore) (1987-88)	Aeromagnetic Total Field Gradiometer VLF	16,725	200 m	150 Radar
Manitoba (1986-87)	Aeromagnetic Total Field Gradiometer VLF	19,129	300 m	150 Radar
Grand Banks (1987-88)	Regional Aeromagnetics	37,304	4 km	400 Radar
S.E. B.C./Alberta (1987-88)	Regional Aeromagnetics	53,548	Williams Lake 1 km Lethbridge 1.5 km	Variable Altitudes Depending on Topography (by blocks)
Lake Superior (1987-88)	Regional Aeromagnetics	56,916	1.9 km	300 Radar
Vancouver Island (1986-87)	Regional Aeromagnetics	37,678	1.5 km	Variable Altitudes Depending on Topography (by blocks)

board Global Positioning System (GPS) and Loran-'C' system provided by Nortech Ltd. which resulted in both accurate flight path recovery and real-time guidance to the pilots, essential for a high resolution survey in this area.

DETAILED SURVEYS

The detailed total field/gradiometer/VLF surveys except that in Quebec were funded under Mineral Development Agreements; with the provinces as was the central B.C. regional survey. These areas were selected by the relevant provincial agencies in co-operation with the Geological Survey of Canada to stimulate, guide and improve the effectiveness of mineral exploration in these areas. The Gaspé survey which combines total field/gradiometer and active EM was funded under the Canada Initiatives-Gaspé and Lower St.Lawrence program.

Contractors involved in the current program are: Aerodat Ltd., Toronto, Geoterrex Ltd., Ottawa, Kenting Earth Sciences, Ottawa, Les Relèves Géophysiques, Quebec City, Questor Ltd., Toronto, and Sander Geophysics, Ottawa. Nortech Ltd. of Calgary provided the integrated GPS-Loran-'C' system for the Grand Banks survey as a subcontractor to Geoterrex.

CURRENT RESEARCH PART B
EASTERN AND ATLANTIC CANADA

RECHERCHES EN COURS PARTIE B
EST ET RÉGION ATLANTIQUE DU CANADA

CONTENTS

1 | Y.T. MAURICE
Répartition du Cr, Pt, Pd, et Ir dans les dépôts de surface de l'Estrie-Beauce, Québec

9 | K.L. CURRIE
Saint George map area: the end of the Avalon zone in southern New Brunswick

17 | A.P. HAMBLIN
A preliminary report on the sedimentology, tectonic control and resource potential of the Upper Devonian-Lower Carboniferous Horton Group, Cape Breton Island

23 | E.J. SCHWARZ, G.J. PALACKY, L.E. STEPHENS, D.-J. DION, D.L. LEFEBRE, H. CHURCH, et C. GRAVEL
Levé héliporté magnétique et électromagnétique des monts Stoke, Québec, et interprétation géologique préliminaire

29 | G.M. YEO, W.D. KALKREUTH, G. DOLBY, and J.C. WHITE
Preliminary report on petrographic, palynological, and geochemical studies of coals from the Pictou Coalfield, Nova Scotia

41 | D. FOX and J.T. VAN BERKEL
Mafic-ultramafic occurrences in metasedimentary rocks of southwestern Newfoundland

49 | M. RAPPOL
Glacial dispersal of Deboullie syenite, northern Maine, into western New Brunswick

55 | S.M. BARR and C.E. WHITE
Field relations, petrology, and age of the northeastern Point Wolfe River pluton and associated metavolcanic and metasedimentary rocks, eastern Caledonian Highlands, New Brunswick

69 | N.A. VAN WAGONER and V.K. FAY
Stratigraphy and volcanology of a portion of the Lower Devonian volcanic rocks of southwestern New Brunswick

79 | E.I. TANCZYK
Paleomagnetic investigations on the Îles de la Madeleine, Gulf of St. Lawrence

91 | H. WILLIAMS, S.P. COLMAN-SADD, and H.S. SWINDEN
Tectonic-stratigraphic subdivisions of central Newfoundland

99 | J.B. MURPHY, G. PE-PIPER, R.D. NANCE, and D. TURNER
A preliminary report on geology of the eastern Cobequid Highlands, Nova Scotia

109 | P. TALLMAN, A. SANGSTER, and R.A. JAMIESON
Geology and mineralization of the Jumping Brook metamorphic suite, Faribault Brook area, western Cape Breton Island, Nova Scotia

119 | L. QUINN
Distribution and significance of Ordovician flysch units in western Newfoundland

127 | R. GRENIER and P.A. CAWOOD
Variations in structural style along the Long Range Front, western Newfoundland

135 | C.R. VAN STAAL, J. WINCHESTER, and R. CULLEN
Evidence for D_1-related thrusting and folding in the Bathurst-Millstream River area, New Brunswick

149 | A.D. PAKTUNC
The Portage Brook troctolite, a layered intrusion in the New Brunswick Appalachians

155 | A.D. PAKTUNC
Nickel-copper sulphide mineralization associated with the Goodwin Lake intrusion, northern New Brunswick

163 | J.M. RICHARDSON, K. BELL, J. BLENKINSOP, and D.H. WATKINSON
Fluid-saturation textures and Rb-Sr isotopic data from the East Kemptville tin deposit, southwestern Nova Scotia

173 J.R. HILL
Geochemical differentiation of Precambrian metacarbonate assemblages, Cape Breton Island, Nova Scotia

187 P.P. DAVID, P. BÉDARD, and R. CHARBONNEAU
Stratigraphy and geochemistry of the McGerrigle granite trains of Gaspésie, Quebec

201 W.D. SINCLAIR, G.J.A. KOOIMAN, and D.A. MARTIN
Geological setting of granites and related tin deposits in the North Zone, Mount Pleasant, New Brunswick

209 J.J. VEILLETTE
Observations sur la géologie glaciaire du nord-est de la Gaspésie, Québec

221 H.S. SWINDEN
Re-examination of the Frozen Ocean Group: juxtaposed middle Ordovician and Silurian volcanic sequences in central Newfoundland

227 R.D. NANCE and J.B. MURPHY
Preliminary kinematic analysis of the Bass River Complex, Cobequid Highlands, Nova Scotia

235 G.G.R. BUCHBINDER, A. LAMBERT, R.D. KURTZ, D.R. BOWER, F.M. ANGLIN, and J. PETERS
Summary of multidisciplinary geophysical research in the Charlevoix seismic zone, Québec

245 A.N. RENCZ and G.P. WATSON
Spatial relationship of mineral occurrences with geological and LANDSAT-derived lineaments, northeastern New Brunswick

251 M.C. GRAVES and M. ZENTILLI
The lithochemistry of metal-enriched coticules in the Goldenville-Halifax transition zone of the Meguma Group, Nova Scotia

263 Z.A. SZYBINSKI
New interpretation of the structural and stratigraphic setting of the Cutwell Group, Notre Dame Bay, Newfoundland

271 H. JOSENHANS, S. BALZER, P. HENDERSON, E. NIELSON, H. THORLIEFSON, and J. ZEVENHUIZEN
Preliminary seismostratigraphic and geomorphic interpretations of the Quaternary sediments of Hudson Bay

287 A.C. GRANT and B.V. SANFORD
Bedrock geological mapping and basin studies in the Hudson Bay region

297 P.J. KURFURST and B.V. SANFORD
Acoustic tests of seabottom core in Hudson Bay

CURRENT RESEARCH PART C
CANADIAN SHIELD

RECHERCHES EN COURS PARTIE C
BOUCLIER CANADIAN

CONTENTS

1 | M.R. ST-ONGE, S.B. LUCAS, D.J. SCOTT, N.J. BÉGIN, H. HELMSTAEDT, and D.M. CARMICHAEL
Thin-skinned imbrication and subsequent thick-skinned folding of rift-fill, transitional-crust, and ophiolite suites in the 1.9 Ga Cape Smith Belt, northern Quebec

19 | I.F. ERMANOVICS, M. VAN KRANENDONK, L. CORRIVEAU, D. BRIDGWATER, F. MENGEL, and L. SCHIØTTE
Geology of North River-Nutak map areas, Nain-Churchill provinces, Labrador

27 | R.F. EMSLIE and W.J. RUSSELL
Umiakovik Lake batholith and other felsic intrusions, Okak Bay area, Labrador

33 | S. HANMER and T. NEEDHAM
Great Slave Lake shear zone meets Thelon Tectonic Zone, District of Mackenzie, N.W.T.

51 | J.A. PERCIVAL and R. GIRARD
Structural character and history of the Ashuanipi complex in the Schefferville area, Quebec-Labrador

61 | R.N.W. DILABIO, R.F. MILLER, R.J. MOTT, and W.B. COKER
The Quaternary stratigraphy of the Timmins area, Ontario, as an aid to mineral exploration by drift prospecting

67 | R.N.W. DILABIO and C.A. KASZYCKI
An ultramafic dispersal train and associated gold anomaly in till near Osik Lake, Manitoba

73 | E. ZALESKI and N.M. HALDEN
Reconstruction of synvolcanic alteration associated with the Linda massive sulphide deposit, Snow Lake, Manitoba

83 | A.D. LECLAIR and P. NAGERL
Geology of the Chapleau, Groundhog River and Val Rita blocks, Kapuskasing area, Ontario

93 | D. MOSER
Structure of the Wawa gneiss terrane near Chapleau, Ontario

101 | J.R. HENDERSON, J. GROCOTT, M.N. HENDERSON, F. FALARDEAU, and P. HEIJKE
Results of fieldwork in Foxe Fold Belt near Dewar Lakes, Baffin Island, N.W.T.

109 | R.D. KLASSEN and F.J. THOMPSON
Glacial studies in Labrador

117 | S.M. ROSCOE and J.A. DONALDSON
Uraniferous pyritic quartz pebble conglomerate and layered ultramafic intrusions in a sequence of quartzite, carbonate, iron formation and basalt of probable Archean age at Lac Sakami, Quebec

123 | J.W. NORTH and D.H.C. WILTON
Stratigraphy of the Warren Creek Formation, Moran Lake Group, Central Mineral Belt of Labrador

129 | N.G. CULSHAW, D. CORRIGAN, J. DRAGE, and P. WALLACE
Georgian Bay geological synthesis, Key Harbour to Dillon, Grenville Province of Ontario

135 | A. DAVIDSON and K.M. BETHUNE
Geology of the north shore of Georgian Bay, Grenville Province of Ontario

145 | P.H. MCGRATH., D.W. HALLIDAY, and B. FELIX
An extension of the Killarney complex into the Grenville Province based on a preliminary interpretation of a new gravity survey, Georgian Bay, Ontario

151 | K.M. BETHUNE and A. DAVIDSON
Diabase dykes and the Grenville Front southwest of Sudbury, Ontario

161 | J.E. KING, W.J. DAVIS, C. RELF, and R.W. AVERY
Deformation and plutonism in the western Contwoyto Lake map area, central Slave Province, District of Mackenzie, N.W.T.

177 | S.S. GANDHI
Volcano-plutonic setting of U-Cu bearing magnetite veins of FAB claims, southern Great Bear magmatic zone, Northwest Territories

189 H.H. BOSTOCK
Geology of the north half of the Taltson Lake map area, District of Mackenzie

199 R.S. HILDEBRAND and S.A. BOWRING
Geology of parts of the Calder River map area, central Wopmay Orogen, District of Mackenzie

207 S.L. SMITH and P.H. WYATT
Quaternary stratigraphy of overburden drill cores, Timmins to Smoky Falls, Ontario

217 L.H. THORLEIFSON and F.J. KRISTJANSSON
Stratigraphy and visible gold content of till in the Beardmore-Geraldton area, northern Ontario

223 L. COVELLO, S.M. ROSCOE, J.A. DONALDSON, D. ROACH, and W.K. FYSON
Archean quartz arenite and ultramafic rocks at Beniah Lake, Slave Structural Province, N.W.T.

233 L.M. MACKENZIE and D.H.C. WILTON
The Grenville Province boundary in the Burnt Lake area, Central Mineral Belt of Labrador

239 I.M. KETTLES and P.H. WYATT
Stratigraphy and lithological composition of Quaternary sediments from five boreholes, Kipling Township, Ontario

245 J. VAN GOOL, D. BROWN, T. CALON, and T. RIVERS
The Grenville Front thrust belt in western Labrador

255 B.W. CHARBONNEAU
Gamma spectrometric and magnetic anomalies associated with Cu-U mineralization, Faber Lake volcanic belt, District of Mackenzie, N.W.T.

259 B.W. CHARBONNEAU and D.D. HOGARTH
Geophysical expression of the carbonatites and fenites, east of Cantley, Quebec

271 C.S. MACDOUGALL and D.H.C. WILTON
Geology of radioactive zones in the Round Pond area, Labrador

277 D.H.C. WILTON, C.S. MACDOUGALL, L.M. MACKENZIE, and C. PUMPHREY
Stratigraphic and metallogenic relationships along the unconformity between Archean granite basement and the early Proterozoic Moran Lake Group, central Labrador

283 S. TELLA and I.R. ANNESLEY
Hanbury Island Shear Zone, a deformed remnant of a ductile thrust, District of Keewatin, N.W.T.

291 D.H.C. WILTON
Copper occurrences in the Bruce River Group, Central Mineral Belt of Labrador

299 S.M. PELECHATY, J.P. GROTZINGER, F. GOODARZI, L.R. SNOWDON, and V. STASIUK
A preliminary analysis of middle Proterozoic karst development and bitumen emplacement, Parry Bay Formation (dolomite), Bathurst Inlet area, District of Mackenzie

313 J.P. GROTZINGER, C. GAMBA, S.M. PELECHATY, and D.S. MCCORMICK
Stratigraphy of a 1.9 Ga foreland basin shelf-to-slope transition: Bear Creek Group, Tinney Hills area of Kilohigok Basin, District of Mackenzie

321 D.S. MCCORMICK and J.P. GROTZINGER
Aspects of the Burnside Formation, Bear Creek Group, Kilohigok Basin, District of Mackenzie, N.W.T.

341 C.A. KASZYCKI, W. SUTTNER, and R.N.W. DILABIO
Gold and arsenic in till, Wheatcroft Lake dispersal train, Manitoba

353 A. CIESIELSKI
Geological and structural context of the Grenville Front, southeast of Chibougamau, Quebec

367 S.M. ROSCOE, C.F. STAARGAARD, and S. FRASER
Stratigraphic setting of gold concentrations in Archean supracrustal rocks near the west side of Bathurst Inlet, N.W.T.

CURRENT RESEARCH PART D
INTERIOR PLAINS AND ARCTIC CANADA

RECHERCHES EN COURS PARTIE D
PLAINES INTÉRIEURS ET RÉGION ARCTIQUE DU CANADA

CONTENTS

1 | E.C. PROSH, K.A. LESACK, and U. MAYR
Devonian stratigraphy of northwestern Devon Island, District of Franklin

11 | P.W. BROOKS, K.G. OSADETZ, and L.R. SNOWDON
Geochemistry of Winnipegosis discoveries near Tablelands, Saskatchewan

21 | H.P. TRETTIN
Early Namurian (or older) alkali basalt in the Borup Fiord Formation, northern Axel Heiberg Island, Arctic Canada

27 | K.C. PRATT
Geographic variations in relationships between random and maximum vitrinite reflectance, Western Canadian coals

33 | L.R. SNOWDON and K.G. OSADETZ
Geological processes interpreted from gasoline range analyses of oils from southeast Saskatchewan and Manitoba

41 | J.C. HARRISON, A.F. EMBRY, and T.P. POULTON
Field observations on the structural and depositional history of Prince Patrick Island and adjacent areas, Canadian Arctic Islands

51 | L.D. STASIUK, K.G. OSADETZ, and F. GOODARZI
Preliminary source rock evaluation of the Nordegg Member (lower Jurassic), Alberta

57 | R.L. CHRISTIE
Field studies at 'fossil forest' sites in the Arctic Islands

61 | J. DIXON
Depositional setting of the Maastrichtian Cuesta Creek Member, Tent Island Formation, northern Yukon

67 | A.R. CAMERON, C. BOONSTRA, and K.C. PRATT
Compositional characteristics of anthracitic coals in the Hoidahl Dome area, northern Yukon Territory

75 | Q.H. GOODBODY, T.T. UYENO, and D.C. MCGREGOR
The Devonian sequence on Grinnell Peninsula and in the region of Arthur Fiord, Devon Island, Arctic Archipelago

83 J.R. MACKAY
Catastrophic lake drainage, Tuktoyaktuk Peninsula area, District of Mackenzie

91 D.G. HARRY and K.L. MACINNES
The effect of forest fires on permafrost terrain stability, Little Chicago-Travaillant Lake area, Mackenzie Valley, N.W.T.

95 L.S. LANE
The Rapid Fault Array: a foldbelt in Arctic Yukon

99 M.P. CECILE
Corridor traverse through Barn Mountains, northernmost Yukon

105 M.R. MCDONOUGH and P.S. SIMONY
Stratigraphy and structure of the late Proterozoic Miette Group, northern Selwyn Range, Rocky Mountains, British Columbia

115 G.V. SONNICHSEN and B. MACLEAN
A reconnaissance study of the marine geology of the Lougheed-King Christian — Cameron islands region, northwest Arctic Island channels

121 LI BAOFANG and F.M. DAWSON
Stratigraphic framework and depositional setting, Judy Creek coalfield, northern Alberta

129 P.T. LAFLECHE, A.S. JUDGE, B.J. MOORMAN, B. CASSIDY, and R. BEDARD
Ground probing radar investigations of gravel roadbed failures, Rae Access road, N.W.T.

137 A. TAYLOR AND A. JUDGE
Reconstruction of marine transgression history from an offshore ground temperature profile, Esso Angasak L-03 wellsite, Beaufort Sea

143 A.D. MIALL
The Eureka Sound Group: alternative interpretations of the stratigraphy and paleogeographic evolution — Discussion

149 B.D. RICKETTS
The Eureka Sound Group: alternative interpretations of the stratigraphy and paleogeographic evolution — Reply

CURRENT RESEARCH PART E
CORDILLERA AND PACIFIC MARGIN

RECHERCHES EN COURS PARTIE E
CORDILLÈRE ET MARGE DU PACIFIQUE

CONTENTS

1 K.R. McCLAY, M.W. INSLEY, N.A. WAY, and R. ANDERTON
Tectonics and mineralization of the Kechika Trough, Gataga area, northeastern British Columbia

13 S.P. GORDEY
The South Fork Volcanics: mid-Cretaceous caldera fill tuffs in east-central Yukon

19 R. BOSDACHIN and R.M. HARRAP
Stratigraphy and structure of the Monashee complex and overlying rocks adjacent to the Trans-Canada Highway, west of Revelstoke, B.C.

25 B. BLAISE and J.J. CLAGUE
Clay mineralogy of late Pleistocene glacial deposits in Chilliwack Valley, southwestern British Columbia

31 B. BLAISE, J.M. FRANKLIN, W.D. GOODFELLOW, I.R. JONASSON, F.E.L. HARVEY-KELLY, et C.D. ANGLIN
Activité hydrothermale et altération de sédiments hémipélagiques dans une ancienne vallée axiale, vallée Middle, dorsale de Juan de Fuca, nord-est du Pacifique

39 L.C. STRUIK and E.A. FULLER
Preliminary report on the geology of McLeod Lake area, British Columbia

43 D.J. THORKELSON
Jurassic and Triassic volcanic and sedimentary rocks in Spatsizi map area, north-central British Columbia

49 S.A. GAREAU
Preliminary study of the Work Channel lineament in the Ecstall River area, Coast Plutonic Complex, British Columbia

57 D.W.A. McMULLIN and H.J. GREENWOOD
Metamorphism in and near the northern end of the Shuswap Metamorphic Complex, south-central British Columbia

65 C.J. DODDS
Geological mapping in Tatshenshini River map area, British Columbia

73 J.K. MORTENSEN
Geology of southwestern Dawson map area, Yukon Territory

79 J.J. CLAGUE
Holocene sediments at McNaughton Lake, British Columbia

85 F. GOODARZI and E. VAN DER FLIER-KELLER
Organic petrology and depositional environment of a coal-bearing section from Blakeburn open cast mine in Tulameen, British Columbia

91 C.A. EVENCHICK
Structural style and stratigraphy in northeast Bowser and Sustut basins, north-central British Columbia

97 E.W. MOUNTJOY
The Hugh Allan (Purcell) fault (a low-angle west-dipping thrust) at Hugh Allan Creek, British Columbia

105 J.L. LUTERNAUER
Geoarchitecture, evolution, and seismic risk assessment of the southern Fraser River delta, B.C.

111 M.D. THOMAS, D.W. HALLIDAY, and B. FELIX
Preliminary results of gravity surveys along the Lithoprobe southern Canadian Cordilleran transect

117 W.A. SPIRITO, C.W. JEFFERSON, and D. PARÉ
Comparison of gold, tungsten and zinc in stream silts and heavy mineral concentrates, South Nahanni resource assessment area, District of Mackenzie

127 S.M. HAMILTON, F.A. MICHEL, and C.W. JEFFERSON
Groundwater geochemistry, South Nahanni resource assessment area, District of Mackenzie

137 B.I.A. McINNES, W.D. GOODFELLOW, J.H. CROCKET, and R.H. McNUTT
Geology, geochemistry and geochronology of subvolcanic intrusions associated with gold deposits at Freegold Mountain, Dawson Range, Yukon

153 B.I.A McINNES, W.D. GOODFELLOW, and J.H. CROCKET
Role of structure in the emplacement of gold-quartz veins and rhyolite dykes at Freegold Mountain, Dawson Range, Yukon

159 M.J. ORCHARD and J. BEYERS
Conodont biostratigraphy of the Cache Creek Group in the Marble Range of south-central British Columbia

163 G.A. KLEIN and E.W. MOUNTJOY
Northern Porcupine Creek anticlinorium and footwall of the Purcell Thrust, Northern Park Ranges, B.C.

171 R.G. DECHESNE and E.W. MOUNTJOY
Structural geology of part of the Main Ranges near Jasper, Alberta

177 C.J. GREIG
Geology and geochronometry of the Eagle plutonic complex, Hope map area, southwestern British Columbia

185 M.E. RUSMORE and G.J. WOODSWORTH
Eastern margin of the Coast Plutonic Complex, Mount Waddington map area, B.C.

191 E.A. FULLER
Paleomagnetism of lake sediment cores from McLeod Lake and McBride map areas, central British Columbia

197 P.S. MUSTARD, J.A. DONALDSON, and R.I. THOMPSON
Trace fossils and stratigraphy of the Precambrian-Cambrian boundary sequence, upper Harper group, Ogilvie Mountains, Yukon

205 **CONTRIBUTIONS TO FRONTIER GEOSCIENCE PROGRAM**

207 R.I. THOMPSON
Introduction to the Frontier Geoscience Program, Queen Charlotte Islands, British Columbia

209 G.J. WOODSWORTH
Karmutsen Formation and the east boundary of Wrangellia, Queen Charlotte Basin, British Columbia

213 R.G. ANDERSON
Jurassic and Cretaceous-Tertiary plutonic rocks on the Queen Charlotte Islands, British Columbia

217 R.I. THOMPSON
Late Triassic through Cretaceous geological evolution, Queen Charlotte Islands, British Columbia

221 B.E.B. CAMERON and T.S. HAMILTON
Contributions to the stratigraphy and tectonics of the Queen Charlotte Basin, British Columbia

229 M.J. ORCHARD
Studies on the Triassic Kunga Group, Queen Charlotte Islands, British Columbia

231 H.W. TIPPER, P.L. SMITH, and G. JAKOBS
A note on the status of Lower Jurassic ammonite biostratigraphy and paleontology of Queen Charlotte Islands, British Columbia

233 T.P. POULTON and H.W. TIPPER
New developments and current research on Middle Jurassic ammonite biostratigraphy, Queen Charlotte Islands, British Columbia

235 E.S. CARTER
Radiolarian studies in the Queen Charlotte Islands, British Columbia

239 J.M. WHITE
Tertiary biostratigraphy, Queen Charlotte Basin, British Columbia

241 J.G. SOUTHER
Implications for hydrocarbon exploration of dyke emplacement in the Queen Charlotte Islands, British Columbia

247 T.J. LEWIS, W.H. BENTKOWSKI, M. BONE, R. MACDONALD, and J.A. WRIGHT
Geothermal studies in Queen Charlotte Basin, British Columbia

251 L.R. SNOWDON, M.G. FOWLER, and T.S. HAMILTON
Progress report on organic geochemistry, Queen Charlotte Islands, British Columbia

255 D. VELLUTINI and R.M. BUSTIN
Preliminary results on organic maturation of the Tertiary Skonun Formation, Queen Charlotte Islands, British Columbia

259 D. VELLUTINI and R.M. BUSTIN
A progress report on organic maturation and source rock potential of the Mesozoic and Tertiary strata of the Queen Charlotte Islands, British Columbia

261 R. HIGGS
Cretaceous and Tertiary sedimentology, Queen Charlotte Islands, British Columbia

265 J.A.S. FOGARASSY and W.C. BARNES
Stratigraphy, diagenesis and petroleum reservoir potential of the mid- to Upper Cretaceous Haida and Honna formations of the Queen Charlotte Islands, British Columbia

269 C.J. HICKSON
Structure and stratigraphy of the Masset Formation, Queen Charlotte Islands, British Columbia

275 P.D. LEWIS and J.V. ROSS
Preliminary investigations of structural styles in Mesozoic strata of the Queen Charlotte Islands, British Columbia

281 J.L. LUTERNAUER, J.V. BARRIE, and K.W. CONWAY
Surficial geology and geohazards on the continental shelf off Western Canada

283 D.A. SEEMANN, A. COLLINS, and J.F. SWEENEY
Gravity measurements on the Queen Charlotte Islands, British Columbia

287 R.G. CURRIE and D.J. TESKEY
Magnetics component of the Frontier Geoscience Program on the West Coast of Canada

289 G. ROGERS, B. HORNER, and D. WEICHERT
Lithospheric structure from earthquake depth, Queen Charlotte Islands, British Columbia